REPUBLIC OF IRAQ
MINISTRY OF HIGHER EDUCATION
AND SCIENTIFIC RESEARCH
AL-FURAT AL-AWSAT TECHNICAL
UNIVERSITY
ENGINEERING TECHNICAL
COLLEGE- NAJAF

ENHANCEMENT OF TWINS FETUSES ECG SIGNAL EXTRACTION BASED ON MODIFIED STONE BLIND SOURCE SEPARATION TECHNIQUE

A THESIS
SUBMITTED TO THE COMMUNICATION
TECHNIQUES ENGINEERING DEPARTMENT
IN PARTIAL FULFILLMENT OF THE REQUIREMENTS
FOR THE MASTER DEGREE
IN COMMUNICATION TECHNIQUES ENGINEERING

BY

Mushtaq Talib Mezaal

(B. Sc. in Communication Techniques Engineering)

Supervised by

Asst. Pro. Dr. **Ali A. A. Al-Bakri**

Asst. Pro. Dr. **Ahmed K. A. Al-Bakri**

September 2019

جمهورية العراق
وزارة التعليم العالي والبحث العلمي
جامعة الفرات الاوسط التقنية
الكلية التقنية الهندسية- نجف

تقوية وتعزيز استخراج اشارة قلب الاجنة التوأم بالاعتماد على تقنية ستون لفصل مصادر الاشارة العمياء المعدلة

رسالة مقدمة الى
قسم هندسة تقنيات الاتصالات
كجزء من متطلبات نيل درجة ماجستير في هندسة تقنيات الاتصالات

تقدم بها
مشتاق طالب مزعل
بكالوريوس في هندسة تقنيات الاتصالات

إشراف

أ.م.د.
علي عبد العباس البكري

أ.م.د
احمد كريم البكري

ايلول / 2019

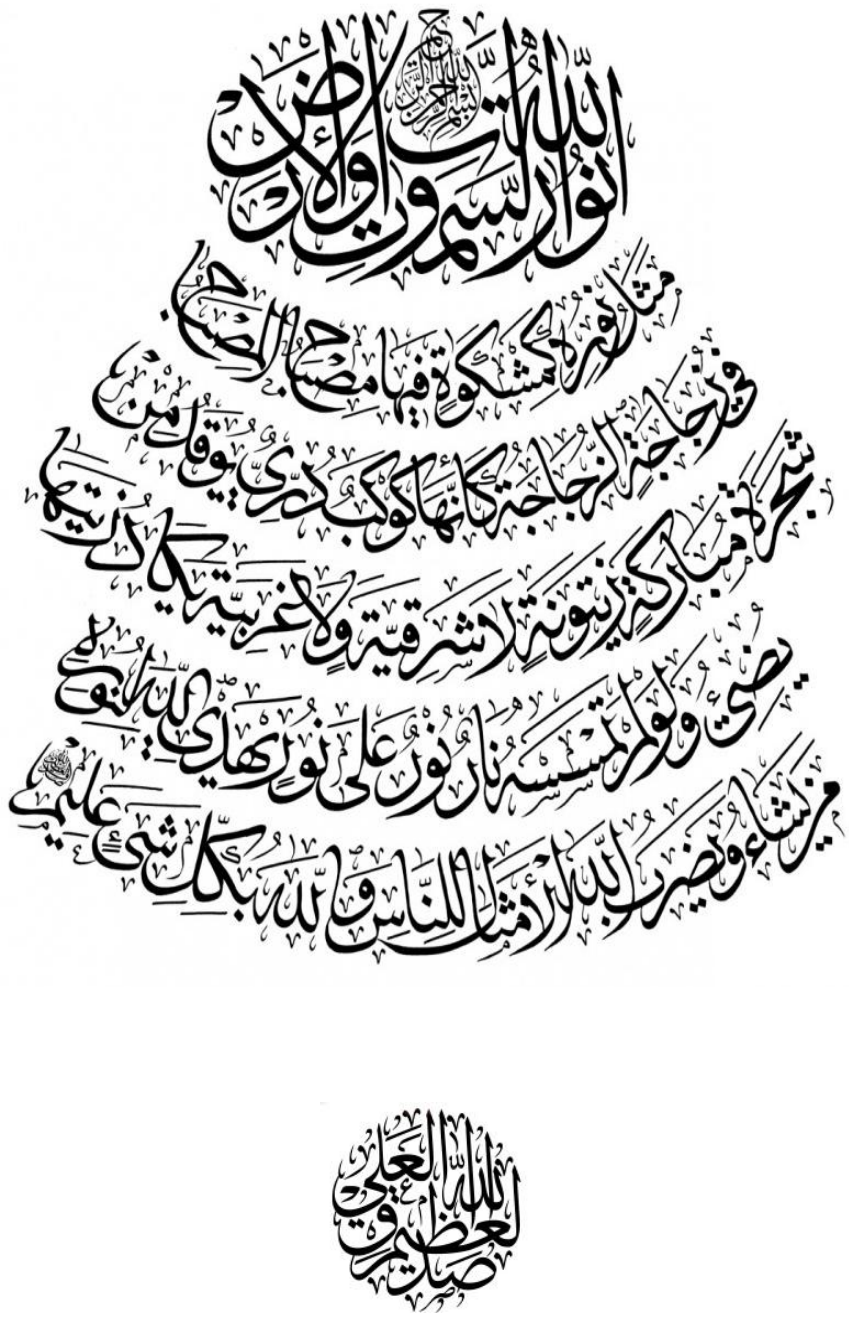
الله نور السموات والأرض
مثل نوره كمشكوة فيها مصباح المصباح
في زجاجة الزجاجة كأنها كوكب دري يوقد من
شجرة مباركة زيتونة لا شرقية ولا غربية يكاد زيتها
يضيء ولو لم تمسسه نار نور على نور يهدي الله لنوره
من يشاء ويضرب الله الأمثال للناس والله بكل شيء عليم
لله العظيم صدق العلي

Dedication

To the greatest person that Allah has ever created,
Prophet Mohammad peace be on him.

To the best person that Allah has ever created after His Prophet,
Imam Ali peace be upon him.

To those who have all the credit on me, to those who were the cause of my existence, to my beloved **parent**.

To my **brothers**, my **wife** and my **friends**...

To all who supported and encouraged me to achieve my success.

Acknowledgment

Before everything, I would like to express my gratitude to Allah Almighty for His kindness and mercy and for giving me the opportunity to complete my study.

I would like to appreciate the extraordinary efforts and advices of **Asst. Prof. Dr. Ali A. A. Al-Bakri** and **Asst. Prof. Dr. Ahmed K. A. Al-Bakri** who had the greatest impact in fulfilling the requirement of the present study.

I would like also to thank **Asst. Prof. Zainab Hasan, Eng. Baha'a Hamza** and **Eng. Mohammad Jawad** for helping me to complete this thesis.

Finally, I would like to express my thanks to my family for their patience and for supporting me during the study period.

Supervisor Certification

We certify that this thesis titled **"Enhancement of Twins Fetuses ECG Signal Extraction Based on Modified Stone Blind Source Separation Technique"** which is being submitted by **Mushtaq Talib** was prepared under our supervision at the Communication Techniques Engineering Department, Engineering Technical College-Najaf, AL-Furat Al-Awsat Technical University, as a partial fulfillment of the requirements for the degree of Master in Communication Techniques Engineering.

Signature:
Name: **Asst. Prof. Dr. Ali A. A. Al-Bakri**
(Supervisor)
Date: / / 2019

Signature:
Name: **Asst. Prof. Dr. Ahmed K. A. Al-Bakri**
(Supervisor)
Date: / / 2019

In view of the available recommendation, we forward this thesis for debate by the examining committee.

Signature:
Name: **Dr. Salem M. W.**
(Head of Communication Tech. Eng. Dept.)
Date: / / 2019

Committee Report

We certify that we have read this thesis titled **" Enhancement of Twins Fetuses ECG Signal Extraction Based on Modified Stone Blind Source Separation Technique "** which is being submitted by **Mushtaq Talib** and as Examining Committee, examined the student in its contents. In our opinion, the thesis is adequate for award of Master degree in Communication Techniques Engineering.

Signature:
Name: **Asst. Prof. Dr. Ali A. A. Al-Bakri**
(Supervisor)
Date: / / 2019

Signature:
Name: **Asst. Prof. Dr. Ahmed K. A. Al-Bakri**
(Supervisor)
Date: / / 2019

Signature:
Name: **Asst. Prof. Dr. Bashar J. Hamza**
(Member)
Date: / / 2019

Signature:
Name: **Asst. Prof. Dr. Faris Mohammad Ali**
(Member)
Date: / / 2019

Signature:
Name: **Prof. Dr. Adheed Hasan Sallomi**
(Chairman)
Date: / / 2019

Approval of the Engineering Technical College- Najaf

Signature:
Name: **Asst. Prof. Dr. Ali A. A. Al-Bakri**
Dean of Engineering Technical College- Najaf
Date: / / 2019

Abstract

One of the most used traditional methods for measuring heart conductivity is the fetal Electrocardiography. Many indicators related to the health of fetal can be determined depending on FECG since fetal heart rate (FHR) is obtained from the components of FECG signal. Recording fetal ECG in a clinic forms a problem due to the interferences of other signals which corrupt the ECG signal. Another problem happen as a result to the location of the used electrodes for recording ECG since these electrodes are placed on the mother abdomen. The obtained abdominal ECG signal also contains different types of interferences.

The maternal ECG (MECG) represents the first big interference source with the FECG signal. Breathing, activity of mother's muscle, electrode contact with the mother's skin, power line interference and thermal noise represent a possible noise source. In case of extraction ECG signal for twin gestation, clear FECG for every fetal would be more difficult because in addition to the all mentioned sources of interferences and noise, both fetuses may share the same morphology and FHR. Close monitoring to the heart of twin is required for early diagnose of congenial problems which infect heart.

Signal separation techniques such as blind source separation (BSS) are used to overcome the artifact problem by separate the artifacts from ECG mixture as independent components. The BSS is a method of separating the underlying sources from their mixtures without or little information about the original sources or the mixing process.

In this thesis extraction of FECG, specially for single and twin case, will be discussed. The obtained results is divide into two parts.

The first part of the results discuses the extraction of single and twin fetuses ECG based on Stone blind source separation. The obtained

results by Stone algorithm are compared with other two BSS algorithms (EFICA and JADE).

The second part of the results is obtained by the Modified Stone Blind Source Separation (MSBSS). A combination between conventional Stone BSS and Particle Swarm Optimization (PSO) have been used for producing (MSBSS). The obtained results are compared with other two BSS algorithms (EFICA and JADE) in addition to the obtained results using conventional Stone BSS in part one. MSBSS method has revealed better performance comparing with the other BSS techniques including Stone BSS.

Table of Content

List of Figures

List of Figures

List of Tables

Nomenclature

Symbol	Definition	Unit
$\bar{C}_{LXX}$	Long-term covariance matrix	----
C_{xx}^{long}	Long-term covariance matrix	----
C_{xx}^{short}	Short-term covariance matrix	----
A	Mixing matrix	----
c_1, c_2	Acceleration coefficients	----
F(y)	Temporal predictability of signal y(k)	----
h_{long}	long-term half parameter	----
h_{short}	Short-term half parameter	----
V	Eigenvector matrix	----
W	Separation Matrix	----
w	Inertial coefficient	----
X_L (k)	Filter Response (Long)	----
X_S (k)	Filter Response (Short)	----
β_L	Long-term constant value	----
β_S	Short-term constant value	----
S(t)	Original signal sources	----
X(t)	Observed signal	----
$\tilde{C}_{S\,XX}$	Short-term covariance matrix	----

Abbreviations

Symbol	Description
BPF	Band Pass Filter
bpm	Beat Per Minute
BSS	Blind Source Separation technique
ECG	Electrocardiogram
EFICA	Efficient Fast-ICA
EMG	Electromyogram
FECG	Fetal Electrocardiogram
FHR	Fetal Heart Rate
FICA	Fast-Independent Component Analysis
GEVD	Generalized Eigen Value Decomposition
HR	Heart Rate
HRV	Heart Rate Variability
ICA	Independent Component Analysis
ISR	Interference Signal Ratio
JADE	Joint Approximate Diagonalization of Eigen
MECG	Maternal Electrocardiogram
MHR	Mother Heart Rate
MSBSS	Modified Stone Blind Source Separation
PLI	Power Line Interference
PSD	Power Spectral Density
PSO	Particle Swarm Optimization technique
SNR	Signal to Noise Ratio
SVD	Singular Value Decomposition
TTTS	Twin - Twin Transfusion Syndrome
WGN	White Gaussian Noise
eig	Eigen Value

List of Publications

1) Mushtaq Talib, Ali A. Al-bakri and Ahmed Kareem Abdullah, "Enhancement Separation of ECG signals for Twin Fetuses Based on modified Blind Source Separation," IEEE International Conference (4th-SICN), 2019.

2) Mushtaq Talib, Ali A. Al-bakri, Ahmed Kareem Abdullah and Bahaa Hamza, "Twin Fetus ECG Signal Extraction Based on Temporal Predictability," Kufa Journal of Engineering, Vol. 10, No. 3, P.P. 1, 2019**.**

Chapter One

Introduction

CHAPTER ONE
Introduction

1.1 Background

Observing fetal through Electrocardiogram (ECG) provides the necessary information to check on the status of the fetal. There are two methods to get the fetal electric diagram Fetal Electrocardiogram (FECG). Invasive and non- invasive, in case of invasive labors are used to connect the electrodes to the head of the fetal (scalp) inside the uterus where the signals record directly from the mother abdomen. Non- invasive ECG recording can be classified as an external ECG collection method. This method can be done in any stage of the pregnancy by using tens of electric labors place on mother abdomen. The recorded signal by the invasive method of a higher quality compared with non- invasive. However, this procedure sometimes not suitable to get The (ECG) and is used only to record during parturition. Generally speaking, lower SNR for FECG and interference as result of Mother Electrocardiogram (MECG), base line wonder, power line interference (PLI), random electric noise and Electromyogram (EMG) of wide frequency noise could be the conditions to reduce the use of non- invasive ECG [1].Between 6 to 22 weeks of the fetal age echocardiograph provides 25 - 60% of the heart major defects and does not give enough information about the cardiac system. Besides, all ultrasonic techniques require professional and trained physical technicians and it is also cannot be done in home [2][3]. Figure 1.1 below shows the invasive and noninvasive ECG.

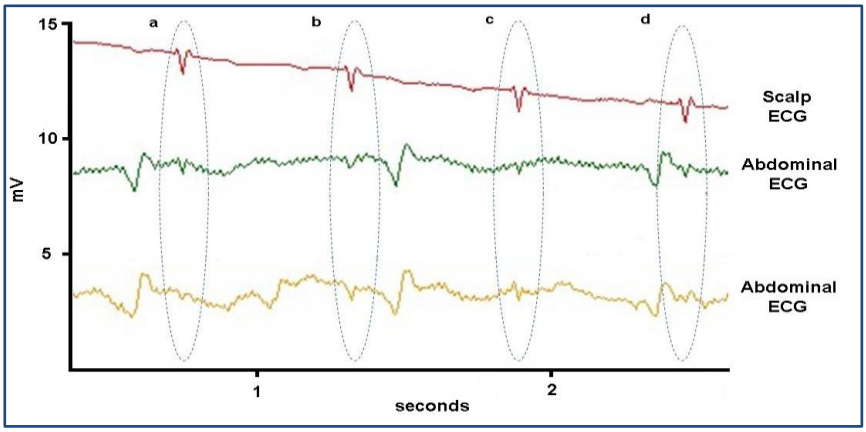

Fig. 1.1 The difference between invasive and non-invasive ECG signal [2]

The electrocardiogram (ECG) could be the best choice to measure conductive signals of heart and can be obtained by putting electrodes on the mother venture. The basic components of ECG is a set of standard waves (P, Q, R, S and T). Fetal ECG permits to determine the fetal heart rate (FHR) and other features like the morphologic ones. One of the most important indicators that could give us an idea about the fetal heart activity is the relative amplitude and timing related to ECG signal like (P/R, Q/R, S/R,R-R interval and T/QRS ratio which gives us information about (FHR). T/QRS is useful to determine some cases like tachycardia (FHR>180 b.p.m) or branchy cardiac (FHR<110 b.p.m) [4]. By monitoring P-R and R-R interval along ST segment, the lack of oxygen "hypoxia" that infects the fetal could be revealed [4]. A comparison between FECG and other biomedical signals has been made as illustrated in Fig. 1.2 that also shows how the amplitude and frequency of FECG is weak as compared to the other signals. Figure 1.2 also shows how difficult to separate the FECG signal from interferences with other signals since it has no limited domain (frequency, time and features).

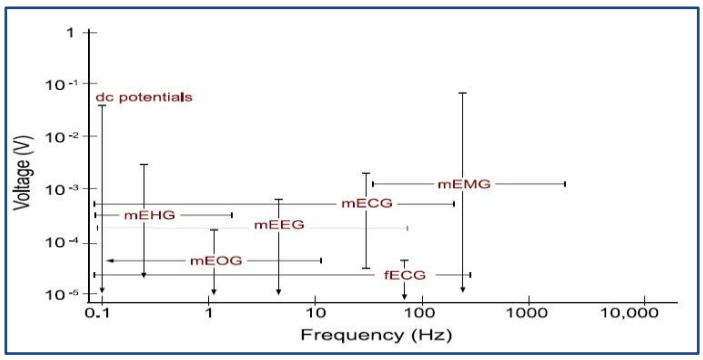

Fig. 1.2 Some biomedical signals that affect on Fetal ECG [2]

Figure 1.3 shows the location of (QRS complex which represent the main part of the signal) among the mother QRS complex and in-vivo signals.

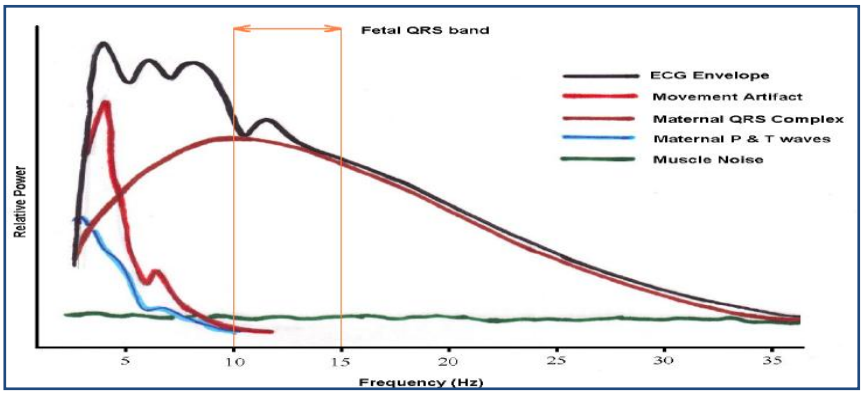

Fig. 1.3 Location of QRS band of fetal ECG among other band frequencies [2]

1.2 Motivation

Obviously, ECG seems very attractive to be used, but formerly the use of ECG in clinics was very limited because of the shortage in clinical technology in reading and displaying that signal. Besides, the FECG is an abdominal ECG that contains many interferences where as the recorded signal would be the mix of many signals due to the bioelectric phenomenon. This phenomenon is caused by breathing, stomach activity and muscles activity. The ECG also is affected by different types of noise like thermal noise, noise caused by electrode –skin contact, electronic

noise and power line interference. The problem would be more complicated in twins case as they may have the same morphology, amplitude and FHR [5]. Frequent use of the reproduction technology like IVF that results in identical twins with 40% percentage gives the observation of fetal ECG more importance. From 9 to 10 cases of the increasing in heart defects that are recorded for gestation of twins are caused by twin- twin transfusion syndrome (TTTS). For example (TTTS) both fetuses are susceptible to heart failure. Thus, this condition needs synchronized monitoring for heart side effects to every fetal so to highlight some signs, like cardiac overload and any other defects. Due to the mentioned reasons there is persistent need to find a method for processing the signal so as to extract and enhance FECG and.To highlight how this field of science is fresh and thus encourages researchers to further investigate it, a statistical survey for the published researches on the extraction of fetal ECG has been made depending on PubMed, which registers the published researches in this field as shown in Fig. 1.4.

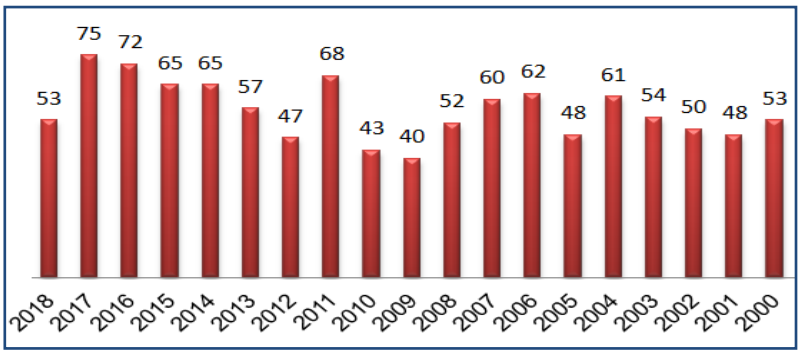

Fig. 1.4 Numbers of the published literatures on fetal ECG extraction in each year according to the statistics prepared by PubMed [6]

1.3 Problem Statement

1- Generally the current methods that are used to observe fetal inside the intrauterine does not give a comprehensive evaluation to the fetal hygienic case.

2- Observing fetal heart, specially observing heart functions become more complicated in the case of the twins pregnancy. As a result of the case of twins gestation, defects increase.

3- Extract ECG signal for each fetal is very difficult since its interfere with may signals like MECG, EMG, PLI as well as the fetuses signal share the same signal features. All the mentioned reasons represent a real problem to have clean ECG signal for fetal.

1.4 The scope of work

Figure 1.5 demonstrate the scope of work which is related to this thesis.

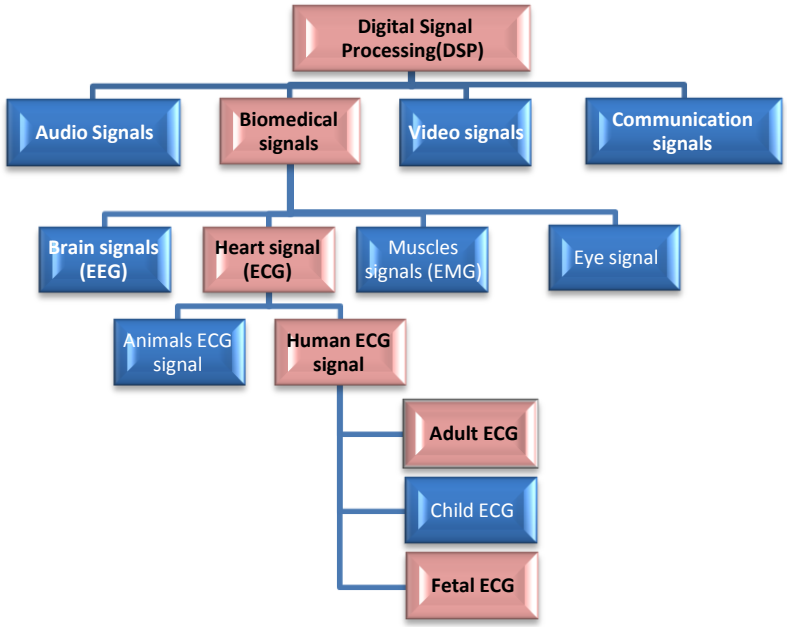

Fig. 1.5 Scope of work

1.5 Objectives

The main objective of this thesis is to extract clean fetal ECG as far as possible for twin fetuses and for mother ECG as well from mixture signals of common artifact and interferences using modified blind source

separation (BSS). The evaluation of modified BSS algorithm is primarily evaluated using different Probability Density Function (PDF) sources (Gaussian, Sub-Gaussian and Supper Gaussian noise) and then tested with simulated and real ECG data.

1.6 Thesis Contribution

- Stone BSS algorithm has been used for the first time to process and extract the fetal ECG signal for single and twin case gestation.
- A new method has been done based on Particle Swarm Optimization technique (PSO) to obtain the suitable values for the parameters of Stone algorithm which controls over the algorithm performance to extract the best signal quality for F-ECG.

1.7 Thesis Layout

Chapter Two : It gives a general background about ECG, Fetal heart features, general introduction for the blind source separation technique and Particle Swarm Optimization (PSO). It covers the literature review of the previous related works.

Chapter Three : It tackles the general description of Stone BSS technique, PSO and our contribution of the method of merging between Stone BSS and PSO technique.

Chapter Four : It highlights the obtained results for the different cases.

Chapter Five : Conclusion and suggestions for future work are presented in this chapter.

Chapter Two

Theoretical Background and Literature Review

CHAPTER TWO
Theoretical Background and Literature Review

2.1 Introduction to ECG

Placing electrodes on human skin allows to record every tiny change "electrical change" that happens due to the electrical activity of the heart muscles. The recording must be in specific time period. The electrical activity comes from the electrocardiographic. The electro physiologic is constructed from depolarizing and re-polarizing of heart during each beat[7].

There are ten electrodes that used to record ECG for human by placing that on chest and limbs. By ECG it is too easy to detect any problem in heart operation. To measure the magnitude of heart, 12 different angles "lands" utilized to satisfy these purposes. The used period of time to record ECG is usually equal to ten seconds. Through this cardiac cycle, the general size of heart and direction of depolarization would be captured [7].

Graphically, the relation between voltage potential and time generate non-invasive medical ECG. ECG is constructed from three major components. P, QRS and T-wave. Depolarization of atria controlled by the P-wave. Depolarization of ventricles controlled by the T-wave [7]. For more clarification, waves are disassembled into small following components:

- O: represents the start point of ECG signal;

- P: this pulse is responsible for shrinking of the atrial systole;

- Q: represents the deflection that comes before ventricular contraction;

- R: the maximum height that the ventricular contraction will reach;

- S: represents the deflection that comes after ventricular contraction;

- T: represents ventricles refresh;

- V: it is so small and can be neglected; it represents the success of T-wave[7]. Figure 2.1 shows the ECG signal components.

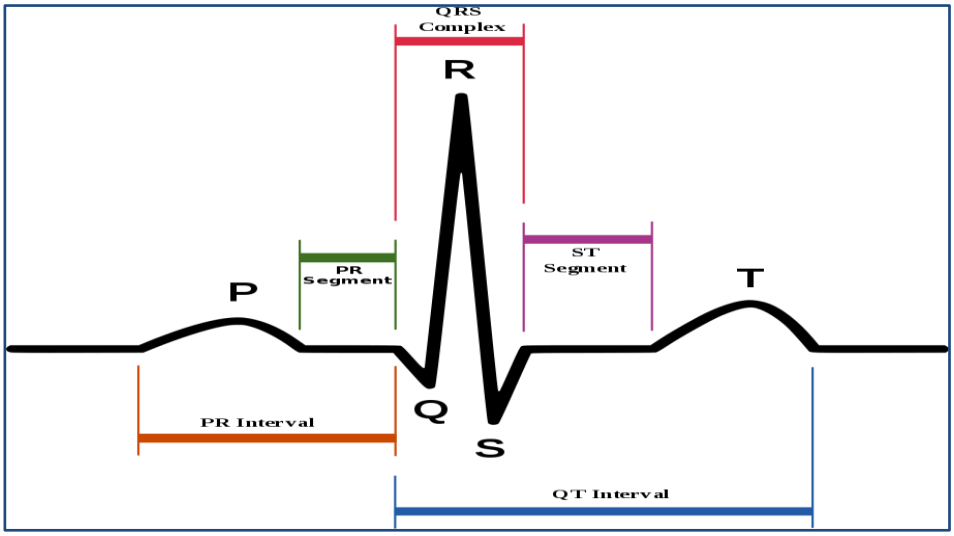

Fig. 2.1 The general form of ECG signal [7]

2.1.1 ECG History

The origin of ECG word comes from Greek word 'electro', which refers to the relation between the word and the electrical activity of heart. The word 'Kardia' in Greek, specially for heart, means write and graph. In 1872 and exactly at St. Bartholomew's hospital, Alexander Muirhead linked the wrist of a patient suffering from fever, with wires to record his heart beat. In St. Mary's Hospital in London, Augustus Waller made the first successful attempt to produce machine for recording heart beat rate. His electrocardiographic machine consisted of Lippman poetical electrometer. The result on photographic plate that was placed on a toy and that toy was a train. Augustus machine allowed to record ECG for the first time on real time [8]. In 1901, Willem Einthoven invented the first

practical ECG device. He used sting galvanometer instead of capillary electrometer. The galvanometer was more sensitive than the capillary electrometer[9]. The letters (P, Q, R, S and T) were assigned by Einthoven in 1895 to point to the deflection theoretically in the wave form. He assigned these letters using equations for correcting the real wave form of signal that was captured by capillary electrometer. The equations were used to compensate the error comes from the instrument of capillary electrometer[9]. Einthoven described the features of ECG and thus he got Nobel Prize in Medicine in 1924 for his discovery [9]. In 1927 General Electric Company developed a new generation of ECG device. The device was portable and didn't use galvanometer. It used amplifier tube which is similar to the one used in radio, lamb and moving mirror. The role of moving mirror was to derive electrical pulse on a film [9]. By 1937 Taro Takemi invented a new ECG device [9]. In spite of the big development in science, the principles of ECG which were invented in the past are still being use today. The electrocardiographic has developed from big machine hard to work to portable electronic small device. Figure 2.2 demonstrate the first ECG device.

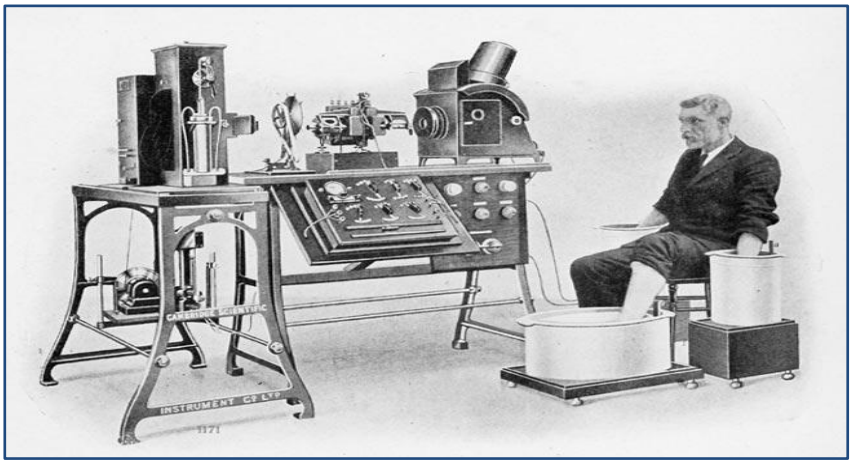

Fig. 2.2 The first commercial device allocated to record heart signal [9]

2.1.2 ECG medical uses

The general purpose of obtaining ECG is to gain as much as possible information about the structure, function and activity of heart. ECG explains and diagnoses any defect that affects heart. ECG must be available to provide information that helps to make decision. Here come some indications about what ECG diagnoses [10]

- Myocardial infarction which is known as heart attack or chest pain.
- STEMI: (ST elevated myocardial infarction).
- (NSEMI): (non-ST elevated myocardial infarction).
- Pulmonary embolism and hard breathing.
- The disease of structural heart.
- Diagnosis arrhythmia by pulse or palpitations.
- Diagnosis collapse or fainting.
- Seizures.
- Check if any medication has any effects on heart.
- Evaluate electrolyte abnormalities like hyperlcalmia.
- Monitoring hypertrophic cardiomyopathy in teenagers to reduce the case of sudden death.
- Monitoring heart during any surgical operation which requires any kind of anesthesia.
- Evaluate the status of patient before any surgical operation, specially for people who already suffer from heart defect.
- CST (cardiac stress testing).
- CTA (computed tomography angiography).
- MRA (magnetic resonance angiography).

2.1.3 The device of Electrocardiographs:

One of the non-surgical devices is the electrocardiograph. This device is used to register every tiny electrical change that arrives to the surface of human body which is generated from the electrical activity of heart. This process will produce electro cardiodiagram [10]. Electrocardiograph consist of amplifier, which is responsible for computing the difference in voltage among leads and starting to amplify the signal of ECG. The range of voltages is measured in micro volts (from 1 to 100 μv). the low voltage level that the ECG signal comes with requires the use of some specific circuit that has low noise and has instrumentation amplifiers as well. Previously, ECG devices used motor which helps the ECG device to record the signal on paper. This mean that ECG device were contain developing in electronics. Development in electronic field leads to the use of analog to digital convertor to get the analog ECG signals into digital that helps to preview the ECG on computers. Below Fig. 2.3 is a simple block diagram of ECG circuit..

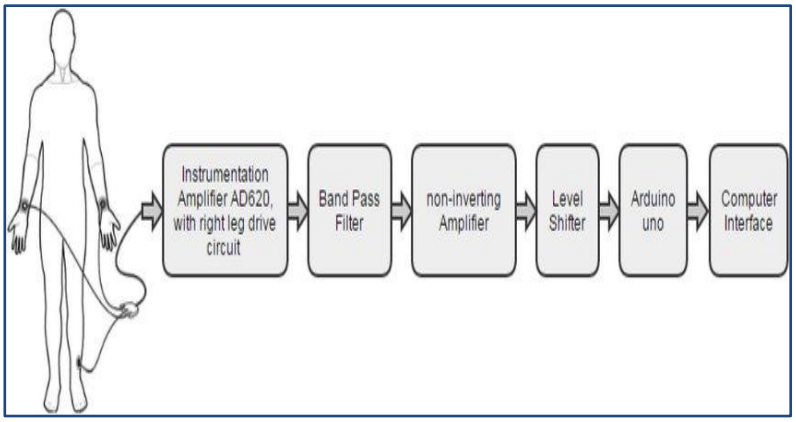

Fig. 2.3 The simplest block diagram of ECG circuit[10]

The following points illustrate shortly the role of every signal part in the simple ECG device.

- Electrode: it represent the first stage. It can be shortly describe as transducer which used to convert ECG signal to electrical voltage for the range of (1 to 5mv).
- Instrumentation amplifier: it has a very high CMRR equal to (90ds) and also own high gain power supply of the amplifier which is equal to +90v and -90v [10].
- B.P.F.: the band will be between 0.04Hz to 160Hz.

As the Fig. 2.4 shows, the complete ECG device hardware consist of screen, keyboard and printer. They all form the combined unit of ECG. Just like any electrical device, ECG device is connected to power supply. It also has long cables that connect the device with human body to record the signal [10].

Fig. 2.4 The modern ECG device

2.1.4 Electrodes location

Electrodes is the actual parts that connect human skin surface with the ECG device. Difference in electrical potential can be measured by pair of electrodes exactly by taking in concern them location. “Lead” term form by pair of electrodes, lead also can be formed by real and virtual electrodes forming lead form real and virtual electrode which are called the central terminal of Wilson [10].

To define Wilson’s potential, three limb electrodes are taken to measure the potential: left arm, left foot and right arm. Below Fig. 2.5 illustrate the electrode location on human body.

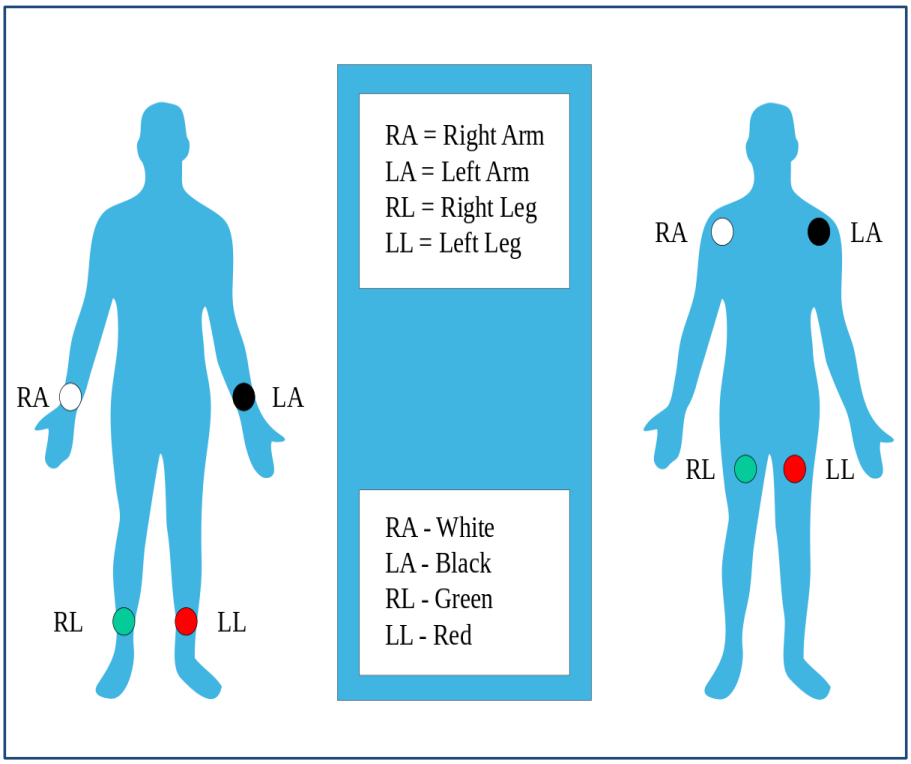

Fig. 2.5 Electrodes location over human body[10]

Generally, there are ten electrodes placed on human body to shape 12 ECG leads. The role of each lead is to record specific difference in the electrical potential. Lead can be classified into three kinds which are limb,

augmented limb and precordial. Sometimes the technicians in the medical field refer to lead as electrodes. This is technically incorrect and can cause confusion [10]. Table 1.1 demonstrate name and location of each electrodes. Figure 2.6 shows the real location for each electrodes over thorax.

Table 1.1 Name and location of each electrodes

Electrode name	Electrode location
RA	**Right arm**
LA	**Left arm**
RL	**Right leg**
LL	**Left leg**
V1	**Lie between rib four and rib five (4th intercostal) close to the breast bone**
V2	**Same as V1 location**
V3	**Its locate between V2 and V4**
V4	**Lie between rib five and rib six (5th intercostal)**
V5	**Left anterior axillary**
V6	**Mid-axillary**

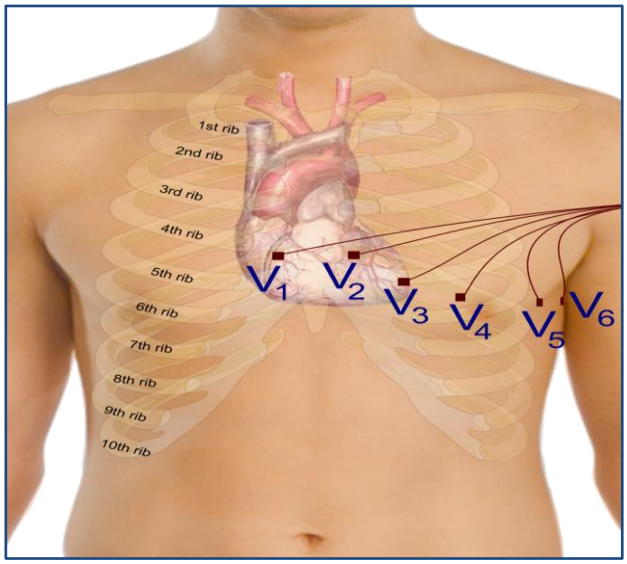

Fig. 2.6 Electrodes location over thorax[10]

The location of electrodes allocated for recording fetal and mother ECG differs from the electrodes location allocated to record normal human. The location changes as in Fig. 2.7. For better conductivity, special gel is placed on each electrodes. Gel gives flexibility to electron to travel between skin and the electrodes since it contains silver/silver chloride and also contains potassium chloride [10].

2.1.5 Obtaining Fetal ECG signal

There are two methods to obtain FECG either invasive method or non-invasive method. Invasive method is better than non-invasive because it has direct contact to the fetal skin as the electrode is placed on the fetal scalp and starts recording ECG directly [11].

This method needs specialists to implement because it requires inserting the electrode inside the mother uterus to reach the fetal. Non-invasive method does not need specialists to implement it because all electrodes are placed on the mother abdomen to record the FECG [11].

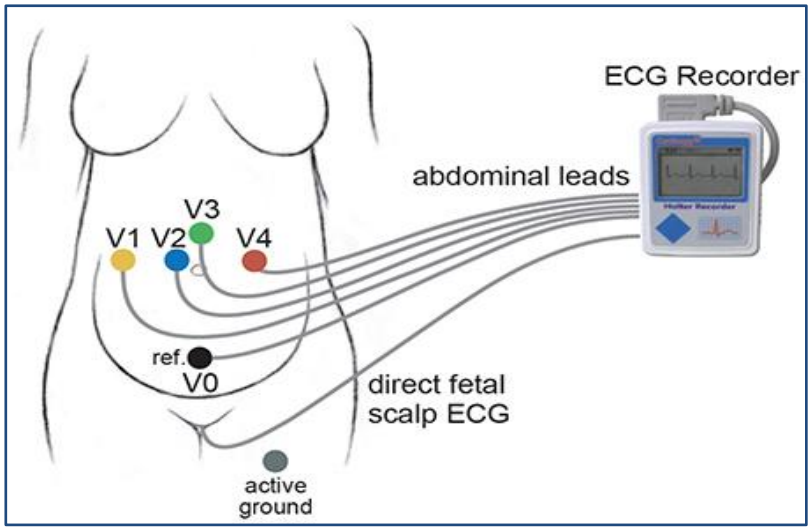

Fig. 2.7 Electrodes location over mother abdomen to record fetal ECG signal[11]

2.1.6 Open database of ECG

To get data of ECG it is too important to check few points in advance such as number of the used electrodes to collect ECG, type of electrodes, age of gestation and the data quality. The data quality mean" sampling frequency, amplitude and noise". The suitable sampling frequency is 2kHz and with 16 bit resolution. There is no specific location of electrodes but it is recommended to make them cover the abdomen of the mother as far as possible [2]. There are two available databases that are widely used by many researchers.

The first one is DaISy database. The recorded signal consist of 8 channels, three channels are placed on thorax for recording mother ECG and four channels are placed on abdomen to get fetal ECG signal. The data set is part of SISTA (Signals, Identification, System Theory and Automation) data set. The recorded ECG signal duration is equal to 10sec and is sampled at 250Hz. The SISTA data set belong to Kathilieke University Leuven, Electrical Engineering Department in Belgium [12].

The other database, which has been used in obtaining result and making simulation in this thesis, is PhysioBank. The recorded signal comes from two thoracic and four abdominal electrodes. The obtained signals are sampled at 1 kHz with resolution of 16 bit. This data set is prepared by Digital Signal Processing Group(DSPG) of Electronic Engineering Department, University of Valencia, Spain [13].

2.1.7 Other techniques used for measuring FECG

There are different techniques that have been used for measuring and monitoring FECG such as:

- Echocardiography: it can be classified as ultrasound technique. It is also known as Sonography [14].
- Phonocardiography: this type is classified as graphic registration to the sound of heart. The recorded signal is obtained from the vibration of the piezoelectric crystal microphone[15].
- Pulse Oximetry: this method is used for measuring the saturation of oxygen in fetal blood. An infra-red light is applied on the skin of fetal to record the amount of oxygen in the fetal blood[16].
- Cardiotocography: method in uterine contractions, this is used for measuring strength and frequency and as a result for this operation FHR would be recorded as well[17].
- Magnetocardiography: this method depends on the calculation of magnetic fields that surround the cardiac signals [18].

2.1.8 The amplitude and internals of ECG signal

All waves of the ECG signals have specific duration of time which separates them. Also they have an amplitude which is acceptable to make the ECG measuring easy. The signal will be printed on grid papers with standard scale. The table 2.2 below illustrates each wave and its duration. It also describes the interval and duration of the ECG components [10].

Table 2.2 The interval and duration of the ECG components

Waves and intervals	Demonstration	Duration
P- wave	**Responsible for shrinking atrial systole, start from SA node toward the AV node (depolarization).**	**Less than 80ms**
PR interval	**Its starts from P-wave and the start point of QRS would be its end.**	**From 120 to 200ms**
QRS	**It represents the quick depolarization for heart and it is caused by the right and left ventricles.**	**80 to 100ms**
J. point	**This point lies between QRS and ST segment. This point determine the start of ST segment and the end of QRS.**	
ST. segment	**Is the link that join QRS with T-wave. It happens when ventricles are depolarized.**	
T-wave	**Denotes to re-polarization of ventricles.**	**100ms**
QTc interval	**It is named as corrected QT. It starts from the beginning of QRs and ends when T-wave finish.**	**<440ms**
U-wave	**It has very low amplitude and always not touchable.**	

2.2 The artifacts

Sometimes mistakes can occur in ECG tracing due to specific motion like patient shivering for example. The patient motion can create wrong diagnosis of cardiac arrhythmia [19]. The artifacts is distorted signals which happen due to the interference between two or more signals. The signals may be internal like in-vivo signals or external like electrical devices[19]. The effect of the artifacts signals are regarded as a big

challenge for the health specialists in extracting pure ECG signal [19]. For fetal ECG, the mother ECG can be an artifact signal in addition to the other artifacts signals as well.

2.3 Noise affecting on ECG signal

There are many different signals that affect ECG extraction such as:

- Power line noise (PLI) : this kind of noise happens due to the electromagnetic interference. Electromagnetic field is caused by equipments, alternating current in cables and ECG equipment and patient miss grounding produce harmonic signal of 50 – 60 Hz. Equipment that consumes heavy current like X-ray, lifts and air conditioners can generate large amount of PLI and could be the best example of PLI generation tools[20].

- Electromyogram (EMG): This type of noise is generated by the muscle activity of human body and here we are pointing exactly to the electric muscle activity. EMG has a maximum frequency that is equal to 10 KHz[20].

- Baseline wonder : This type of noise is coursed by human breathing and it has low frequency exceeding 1 Hz. It has no touchable effect on (ECG) but can only affect the peak analysis [20].

- Electrode contact with skin : this type occurs as a result of losing contact between the electrode and the skin. It gives delay duration of 1 second [20].

- Channel noise : this kind of noise has all frequencies components. It looks like white Gaussian noise and occurs as a result of the channel condition poverty which transmit the signal between patient and the equipment that records ECG[20].

- The device that collects data : this noise happens due to hardware that processes the signal [20].

- Artifacts : in this type we specifically mean motion artifacts. It occurs when electrode moves and changes its position. This leads to changing electrode skin impedance and when the impedance changes the ECG amplifier will notice various source impedance. This change in impedance will creates voltage divider. Voltage divider influences on the ECG since the amplifier input depends on impedance [20].

- Electrosurgical noise : it has no large duration, it lasts from 1 – 10 sec..It is caused by different medical equipments that surrounds the place in which the ECG is recorded. It has frequency between 1-10 MHz [20].

2.4 The development of fetal heart

The first part of the fetal body that starts to develop is the heart. It becomes functional early 3-7 weeks after fertilization. This stage could be the most critical and dangerous one of heart development as the heart shape would be a tube with four chambers. the fetal heart begins beating in 22 days and starts bumping blood through closed circular system. The fetal blood type may differ from the mother's blood. After four weeks of fertilization the other parts of the fetal body starts shaping like ears, eyes

and respiratory system. The uterus sound photograph could be used to observe fetal heart during 7-9 weeks of conception but this technique is poor to determine the heart and the shape of hearts waves [19]. In week 20, fetal heart beats could be heard without the need of the amplification and the heart beat rate of fetal would be from 120 to 160 beats/minute [19]. Mother and fetal ECG have morphology information about the heart activity. This signal could be recorded directly from the mother abdomen in the 18^{th} to 22^{th} week after conception. Fig. 2.8 shows the location of fetal heart while Fig. 2.9 demonstrate the stages of fetal heart development.

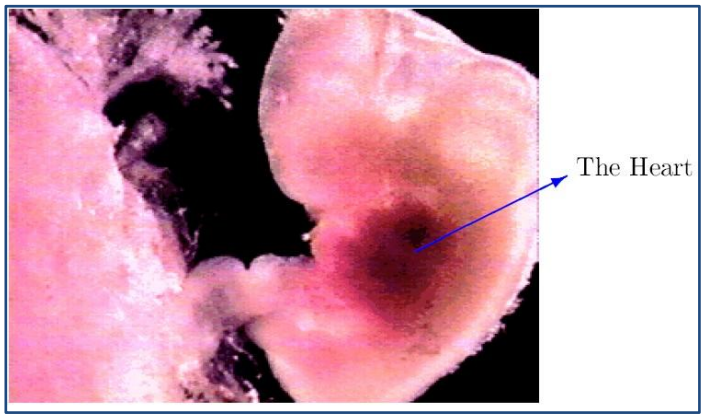

Fig. 2.8 Fetal heart location[21]

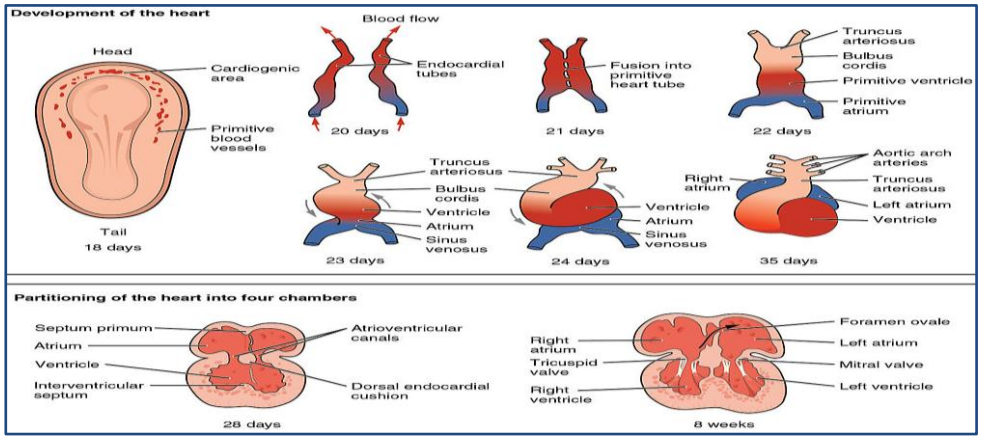

Fig. 2.9 Fetal heart development [21]

2.4.1 Fetal heart anatomy

Fetal heart beats differs from that newborns heart beat because of the difference of the circulatory system. Until birth the fetuses does not need to use its lung so the fetal heart does not pump the blood to the lung to get oxygen, Rather it get the oxygen from the placenta that connects the fetus to its mother. In other words, the fetus does not need to separate between pulmonary artery and aorta. There is blood vessel called ducts arteriosus which connects both vessels [19]. The channel closes in short time after birth. Thus the pulmonary artery and aorta will be separate. The blood travels from mother to fetus stops after disconnecting the placenta. Accordingly, the cardiovascular system and the pulmonary system start to work [19]. Figure 2.10 shows the anatomy of fetal heart.

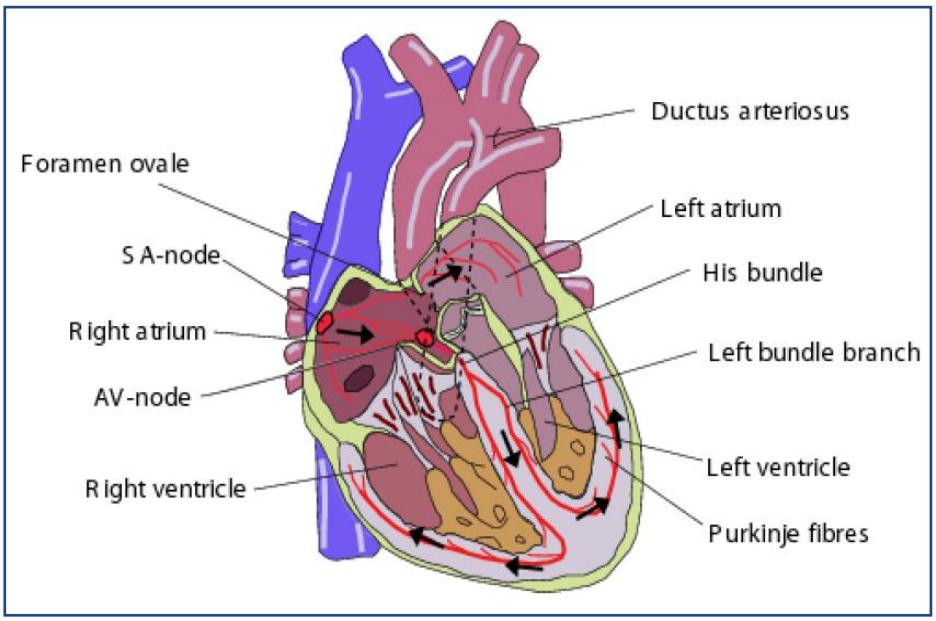

Fig. 2.10 Fetal heart anatomy[19]

The fetal heart activity is similar to adult heart activity, but with little difference in mechanical functions.

2.4.2 Fetal heart electrical activity

There are networks of neural fibers distributed over heart muscle that control the waves related to pumping blood. It also coordinates the contraction and relaxation operation of heart. The SA- node, simply, is set of cells located on the back wall of the right atrium in the right upside which motivate the heart muscle to work. It sends electric pulses to heart muscle that starts the heart beat forming the natural system of heart beating [14]. These pulses lead to more motivation to another cells set called AV node that are located on the down side to the back wall of right atrium [19]. Removing fibers polarity of the ventricular muscles occurs after some delay and through the purkinje. The complete blood circulation is a sequence of heart muscle contract (systole) and heart muscle relax (diastole) which allows the delivery of blood to the pulmonary system [19]. Figure 2.11 clarifies how typically the ECG signal is generated.

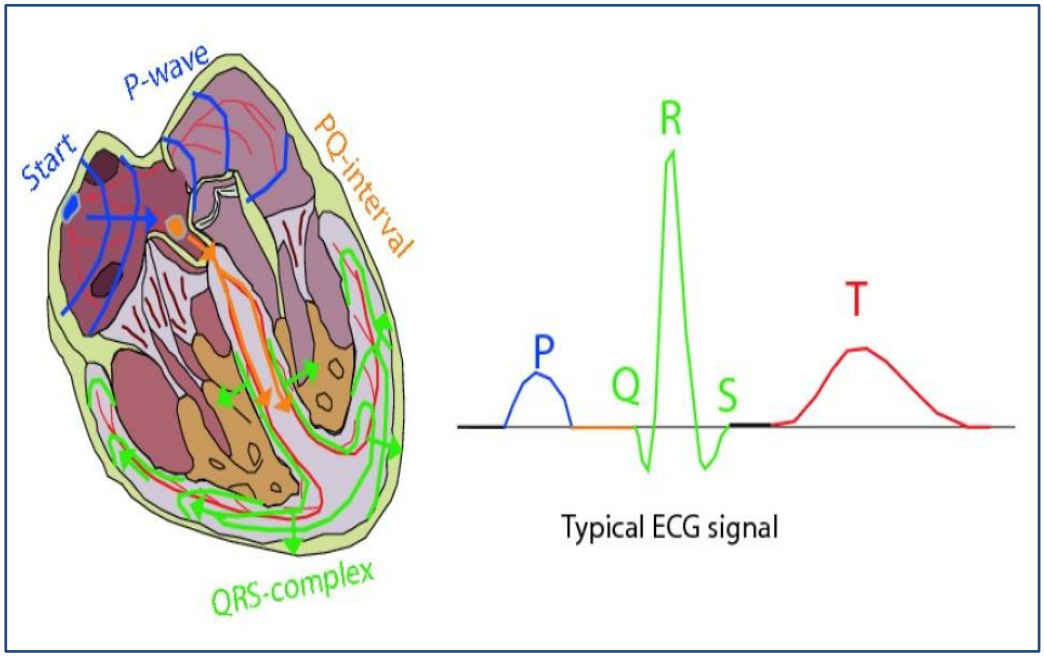

Fig. 2.11 Fetal heart cycle [19]

2.4.3 The morphology of electrocardiogram

ECG measures the electric signal of heart that reaches the surface of body. This signal happens as a result of myocardium activation and it is called PQRST complex. These letters were invented by Einthoven in 1895 [10]. P-wave, is responsible for shrinking the atrial systole; it starts from SA node toward the AV node. It is very weak recordable signal [10]. The next part of the signal will be QRS which represents the quick depolarization of heart and it is caused by right and left ventricles.

The final part of the signal is the T-wave. This wave occurs due to re-polarization of ventricles. There is a weak wave called U-wave. It is located in the end of ECG signal. It has very low amplitude and occurs as a result to the His-Purkinje system re-polarization [10].

The term isoelectrical segment has connection with U-wave. It can be defined as the segment that connects the U-wave of the finished one with the beginning of P-wave of the new one. In this segment the heart has no activity to measure[10]. Adults and fetuses share the same ECG patterns, but with only one difference in the amplitude of FECG since FECG is weaker than the adults ECG because of gestation conditions[10].

2.4.4 Fetal heart Rate (FHR)

Until now fluctuation in fetal heart rate and fetal heart rate variability (FHRV) have not thoroughly explained. Since the nervous system of fetus at birth may not be shaped completely. In spite of the fact that direct neural connection between mother and her fetus is not available, mother still indirectly able to affect the FHR and the pressure of blood. The influence of the mother reaches the fetus through hormones transmission (cortisol /catecholamines).

There is another way in which the effect of mother can reach the fetus. It is called the direct way. In this way, the effect travels by compromised placental vasculature or through blood [22]. Generally, the fetus has independent autonomic nervous system of its mother and connected indirectly as illustrated above [22]. FHR reach from 120 to 160 beats per minute (bpm) when fetus is 20 weeks. Fetal FHR differs from adult, and even children, because FHR changes during gestation [22].

The heart rate variability (HRV)for fetal is less dynamic as compared to adult. During the development of fetal nervous system the HRV pattern would be more complicated [22]. Figure 2.12 gives an example of HVR.

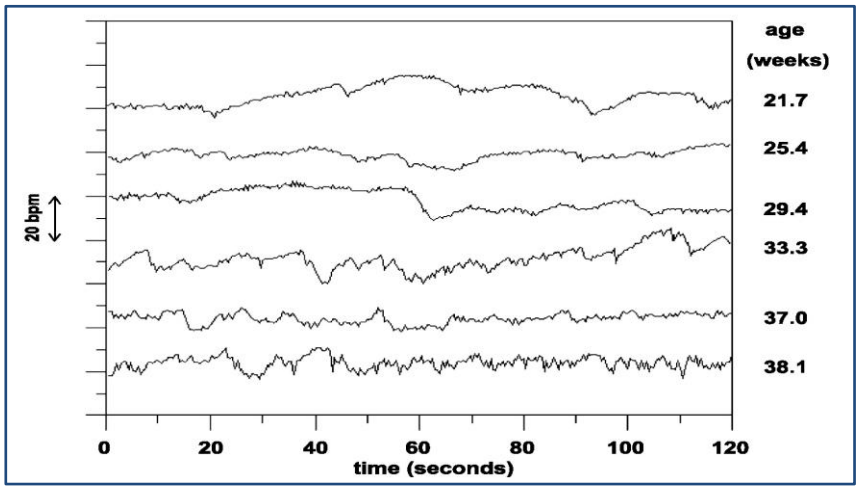

Fig. 2.12 HRV complexity [22]

Linshof and other scientists show that 73% of the studied fetuses are related closely to the tempo of mother HR[22]. Lange et.al., discovered that FHRV changes with the age of gestation and also changes with the mean of HR. They proved that gender and time of day don't have any influence on the FHR [22]. Another point must be taken in consideration is the fetal health since it has a direct effect on FHR.

2.5 Fetal components

The anatomy of fetomaternal components can be noticed in Fig. 2.13. The fetal appears to be surrounded by different layers (anatomical layers). Each layer has different electrical conductivity[21]. There are two layers that have the biggest effect on the conductive which are the amniotic fluid and vernix caseoa. They have the highest and the lowest conductivity and they fully surround the fetal. By concentrating on the mother abdomen we notice how the existence of fats under the skin which affects the conductivity, unlike the muscle tissue [21]. Since both skin and fat, which lie under the skin, have direct contact with the electrode that is responsible for recording FECG and due to the difference of their conductivity they will have the maximum effect on ECG collecting [21]. Because of the layers that surround the fetus, the volume of conductivity will be unsteady and will take a geometric shape. The conductivity changes during pregnancy. From the 20^{th} week forward the electrodes of ECG device are able to record FECG signals because the heart activity and amplitude of fetus will be higher than the previous weeks of fetal age.

From weeks 28 to 32, the vernix caseosa layer will be formed. Since this layer has a very low conductivity, it surrounds the fetus and tries to isolate it electrically. Thus, the process of recording fetal ECG would be more difficult [21]. This problem will vanishes by the weeks 37 to 38 of gestation [21].

Different studies have been carried out for enhancing FECG recording after vernix caseosa layer forming (during the 3^{rd} trimester of pregnancy) [21]. The studies are based on selecting optimum pathway like umbilical cord, during random holes in the vernix caseosa and oronasal cavity[21].

Some of the differences between adult ECG and FECG can be explained by taking into account the path that the FECG uses to reach electrode, intrinsic weakness and the gradually development of FECG[21].

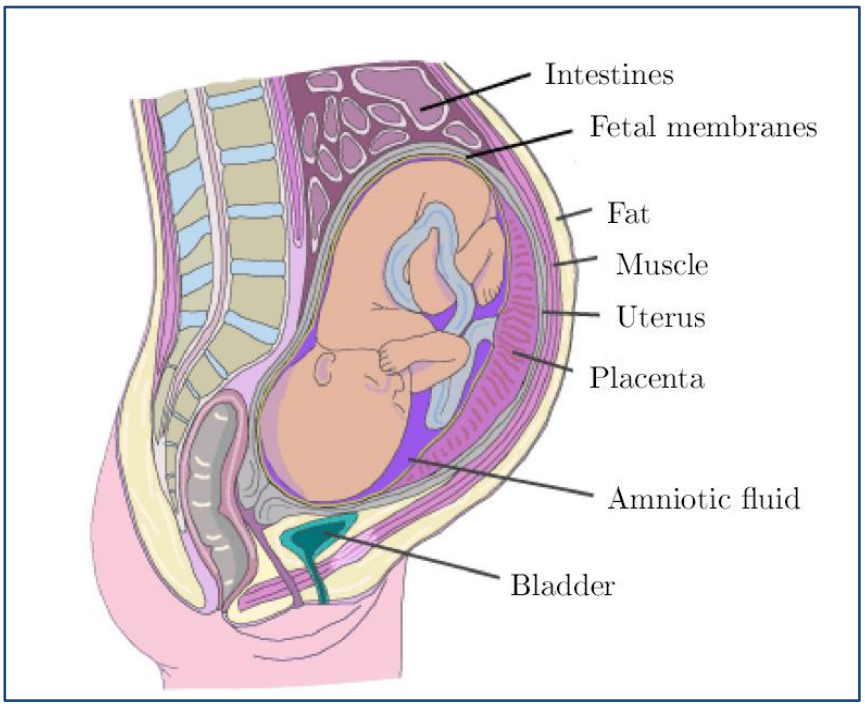

Fig. 2.13 The layers that surrounding the fetal Which affect on the ECG signal[21]

2.5.1 Fetus positions

The fetus don't have a specific position and moves a lot inside the uterus in the first two trimesters of gestation. The fetus takes the vertex position in the mid of 3rd trimester. In this position the head of the fetus are down and it looks like overturned. This position is very suitable for birth [23].

The position of fetus inside uterus influences the ECG recording since its position closes or outs away the fetal heart from the electrodes

[24]. There are many positions that the fetal will passes during gestation as illustrated in Figs. 2.14 and 2.15.

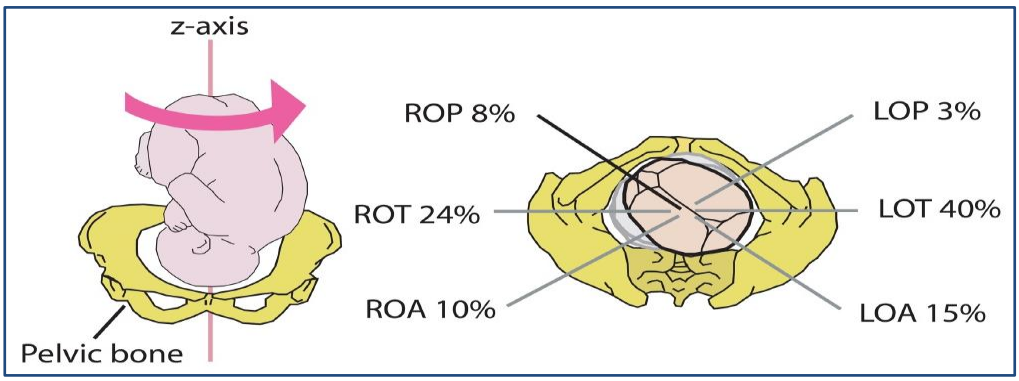

Fig. 2.14 Fetal positions in the last part of gestation where (R&L) represent left and right,(O) point to occiput, (A) mean anterior, (p) represent posterior and T denote to transverse[23]

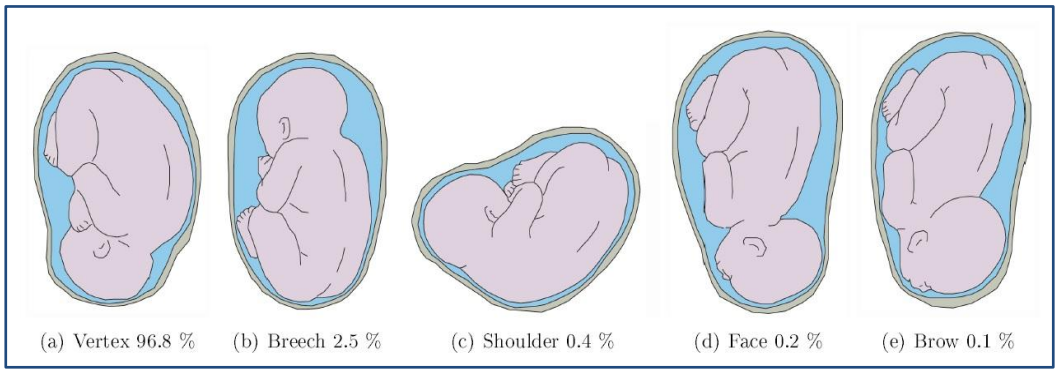

Fig. 2.15 Fetal positions in the last part of gestation [24]

2.6 Blind source separation (BSS)

It also called blind signal separation. Briefly it can be defined as separate set of signals that come from the mix of set of sources without any help or with very simple information about the source signal. Formerly researchers focused only on how to separate temporal signal like audio. Nowadays BSS is applied to many fields like images and tensors

which can be classified as multidimensional data and has no dimension of time[25].

Independent component analysis (ICA), irregular decomposition, principle component analysis stone's blind source separation ect. can be considered as algorithm to treat the problem of blind source separation[26].

ICA is the most used algorithm for solving the problem of BSS and it has been developed. Many algorithms are derived from ICA like FICA, EFICA, block EFICA [25].

2.6.1 The history of blind source separation

In 1980, the first blind technique had been presented. The word "blind" refers to the method since this method utilizes only the observation ability to record signal. In the beginning, the blind source separation technique was exploited to implement adaptive equalizer in the system of digital communication. In 1982, B. Ans, J. Heranlt and C. Jutten presented the first formulation of source separation[27]. In 1984, the problem of blind source separation was formed as a result of using higher-order moments for the approximation of matrix. After that many studies had been published to develop the solution of blind source separation problem [27].

2.6.2 BSS applications

In industry and academic field, BSS earned great interest, medical signal processing wireless communication system, remote sensing, image recognition and pattern analysis etc., all these fields are included BSS application [28].

Another field that the BSS technique is used in is radio communication system [28]. There are many other fields that the BSS technique have been used and can be found [28].

2.6.3 BSS classification

Generally BSS can be classified into two types. The classification of BSS technique depends on the training data. If the BSS comes with trained data then it is named as supervised BSS technique, and if it has no trained data then it is named as unsupervised BSS techniques (blind) [26]. There are three categories (linear/nonlinear, instantaneous/ convolution and underdetermined/ over complete) that are utilized to classify the unsupervised BSS technique [26]. Fig. 2.16 below illustrate the general classification of BSS.

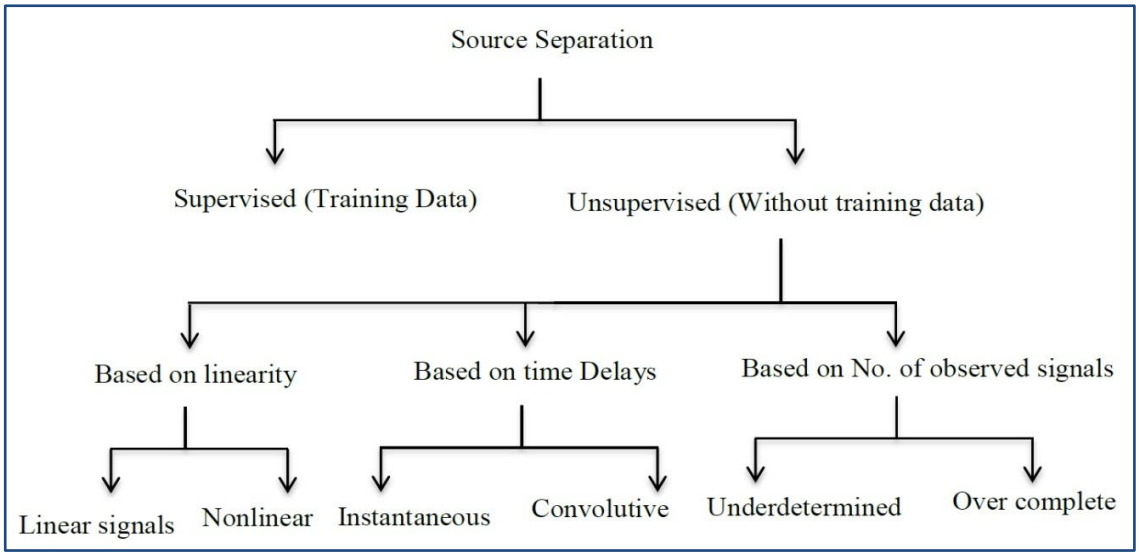

Fig. 2.16 The classification of Blind Source Separation [26]

2.6.4 Preprocessing

Preprocessing can be defined as the process of the data which precedes data entry to BSS technique. There are three preparing technique which are:

- **Centering process**: it simply means the sample mean of the received vectors will remove and add then to the original signal after recovering [29].
- **Whitening process**: It is the process of transferring the received vector to another vector. This transformation is done linearly. All whitened components will have unity variance and they are uncorrelated. The whitening matrix is then restored by the Eigen value decomposition convariance matrix [30].
- **Principle component analysis**: By choosing the components that must be used, and in specific cases, the dimensionality is introduced. Preventing "over learning" is one of this process duty[30].

Generally, the whole work of BSS algorithms can be summarized according to the following steps[31].

- Set the data to zero-mean;
- Whitening the data;
- Select randomly vector W to be initial vector. The selected vector represent column in the inverse matrix W that had been predicted;
- step of "fixed-point iteration" ;
- equalization;
- test the convergence if it is okay, continue and if it is not go back to step 4;

2.6.5 BSS design and mathematical representation

The general mathematical method of BSS is shown Fig. 2.17 below.

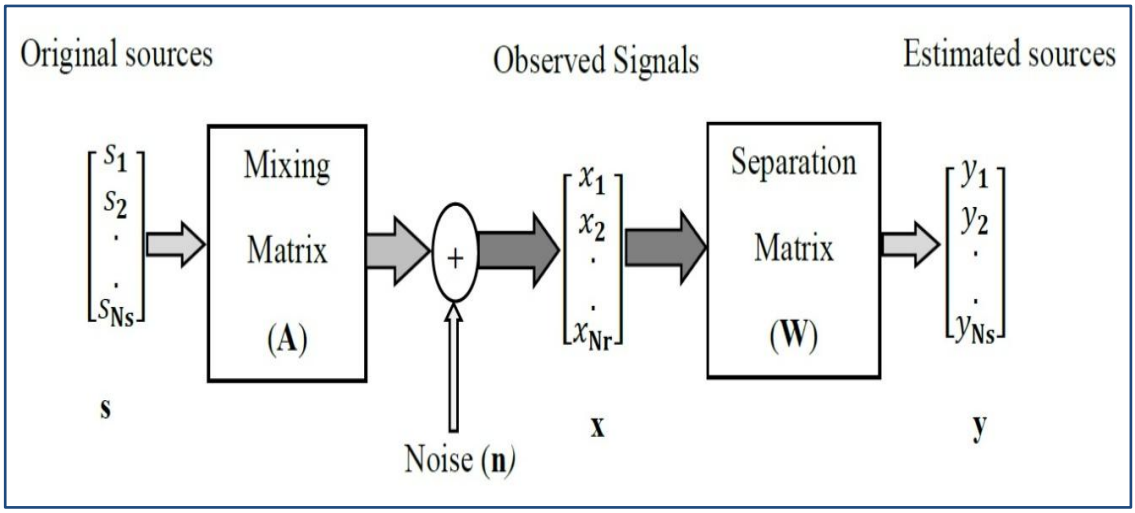

Fig. 2.17 Schematic diagram of Blind source separation[32]

$$S(t) = [S_1(t), S_2(t), S_3(t), \dots, S_{Ns}(t)]^T \quad (2.1)$$

Where $S(t)$ represents the original signal sources. After that all sources are going to be mixed randomly by matrix A to give the mixture matrix [26].

$$X(t) = [X_1(t), X_2(t), \dots, X_{Ns}(t)]^T \quad (2.2)$$

$$\begin{bmatrix} X_1(t) \\ X_2(t) \\ \vdots \\ X_{Ns}(t) \end{bmatrix} = \begin{bmatrix} a_{11} & a_{12} & \cdots & a_{1Ns} \\ a_{21} & a_{22} & \cdots & a_{2Ns} \\ \vdots & & \ddots & \vdots \\ a_{N1} & a_{N2} & \cdots & a_{NNs} \end{bmatrix} \begin{bmatrix} S_1(t) \\ S_2(t) \\ \vdots \\ S_{Ns}(t) \end{bmatrix} \leftrightarrow X(t) = AS(t) \quad (2.3)$$

The above equation illustrates the general mathematical model of blind source separation. The model has no noise.

The principle aim of BSS is to extract source signal. It is done by mixing A or inverse of matrix A. The inverse of matrix A is known as the un-mixing matrix W

$$S(t) = WX(t) \quad (2.4)$$

$$X(t) = AS(t) + n \quad (2.5)$$

Where $n = [n_1(t), n_2(t), \cdots, n_s(t)]^T$ and n represents the noise.

2.6.6 Stone BSS

A scientist named Stone invented a new technique of separation based on blind source separation . It is classify as a kind of second order statistic and the method took the same name of the scientist that invented it "Stone BSS" . This method depends on the feature of signal and the conjecture " The temporal predictability (TP)of any mixture is less than or equal that of any of its component" [33][34][35][36].

Only three helpful features of signal mixtures that could be utilized which are.

- A Gaussian probability density function based on the central limit theorem.
- Degree of statistical independence
- Temporal predictability

The difference between Stone BSS method and any other BSS methods is the utilization of the above three mentioned points in other word Stone BSS depends on its execution on the 3rd point while the other BSS methods utilize the first and the second property to separate signals.

2.6.7 Enhanced Fast Independent Component Analysis EFICA BSS

EFICA algorithm working steps start with removing sample mean and remove the miss- correlation between data and explain that mathematically start with the down below equation [37].

$$X = AS \tag{2.6}$$

To define the above variables it is supposed that X is a matrix with d x N dimension, then N represents the samples number and S represents the original signal samples. A can be described as undefined mixing matrix d x d [37].

Now to remove sample mean and de-correlation of data X it needs the down below equation since the steps is common with all algorithms classify under ICA

$$Z = \hat{C}^{-\frac{1}{2}}(X - \overline{X}) \tag{2.7}$$

whereas $\hat{C}$ is the covariance matrix and $\overline{X}$ represent measured data of sample mean [37].

To finish the operation of EFICA estimation each step of the algorithm works on pulled with the previous or following step in symmetric orthogonalization.

$$W+ \leftarrow g(WZ)ZT - \text{diag}[\acute{g}(WZ)1N]W \tag{2.8}$$

$$W \leftarrow (W+ W+T)-1/2\ W+ \tag{2.9}$$

The above 3 and 4 equation could be as the fixed point of EFICA, g and ǵ represent the second derivative of G where G is appropriate nonlinear function.

$$G= \hat{W}A \tag{2.10}$$

The above equation represent the gain matrix which deals directly with the separation quality since $\hat{W}$ is the de –mixing matrix [37].

From the previous introduction EFICA consider general case while FICA is a special method derived from the ICA since every row would

multiply with appropriate positive number before the symmetric orthogonalization in the iteration number 3.

Every single iteration can be illustrated in the three down below equations

W+ ← g(WZ)ZT - diag[ǵ(WZ)1N]W

W+ ← diag[C1,....,Cd].Ẁ

W ← (W+ W+T)-1/2 W+

The Gaussian distribution gave an opportunity to derive the non-diagonal normalized gain matrix.

$$V_{kl}^{GS} = \frac{C_k^2 \gamma k + C_l^2(\gamma l + \tau_l^2)}{(C_k \tau_k + C_l \tau_l)} \quad (2.11)$$

From the equation 6 it could be noticed that it is invariant with respect to C_k [37].

The coming equation is obtained by keeping k fixed and choosing a value for C_k equal to 1.

$$C_{k,l}^{OPT} = \arg \min_{cl, ck = 1} \quad V_{kl}^{GS} = \frac{\gamma_l \tau_l}{\tau k(\gamma_l + \tau_l^2)} \quad (2.12)$$

from the above equation we can conclude that zero and +∞ lost the ability to minimize the value of equation 6 until $C_{k,l}^{OPT}$ equal to the value of V_{KL}^{GS}.

the down below equation describe the optimum value that would be depended .

$$V_{k,l}^{OPT} = \min_{cl, ck = 1} \quad V_{kl}^{GS} = \frac{\gamma_k(\gamma l + \tau_l^2)}{\tau_l^2 \gamma_l + \tau_k^2(\gamma_l + \gamma_l^2)} \quad (2.13)$$

2.6.8 Joint Approximation Diagonalization of Eigen – Matrix (JADE)

JADE could be consider as one of the algorithms that are used to analysis the independent component to separate mixed signals . It works by exploiting a feature which is called fourth order moment [38]. As we mentioned previously blind source separation techniques works according to one of the following theories "Temporal predictability , Gaussian probability density function and Statistical independence ". JADE is like the other BSS technique , it operates under the Gaussian probability density function which use to determine independence between components . The aim of this determination is to have zero overfull Kurtosis . To predict source vectors which own high amount of overfull Kurtosis . JADE algorithm here search for orthogonal rotation of monitored vectors of the mixture matrix [38].

to represent JADE algorithm mathematically.

Let $X = (x_{ij}) \in R^{m*n}$

Where X is per whitened and the matrix here has n columns and m of variant mixed vector. m by m will represent the identify matrix of sample covariance and the matrix will has zero mean as well .

$$\frac{1}{n} \sum_{j=1}^{m} x_{ij} = 0 \text{ and } \frac{1}{n} X\overline{X} = I_m \qquad (2.14)$$

By treating X with JADE then it will compute first the "fourth order moment" and then to get the rotation matrix by using optimized contrast function .

$$Z = O^{-1}X \qquad (2.15)$$

The above equation is to predict source component

2.7 Particle Swarm Optimization (PSO)

PSO can be defined as swarm intelligence based, approximate and nondeterministic optimization technique. Every optimization technique aims to obtain parameters which give the maximum or minimum values that match the target function. James Kennedy and Russell Eberhart were the first scientists that invented PSO in 1995who had the PSO idea from the bird and fish swarm. PSO algorithm provides multiple solutions at each time. PSO, like genetic algorithm, has fitness function which is used for evaluating each solution during the iteration [39].

In search space each solution is denoted by particle, then the particle flies to reach the max. value depending on the objective function.

The swarm construct from many particles, each particle keeps

- Position inside the search space,
- velocity; and
- individual best position.

The global best position stays at the swarm. The operation of PSO can be summarized in three steps [39].

- Each particle is evaluated according to fitness function;
- updating the bests (global & individual); and
- updating velocity and position.

All the above steps are repeated until the stopping condition is obtained.

The equation below is used for updating the velocity of each particle [39].

$$v_i(t+1) = wv_i(t) + c_1 r_1[\hat{x}_i(t) - x_i(t)] + c_2 r_2[g(t) - x_i(t)] \quad (2.16)$$

i denotes particle index, w denotes inertial coefficient,c_1, c_2 represent the acceleration coefficients and r_1, r_2 represent random values which control the regeneration of each velocity update.

The inertial coefficient "w" value lies between 0.8 to 1.2. The cognitive coefficient c1 value is close to 2. The social coefficient c2 value is close to 2 as well [39].

The equation below is used for updating the particle position.

$$x_i(t+1) = x_i(t) + v_i(t+1) \tag{2.17}$$

PSO approximately covers 4.3% of the papers published in IEEE which deals with biomedical signals and medical fields. ECG signal is classified as biomedical signal; for this reason PSO has been utilized to enhance the extraction of fetal ECG signal [40]. Fig. 2.18 illustrates the general flow chart of PSO technique.

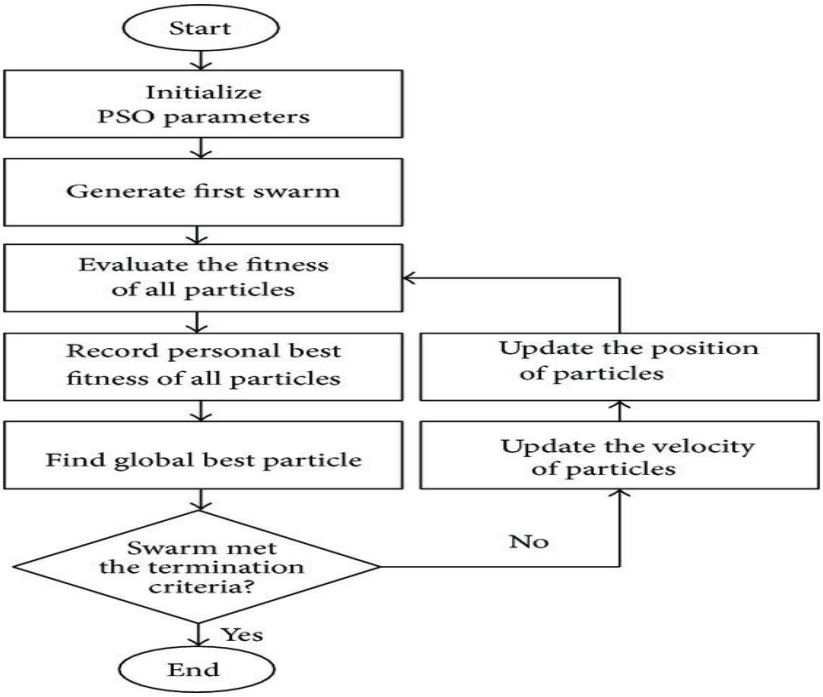

Fig. 2.18 Standard flowchart of Particle Swarm Optimization Technique[39]

2.8 Literature Review

Direct extraction of fetal ECG method is highly depending on fetal position and the age of gestation. Direct detection has been done without any processing for signal. In vertex fetal position the R-peaks of fetal signal will appear positive while the mother appears negative [41].

Different kind of adaptive filter has been used for extracting FECG and cancel the MECG. These filters which used are for extracting FECG included training adaptive filter of matched filter to cancel mother ECG [42][43][44]. Some methods trained the filter directly to extract fetal ECG [45][46]. Partition-based weighted sum filter, least square error fittings are also used for fetal ECG extraction [47][48][49][50]. For extracting FECG by adaptive filter, it requires either reference MECG or independent linear channels [51]. Practically, the above mentioned approaches are not suitable because the morphology of MECG has close link with the electrodes position [52]. Kalman filter has been developed to extract fetal ECG and cancel maternal ECG. In this approach, an arbitrary MECG is used as reference and cancel it while extracting FECG [51][52][53][54].

There is another method which is used for extracting ECG; it is known as linear decomposition. In linear decomposition method, with the help of suitable function, the signals should be decomposed for various components. The selection of that basic function depends on frequency, time and of the feature of fetal signal components. Wavelet decomposition and matching pursuits are the best methods that have been used for the purpose of fetal ECG extraction [55][56][57]. Singular value decomposition (SVD) and blind source separation (BSS) can be classified as “data-driven decomposition method” [58][59][60]. In BSS the required functions are concluded from the used data itself. Using blind source

separation to extract FECG shows that BSS has a better performance than the used adaptive filter[61][62][63]. Depending on, independent components of each mother and fetal or temporal structure existence for either mother signal or fetal signal, will help us to use blind source separation in the extraction of FECG [64][65][66][67][68]. Combination between blind source separation and wavelet decomposition has been also made to enhance the extraction of FECG[56][69]. The main problem in using BSS for fetal ECG extraction is that BSS supposes that all signals (MECG, FECG and noise) mix linearly while in fact some cases like (breathing and when fetus changes its position), do not satisfy the condition of suitable mixing. This explains the error that happens in the extraction operation [70][71].

Adaptive blind source separation which combines model-based signal processing also provides very good results [43][72][73]. Fixed or data-driven basis function are the used functions in linear decomposition. Both fixed and data-driven basis function have less impact for non-linear mixed signals. As mentioned before, the mixed signals (FECG, MECG and noise) may not linearly separable [67][74].

The only solution for this problem is the use of non-linear transforms to isolate all parts that form the mixture. Non-linear methods require prior knowledge about the wavelet signal and even the unwanted signal. Non-linear methods for canceling MECG and extracting FECG have been mentioned in many researches [67][70][72][73]. The point that distinguishes the non-linear method is its ability to apply on one mother abdominal channel [70]. Other projects that have been announced include a combination between linear and non-linear decomposition methods. This combination method has a very good performance specially in the field of fetal ECG extraction [70].

There are few studies that discuss the problem of twin gestation. For instance, Lathauwer discussed twin case "fetal electric cardiogram" extraction by blind source separation. He developed a method to separate both FECG and MECG [2]. Taylor also wrote a general clinical study on both single fetal and twin to record heart time periods in normal pregnancy. He implemented his work using ICA and got 85% rate of success on separating singletons and 79% rate of success on twins and triples [75]. A. Kam and A. Cohen discussed the problem of extracting twin fetus ECG in a published paper with title "SEPARATION OF TWINS FETAL ECG BY MEANS OF BLIND SOURCE SEPARATION (BSS), they used an adaptive filter to cancel the noise and then used the JADE algorithm to separate MECG, F1-ECG and F2-ECG [76]. Comani et al. and Burgoff et,al used the measured magneto cardiograph data of twin. They used ICA-TDSEP algorithm and 9 magnetos cardiograph. They proved that between 28th and 38th week twin fetal ECG could be separated from not only mother ECG but also the noise as well [4][77]. Malika kevalupura, Mehrded Pourfathi and Birsen Sirkeci Mergen wrote a paper under the title of "Impact of Contrast Functions in The ICA on Twin ECG Separation", They used fast ICA with multi and different contrast functions to separate twin fetal ECG from mother ECG. They depend on the performance index as criterion [31]. M. kotas, J.M.LESKI and J.WKOBEL, They published research with title "Sequential Separation of Twin Pregnancy Electrocardiogram". In their research they used a new method of sequential determination of source sub spaces (SDSS) combined with ICA merged with either projective or adaptive filter to separate sources signal [78]. Salman Vardi M, and Z. Einalou also discussed the problem of extracting twin fetal ECG through their research under title "Separation of Twin Fetal ECG From Maternal ECG

Using Empirical Mode Decomposition Techniques " They invented new method by combining principal component analyses (PCA), standard empirical mode decomposition (EMD) and ensemble empirical mode decomposition (EEMD). They used 250HZ as sampling frequency and they got 93.3% and 91.1 % accuracy of separation respectively [79]. Rolant Gini J., Ramachandran K.I. and Ceerthibala U.K. wrote a research under the title "Approach To Extract Twin FECG For Different Cardiac Condition During Prenatal". They invented a new algorithm to detect the R peak for each mother and fetuses. They got results close to 100% of singleton fetal ECG extraction and 80.4% in case of twin [80].

In fact, the published research by Malika Kevalupura,Mehrded Pourfathi and Birsen Sirkeci Mergen under the title "Impact of Contrast Functions in The ICA on Twin ECG Separation" goes in line with our study. Thus, we have used the same dataset (DaISy dataset) of single fetal pregnancy. We have also used the Abio-7 dataset to test the performance of the used BSS algorithms. To satisfy the case of twin gestation The researchers generated fetal -2 signal while we duplicate the same fetal signal that has been extracted in the first stage. They depended on FICA BSS method while we have used Stone BSS method. They used different contrast functions and applied them to check how the extracted signal match the source signal while we calculated the SNR for each signal in addition to the matching index.

Chapter Three

Methodology

CHAPTER THREE
Methodology

3.1 Introduction

In this chapter, conventional Stone BSS will be demonstrated in details. It will also introduce the modification on Stone BSS and the data bases that used to test the performance of the compared algorithms.

3.2 Conventional STONE Blind Source Separation

Stone BSS technique exploits temporal predictability property to separate the mixed signals unlike other BSS technique that use different properties to implement separation . Temporal predictability concept is used for describing the time period which separates a series of events. This period of time may be regular or irregular so when a repeated cases of cause and effect are faced, it face another multi temporal periods. If these periods are constant, then it is possible to predict the next event [81]. Stone estimation depends on very simple principle which is that the temporal predictability must be equal or less than its components and this step helps to select every single weight for each vector to obtain orthogonal projection .

Just like the other BSS techniques Stone system starts with

$$X_k = AS_k \tag{3.1}$$

Since the first equation represents the system without noise. X is the mixed signals, S is the sources matrix and A is the mixing matrix. Symbol K could be sample or time index. The aim of all the operations is to restore [S], which is the sources from [X], which is mixed signal without

prior knowledge of [A] matrix. To get rid of this problem we need to find another matrix known as W which is equal to : W=A-1. Separation model has been established to calculate the record signal.

$$Y(k) = W\,X(k) \tag{3.2}$$

To get the scaling before S is going to be replaced with Y

$$F(y)=\log\frac{V_y}{U_y} = \log\frac{\sum_{k=1}^{N}\left(y_{long}(k)-y(k)\right)^2}{\sum_{k=1}^{N}\left(y_{short}(k)-y(k)\right)^2} \tag{3.3}$$

Equation 3.3 gives a definition to the temporal predictability measured by Stone.

$$y_{short}(k)=\beta_S y_{short}(k-1)+(1-\beta_S)y(k-1) \quad :0\leq\beta_S\leq1 \tag{3.4}$$

$$y_{long}(k)=\beta_L y_{short}(k-1)+(1-\beta_L)y(k-1) \quad :0\leq\beta_L\leq100 \tag{3.5}$$

N equal to number of sample proportion to Y(k), β_L =2-1/h_{long}, β_S =2-1/$h_{short}$where both h_{short} and h_{long} denote to half parameter life. Stone created relation between β_S and β_L. The relation is : half –life h long of β_L is longer than half life h short of β_S with 100 times.

By assuming y(k)= $w_i^T x(k)$, W=[w1,w2,w3,.....,wn].By substituting in equation 3 then we get

$$F(y_i) = \log\frac{w_i C_{xx}^{long} w_i^T}{w_i C_{xx}^{short} w_i^T} \tag{3.6}$$

C_{xx}^{long} and C_{xx}^{short} are respectively long and short term covariance matrix (NxN) of mixed signal.

$$C_{x_i x_j}^{short} = \sum_{\tau}\left(X_{i\tau} - X_{i\tau}^{short}\right)\left(X_{j\tau} - X_{j\tau}^{short}\right) \tag{3.7}$$

$$C_{x_i x_j}^{long} = \sum_{\tau} \left(X_{i\tau} - X_{i\tau}^{long} \right) \left(X_{j\tau} - X_{j\tau}^{long} \right) \quad (3.8)$$

Getting the un-mixing vector by maximizing Rayleigh quotient is the main concern of Stone BSS and here comes the need of using Eigen vectors of $C_{x_i x_j}^{long}$ $[C_{x_i x_j}^{short}]$-1 ,which represents orthogonal of the covariance matrices, to serve the previous purpose .

$$W_i C^{short} W_j^t = 0 \quad (3.9)$$

$$W_i C^{long} W_j^t = 0 \quad (3.10)$$

Where :

$$W_i C^{short} W_j^t = \sum_{\tau} \left(y_{i\tau} - y_{i\tau}^{short} \right) \left(y_{j\tau} - y_{j\tau}^{short} \right) \quad (3.11)$$

$$W_i C^{long} W_j^t = \sum_{\tau} \left(y_{i\tau} - y_{i\tau}^{long} \right) \left(y_{j\tau} - y_{j\tau}^{long} \right) \quad (3.12)$$

When h_{short} goes toward zero ($h_{short} \rightarrow 0$) hence short term would be :

$$y_{\tau}^{short} \approx y_{\tau-1} \quad (3.13)$$

$$\left(y_{\tau} - y_{\tau}^{short} \right) \approx d_{y_{\tau}} / d\tau = \acute{y}_{\tau} \quad (3.14)$$

When h_{long} as well goes towards infinite ($h_{long} \rightarrow \infty$) and in case of y has zero mean, the long term mean would be

$$y_{\tau}^{long} \approx 0 \quad (3.15)$$

$$\left(y_{\tau} - y_{\tau}^{long} \right) \approx y_{\tau} \quad (3.16)$$

According to the above equations the expected value of both yi and yj would be equal to zeros.

$$E[y_i y_j] = 0 \quad (3.17)$$

The previous equations proved that every single restored signal yi is calculated by $y_i=W_iX$ is not correlated with the other mixed signals and could be used to show that all the components are independent and the anticipated value would be zero as well, Stone is very suitable method for linear mixture separation. The anticipated value is equal to zero because the temporal derivative of each restored single signal is uncorrelated with each other.

$$E[\acute{y}_i \acute{y}_j] = 0 \quad (3.18)$$

Separating matrix could be obtained by using the mat lab program and specifically the Eigen value function.

$$W = eig(C^{long} C^{short}) \quad (3.19)$$

Stones BSS has many advantages; one of them is propagate Eigen problem.

3.2.1 Modified Stone Blind Source Separation (MSBSS)

A new method called Modified Stone Blind Source Separation (MSBSS) is introduced based on combination between Stone BSS algorithm and Particle Swarm Optimization (PSO) technique. There are many parameters which control the performance of Stone algorithm. These parameters are the maximum mask length, number of half lives to make mask, long and short term. Stone algorithm sets all the values of the mentioned parameters constant. Any change in the value of these parameters directly affects the signal separation. PSO is utilized to calculate the optimum values for only long and short term (h_{long} and h_{short}). The big search scope which is related to (h_{long} and h_{short}) is the motivation

to use PSO to get them optimum values. There are two linear scalar filters which control the response of Stone algorithm. The linear filters which have been used in Stone algorithm are assumed to be scalar filters and not to be a matrix filters. This explains how Stone BSS algorithm utilizes "Generalized Eigen Value Decomposition" (GEVD) to get the separation matrix [82]. Figure 3.1 illustrate the general Stone algorithm block diagram.

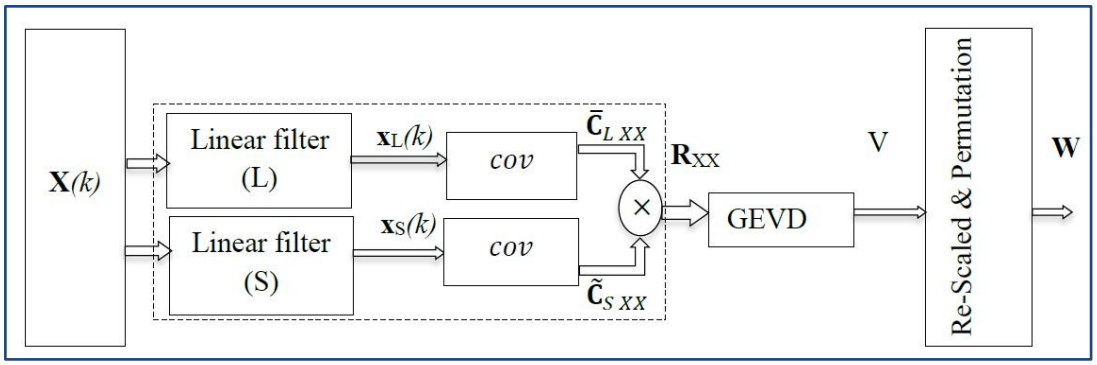

Fig. 3.1 Block diagram of STONE Blind Source Separation Algorithm[33]

Where: X (k) = Mixture observation signals, XL (k) =Filter Response (L)

XS (k) =Filter Response (S), $\bar{\boldsymbol{C}}_{L\,XX}$= Long-term covariance matrix

$\tilde{\boldsymbol{C}}_{S\,XX}$ = Short-term covariance matrix, $R_{XX} = \bar{\boldsymbol{C}}_{L\,XX}\tilde{\boldsymbol{C}}_{S\,XX}$

V= Eigenvector matrix RXXV=VD, W=Un-mixing matrix

The fitness function is defined to ensure the independency between sources. The fitness function is designed depending on equations (3.17) and (3.18)

$$F_1(Y) = \sum_{i=1}^{n} \sum_{j=1,j\neq i}^{n} y_i y_j^T \tag{3.20}$$

$$F_2(Y) = \sum_{i=1}^{n} \sum_{j=1,j\neq i}^{n} \dot{y}_i \dot{y}_j^T \tag{3.21}$$

Where n is the number of sources. The fitness function F should be minimized to ensure the independency between different sources. Then the fitness function would be.

$$F(Y) = \propto_1 . F_1(Y) + \propto_2 . F_2(Y) \quad (3.22)$$

Where $\propto_1$ and $\propto_2$ are two weight parameters.

In this fitness function the objective is to find matrix elements that minimize the fitness function. So PSO continue to search until a lower value of fitness function is reached. The best value for the designed fitness function is zero which shows the independency between sources. The fitness function has been derived from the fact that two vectors a and b are independent if their inner product becomes zero (a*b'=0). It is also important to notice that the inner product of their derivatives become zero ($a'*b'^{T}=0$).

Now the PSO parameters would be

w1=1 weight1 for fitness function(signal independency)

w2= weight2 for fitness function(delta signal independency)

PS=100 Population size in PSO

SL=0.005;%speed limiter (a number between 0.001 and 0.1 depends on the problem)

Maximum Number of Iterations =1000

Fitness Function = $F(Y) = \propto_1 . F_1(Y) + \propto_2 . F_2(Y)$

Figure 3.2 shows the flowchart of Modified Stone Blind Source Separation (MSBSS).

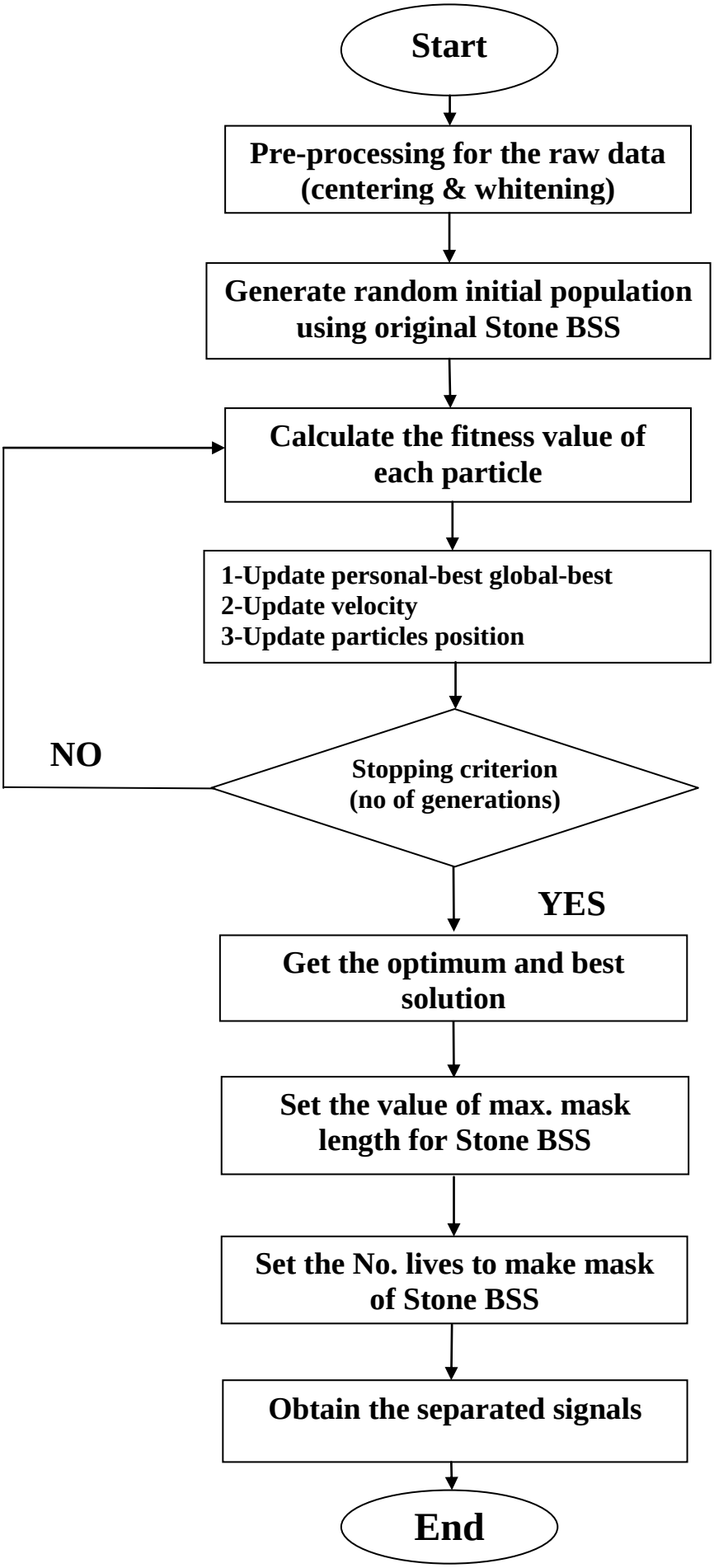

Fig. 3.2 MSBSS flowchart

3.3 DATA SET

3.3.1 ABio 7 Database

It is the criterion of ICALAB [83], the dataset consist of 7 channels, each channel contain one signal with sampling rate equal to 250 Hz. It also has zero mean, unity variance and 500 samples. Signal 1,5 and 6 are Sub Gaussian while signal 4 and 7 are Super Gaussian and finally signal 2 and 3 are Gaussian. Figure 3.3 demonstrate the shape of Abio-7 database signals.

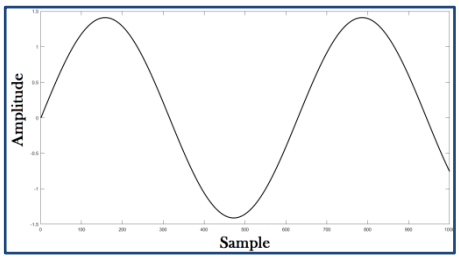

(A) Channel-1 (Sub-Gaussian)

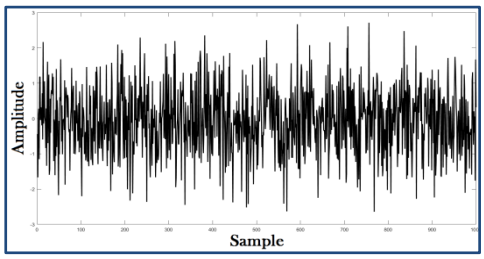

(B) Channel-2 (Gaussian)

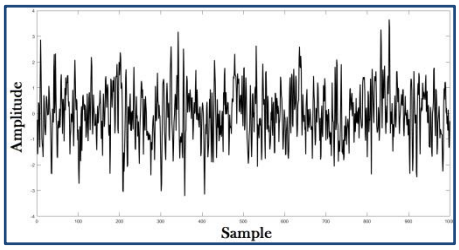

(C) Channel-3 (Gaussian)

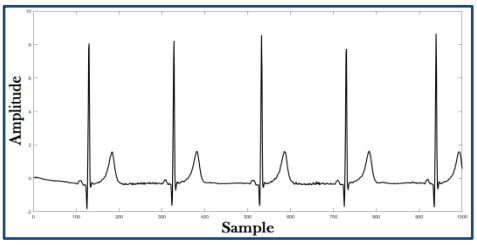

(D) Channel-4 (Supper-Gaussian)

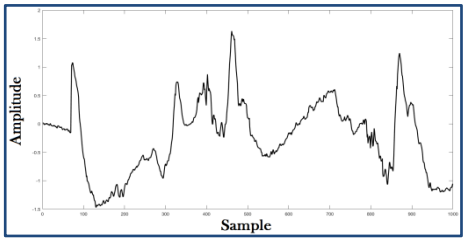

(E) Channel-5 (Sub-Gaussian)

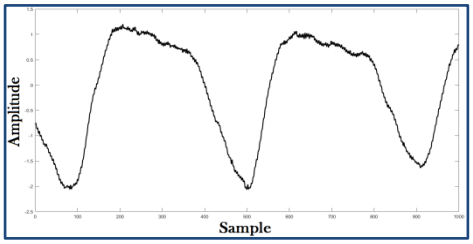

(F) Channel-6 (Sub-Gaussian)

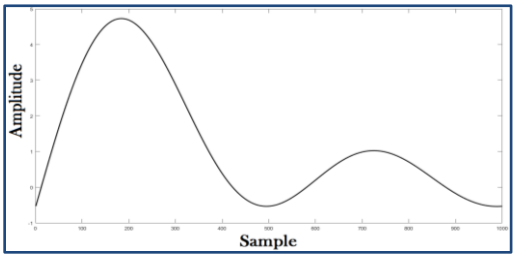

(G) Channel-7 (Supper-Gaussian)

Fig. 3.3 The ABio 7 Database

3.3.2 Real Data

DaISy database has been used [84]. The data is obtained by placing three electrodes (channels 6,7 and 8) over the thorax area of the mother body and five electrodes (channel 1,2,3,4 and 5) on the abdomen. The signals are sampled at 250 Hz and the recording of signals last for 10 seconds. First mother and fetal signal are separated from the real signals of DaISy database by three different blind source separation algorithms.

Figure 3.4 shows the location of electrodes over mother body which is responsible for recording ECG signals for both mother and fetus.

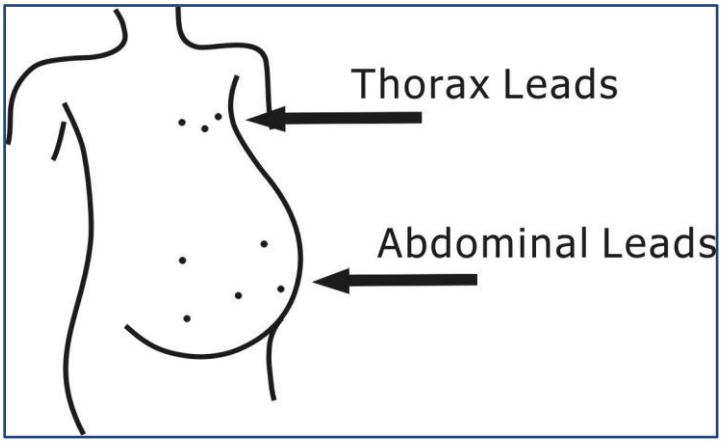

Fig. 3.4 The electrodes location over mother thorax and abdomen[46]

3.3.3- Semi-Simulated Data:

Until now there is no available recorded database online for twin gestation because it needs independent clinical study [31]. Only single fetal pregnancy real database is available. For this reason and to keep all provided data for all algorithms real, the extracted signal of fetal will be repeated and multiplied by factor to make a little change in the shape of the second fetal signal, and to represent the signal of the other fetal to satisfy the study of twin case gestation.

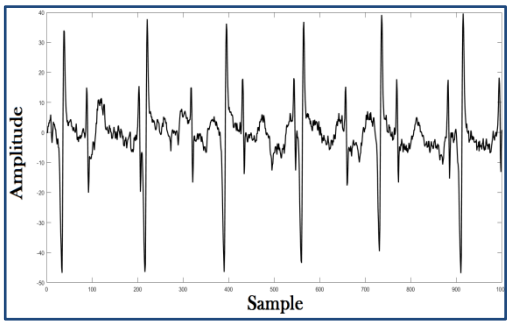

(A) Channel-1

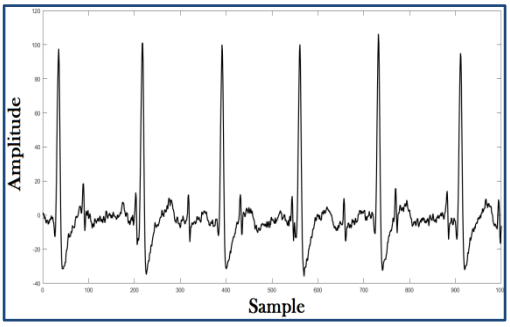

(B) Channel-2

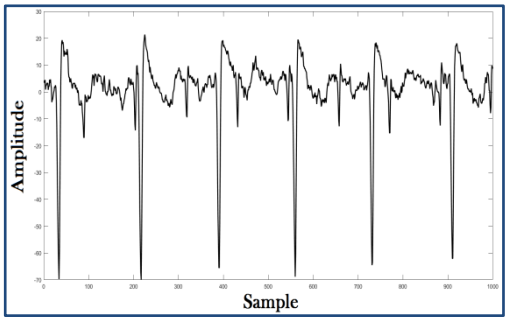

(C) Channel-3

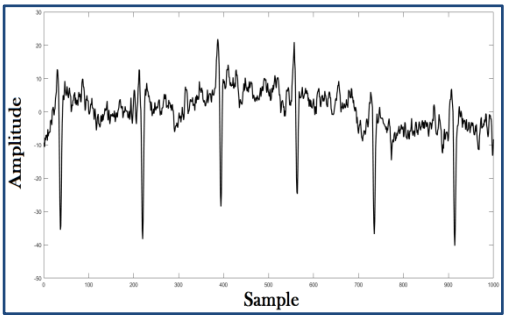

(D) Channel-4

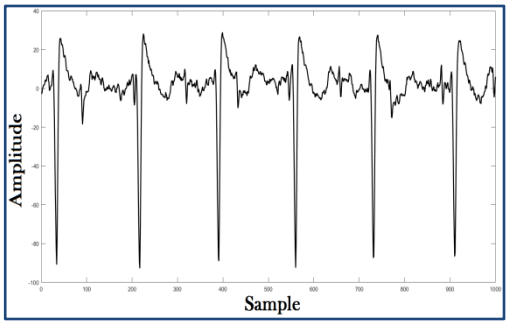

(E) Channel-5

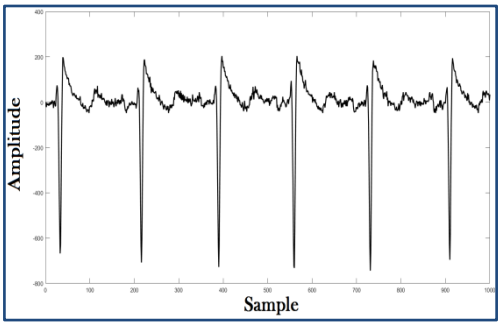

(F) Channel-6

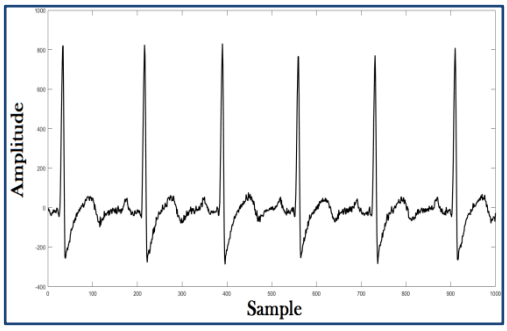

(G) Channel-7

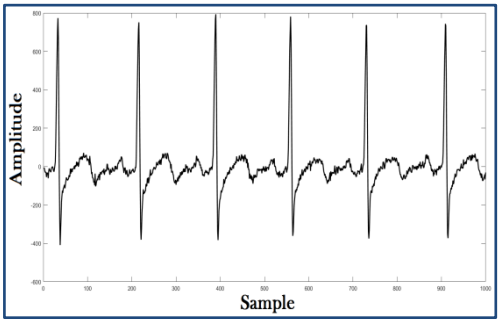

(H) Channel-8

Fig. 3.5 The real in vivo data from the online DaISy database

Traditional techniques try to clarify that thoracic sensor is responsible for recording only the mother heart beat and abdominal sensors are responsible for recording fetal heart beats. In fact all sensors record a mixture of all ECG signals for both mother and its fetuses, even noises are part of the mixture. Filter techniques can isolate only the mother ECG but cannot work to separate between fetal 1 and fetal 2 because their signals have the same features [85]. Fig. (3.5) shows the real obtained data from the online DaISy database before extracting MECG and FECG.

Chapter Four

Results & Discussion

CHAPTER FOUR
Results and Discussion

4.1 Introduction

The results are of two parts. Part-1 demonstrates the calculated results by using BSS only while Part-2 demonstrates the calculated results using Modified Stone BSS technique. Different types of BSS technique are compared with Stone's BSS to check the reliability of this method. Real ECG data for both mother and fetuses are taken from DaISy database. In this work three cases will be discussed.

4.2 PART-1

4.2.1 CASE 1: The Abio-7 dataset

The Abio-7 dataset is used to test the performance of the three selected algorithms (STONE, EFICA and JADE). All the signals in the Abio-7 are mixed randomly together to produce the new input for the algorithms as shown in Fig. 4.1. It also shows how each signal affected by the other channels signal.

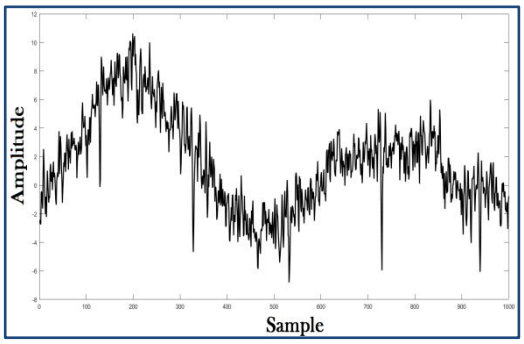

(A) Mixture-1

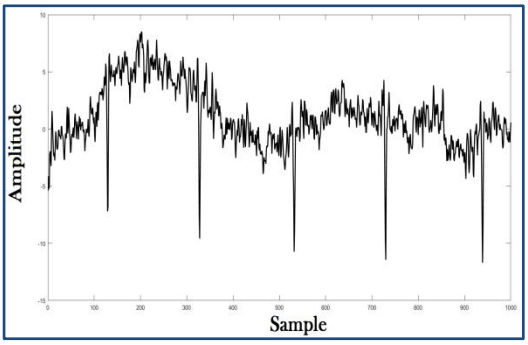

(B) Mixture-2

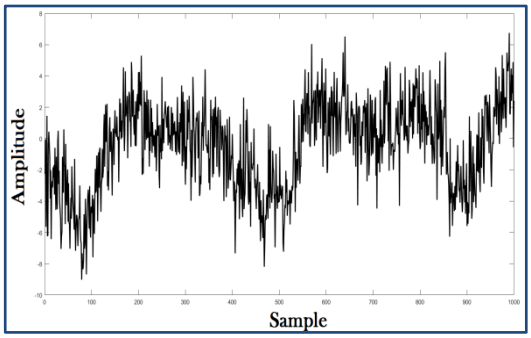

(C) Mixture-3

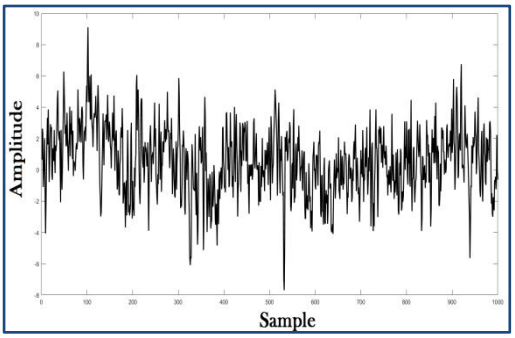

(D) Mixture-4

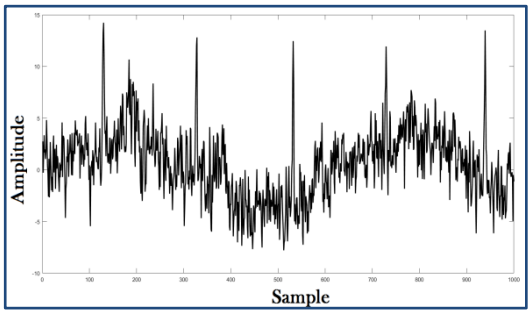

(E) Mixture-5

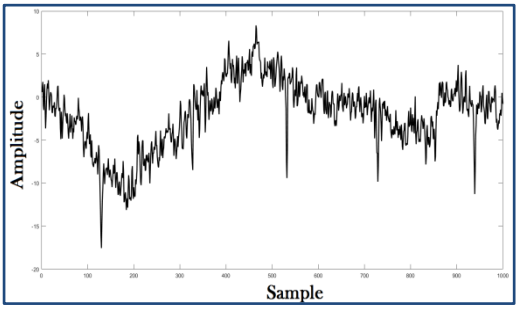

(F) Mixture-6

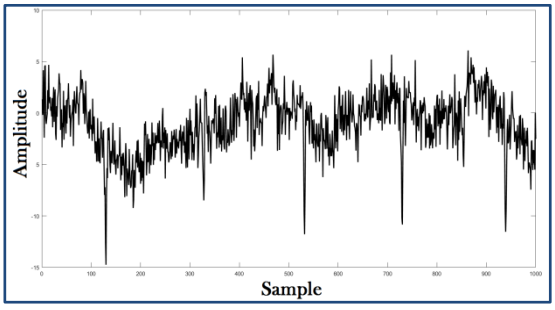

(G) Mixture-7

Fig. 4.1 The mixture of ABio-7 signals

After all signals have been mixed, the mixture matrix is the input for the three algorithms (Stone, EFICA & JADE) so as get the final restored signals. Figures 4.2, 4.3 and 4.4 show the recovered signal after using three BSS algorithms to restore all signal sources. The black signal denotes to source signal while the red one represent the restored signal

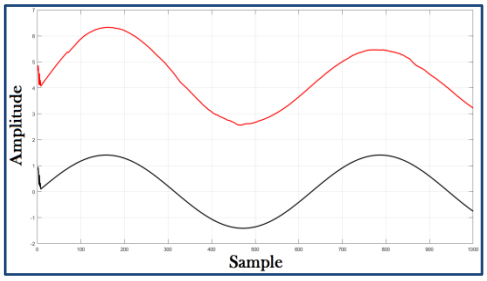

(A) Recovered Channel-1

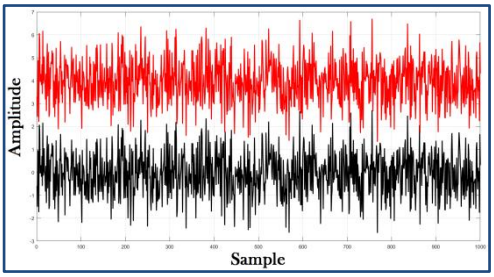

(B) Recovered Channel-2

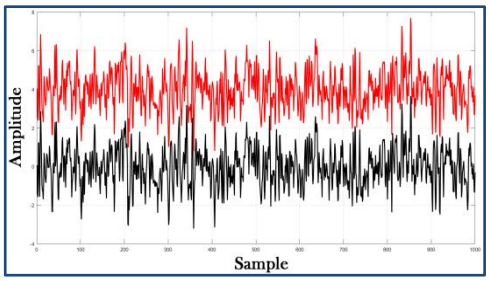

(C) Recovered Channel-3

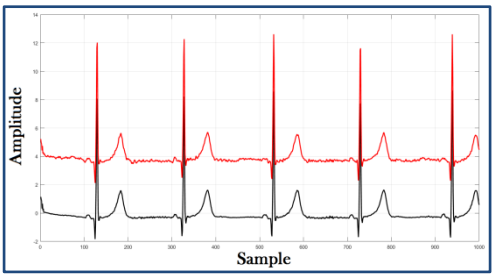

(D) Recovered Channel-4

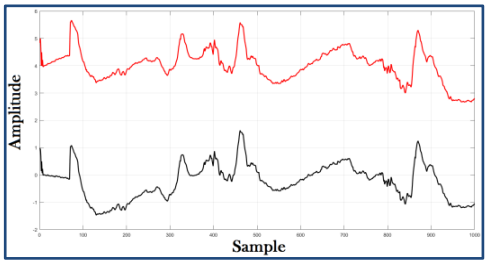

(E) Recovered Channel-5

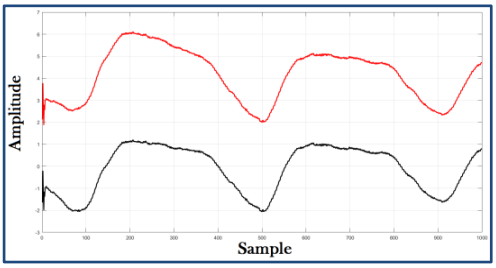

(F) Recovered Channel-6

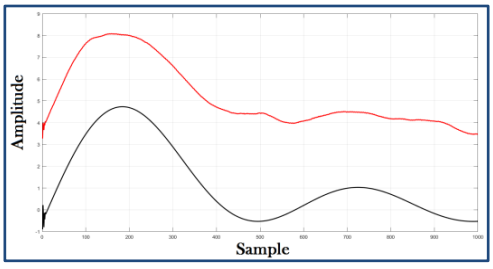

(G) Recovered Channel-7

Fig. 4.2 The source and restored signals by Stone BBS algorithm

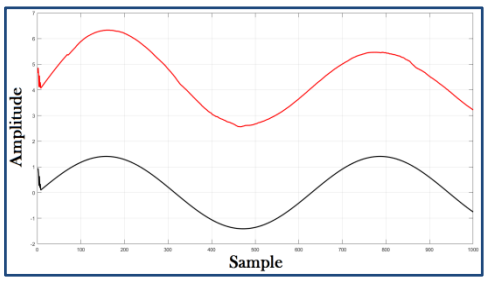

(A) Recovered Channel-1

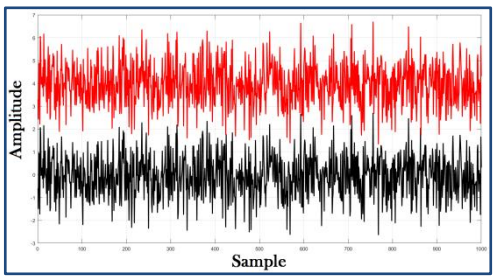

(B) Recovered Channel-2

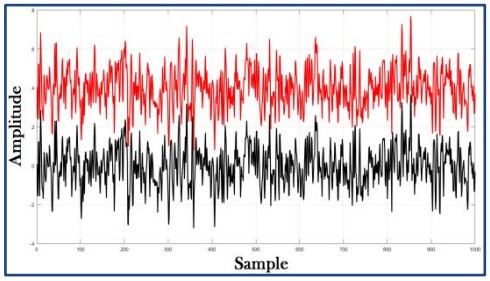

(C) Recovered Channel-3

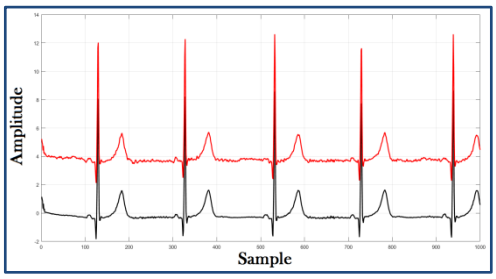

(D) Recovered Channel-4

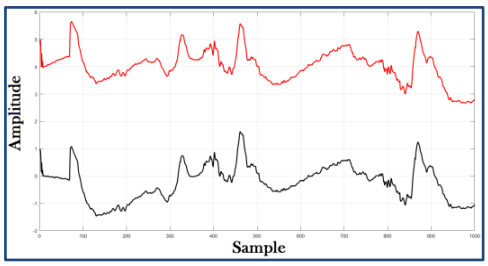

(E) Recovered Channel-5

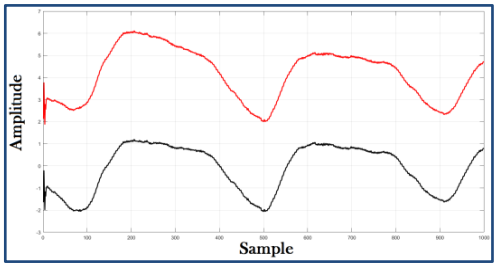

(F) Recovered Channel-6

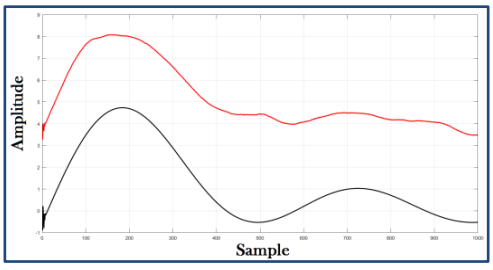

(G) Recovered Channel-7

Fig. 4.3 The source and restored signals by EFICA algorithm

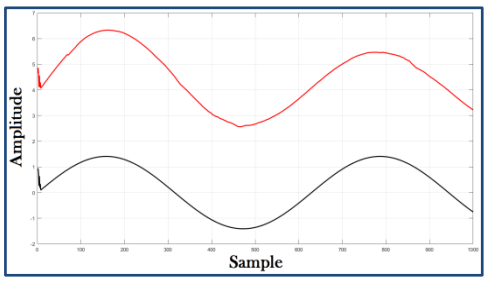

(A) Source and extracted signal

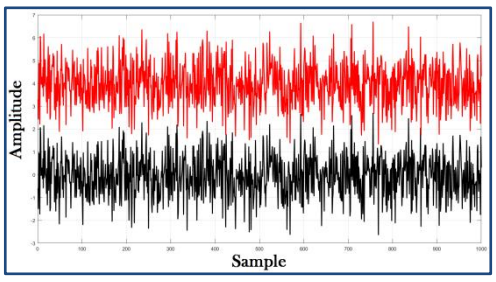

(B) Source and extracted signal

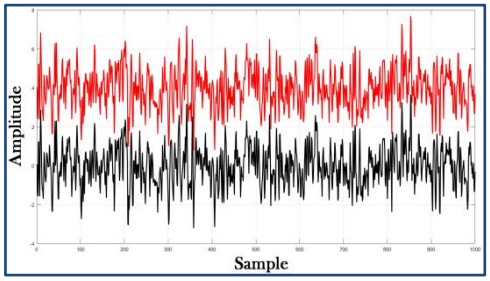

(C) Source and extracted signal

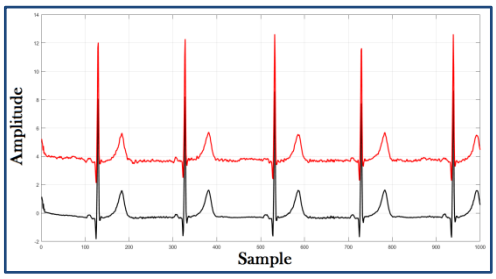

(D) Source and extracted signal

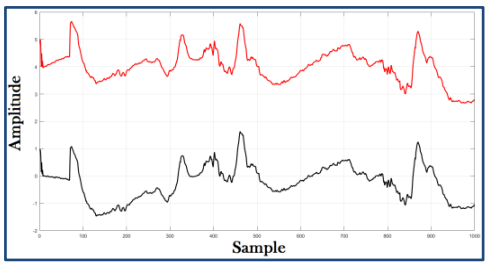

(E) Source and extracted signal

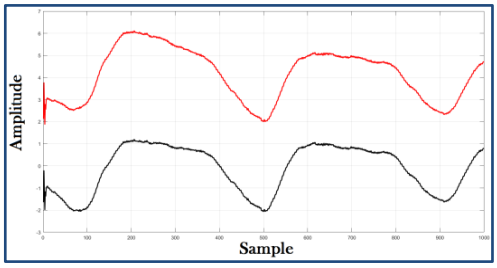

(F) Source and extracted signal

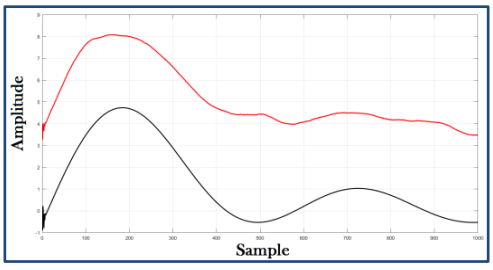

(G) Source and extracted signal

Fig. 4.4 The source and restored signals by JADE algorithm

All algorithms succeeded to recover all signals and to verify which algorithm has the best performance we need to compare them depending on the achieved SNR. Table (4.1) represents a comparison between all algorithms depending on the obtained average signal to noise ratio (SNR) for each method.

SNR is calculated by dividing the total power of the signal over the total power of the noise signal.

Table 4.1 The recorded average SNR in dB for each single algorithm

NO.	BSS Algorithm	Recorded Average SNR
1	**STONE**	**16.88**
2	**EFICA**	**22.36**
3	**JADE**	**14.47**

From table 4.1, EFICA algorithms record the highest value of calculated SNR. STONE algorithm records less SNR than EFICA but is better than JADE algorithm. This supports what has been mentioned in Stone's paper where he states that his algorithm is not the best algorithm to restore the (Gaussion, Sub-Gaussion and Super-Gaussion) signals [34] .

4.2.2 CASE 2: Single Pregnancy

In this part the extraction of both mother and single fetal ECG signal will be discussed depending on the output of the three algorithms. The eight channels of the DaISy dataset, which is illustrated previously in Fig. (3.5), are the input for each BSS algorithm (STONE, EFICA & JADE) after passing through band pass filter (BPF) to check if there is any change in the signals. The BPF cutoff frequency is (f1= 0.1Hz and f2= 140 Hz). The selected values of the cutoff frequency for BPF depends on the fetal heart rate which is equal to 140 beats per minute for a normal

case [22]. Figures 4.5 and 4.6 illustrate the BPF output and the BPF response. Band-pass filter BPF is implemented by a Windowed-Sinc FIR filter to narrow the frequency band and concentrate on the band which has the FECG signal.

$$M \approx \frac{4}{BW} \tag{4.1}$$

BW is the band width

$$h[i] = K \frac{sin\,(2\pi f_c(i-\frac{M}{2})}{i-\frac{M}{2}} \left[0.42 - 0.5\,cos\left(\frac{2\pi i}{M}\right) + 0.08\,cos\left(\frac{4\pi i}{M}\right)\right] \tag{4.2}$$

Where M=1025, Srate= 256, f1= fc1/Srate and f2= fc2/ Srate.

Figure (4.5) illustrates the frequency response of the B.P.F. From Fig. (4.6) there is no noticeable change on the output signals shape which can make distinguish between signals before entering the filter and after coming out. Figures 4.7, 4.8 and 4.9 show the extracted signals by each BSS algorithm.

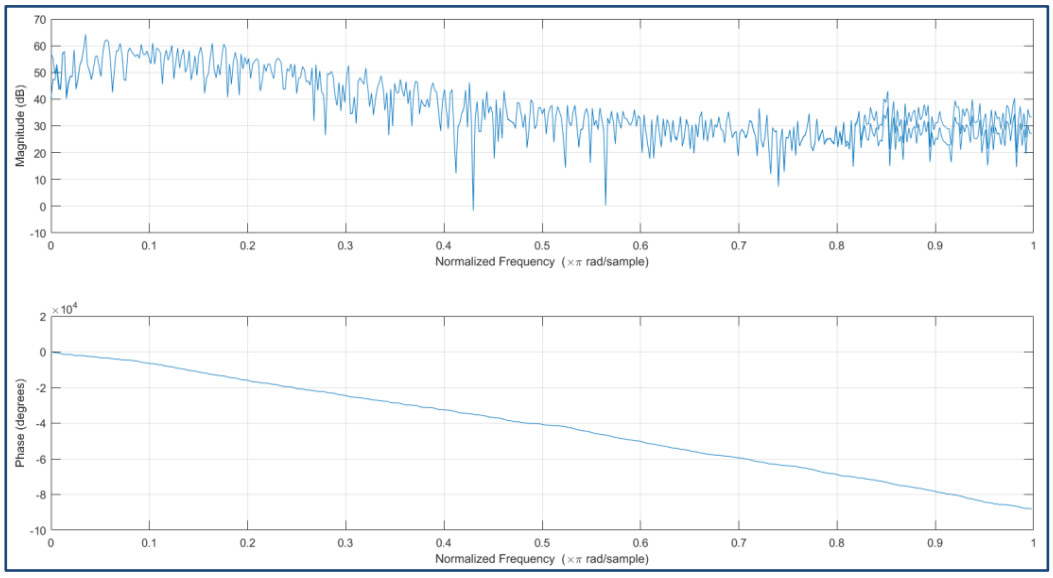

Fig. 4.5 The response of BPF

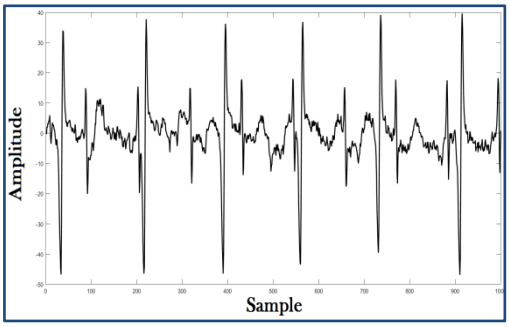

(A) Channel-1

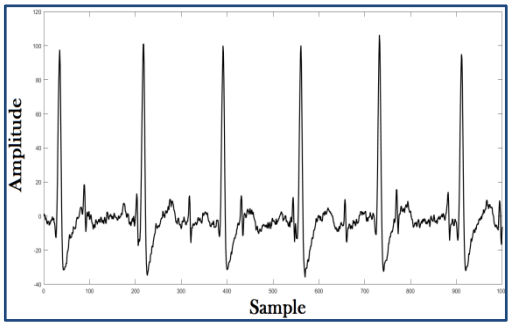

(B) Channel-2

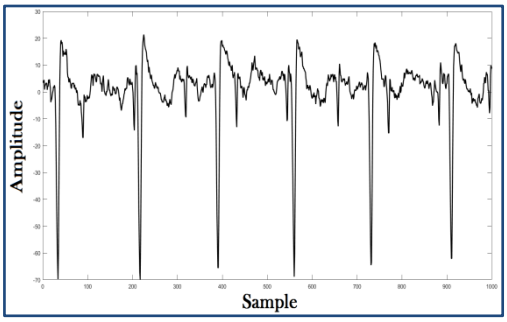

(C) Channel-3

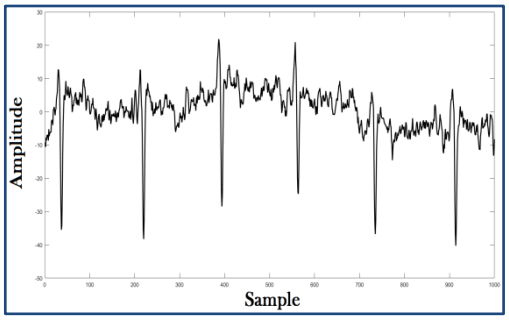

(D) Channel-4

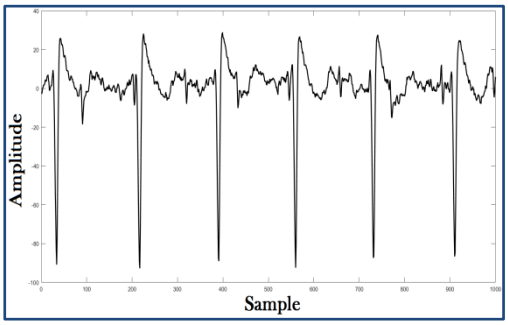

(E) Channel-5

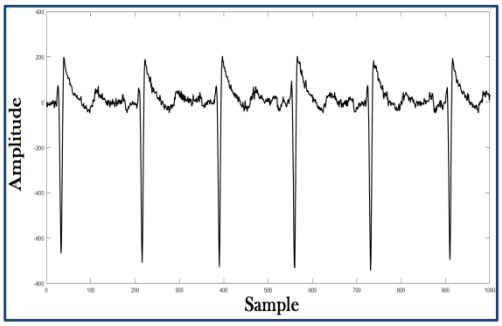

(F) Channel-6

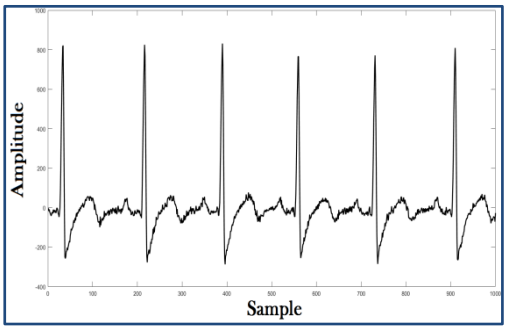

(G) Channel-7

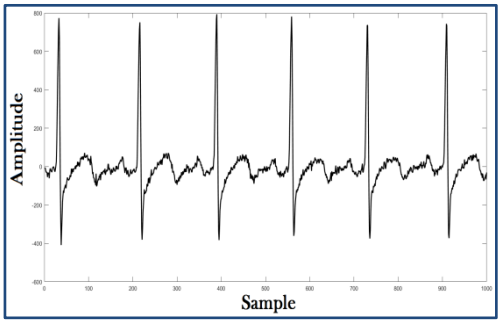

(H) Channel-8

Fig. 4.6 The shape of signals after BPF

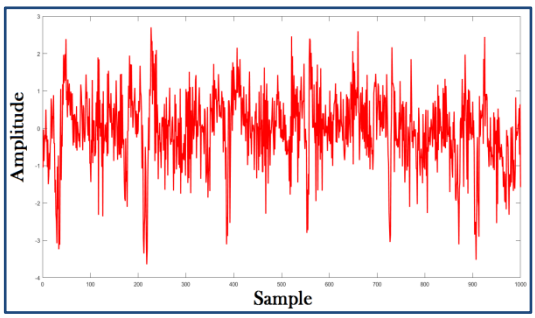

(A) Recovered signal Channel-1

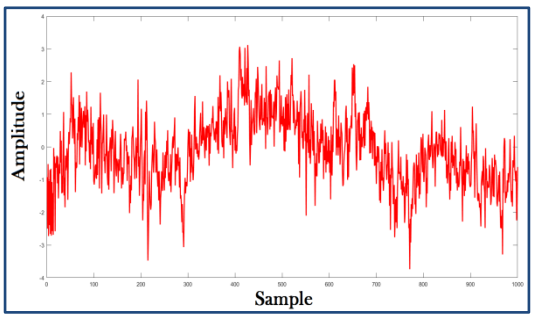

(B) Recovered signal Channel-2

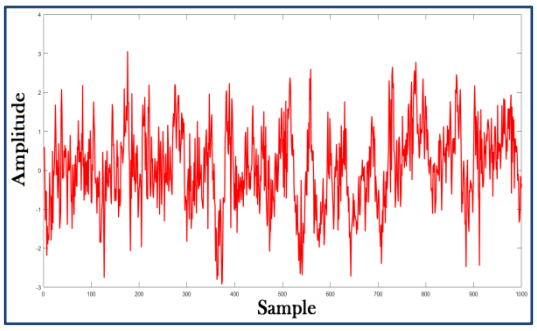

(C) Recovered signal Channel-3

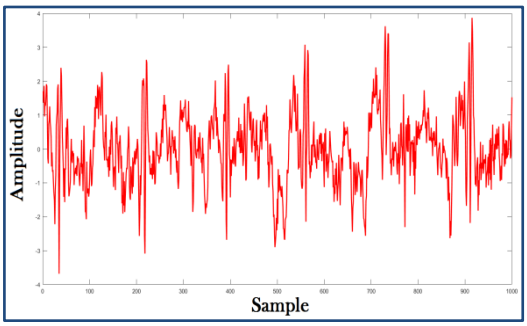

(D) Recovered signal Channel-4

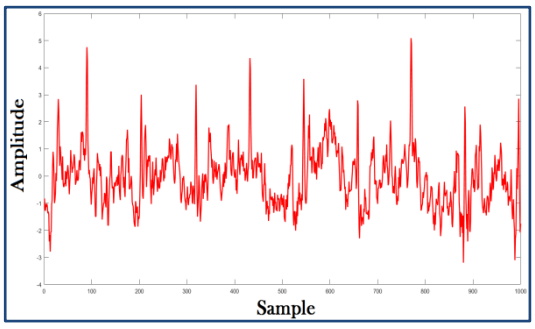

(E) Recovered signal Channel-5

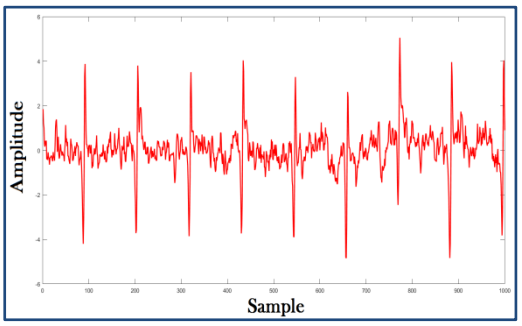

(F) Recovered Fetal signal Channel-6

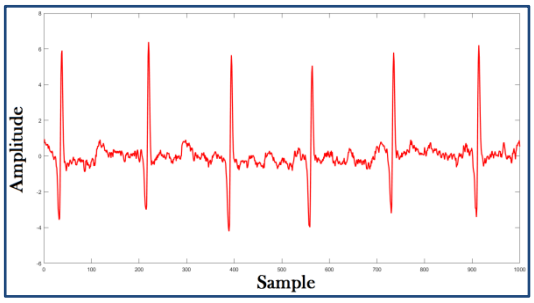

(G) Recovered Mother signal Channel-7

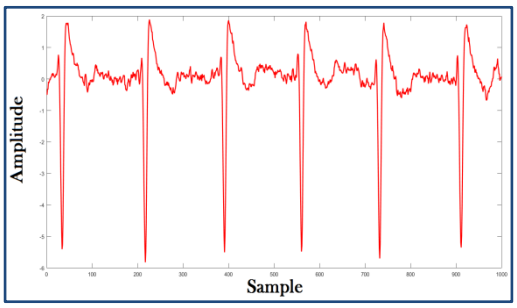

(H) Recovered signal Channel-8

Fig. 4.7 The extracted signals by STONE BBS algorithm

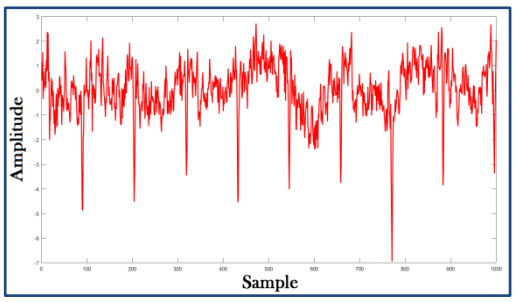

(A) Recovered signal Channel-1

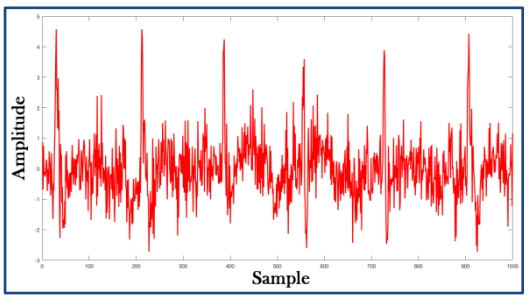

(B) Recovered signal Channel-2

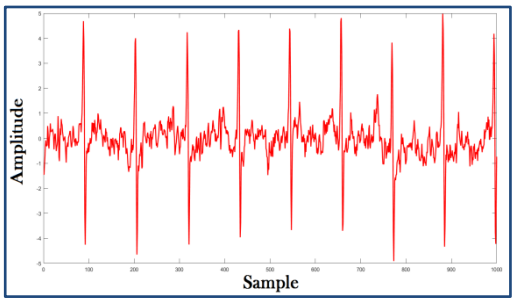

(C) Recovered Fetal signal Channel-3

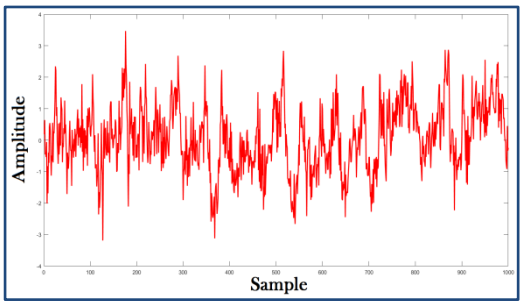

(D) Recovered signal Channel-4

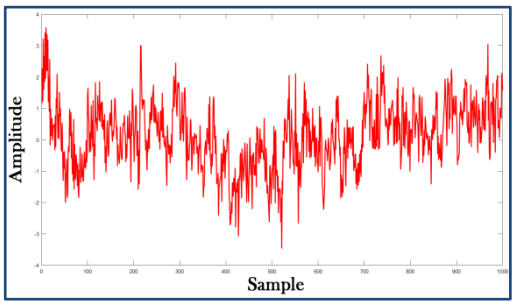

(E) Recovered signal Channel-5

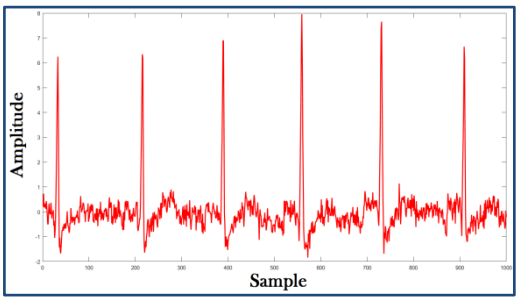

(F) Recovered signal Channel-6

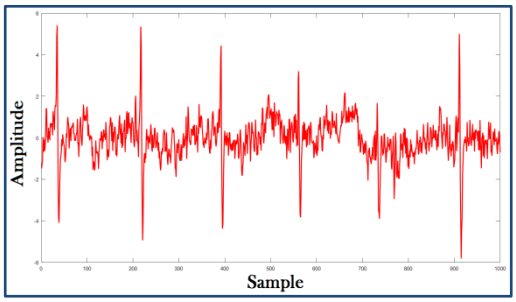

(G) Recovered Mother signal Channel-7

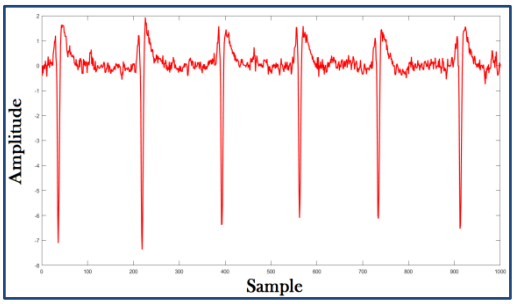

(H) Recovered signal Channel-8

Fig. 4.8 The extracted signals by EFICA BBS algorithm

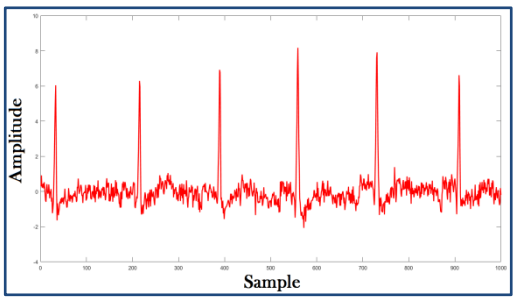

(A) Recovered signal Channel-1

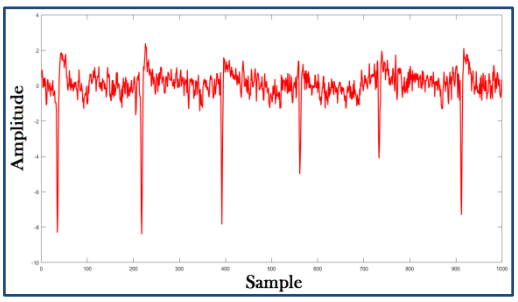

(B) Recovered signal Channel-2

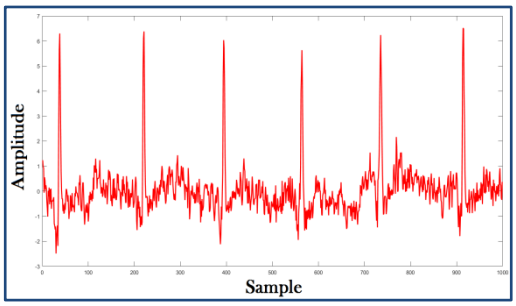

(C) Recovered Mother signal Channel-3

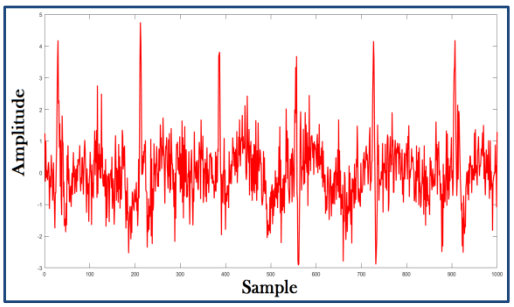

(D) Recovered signal Channel-4

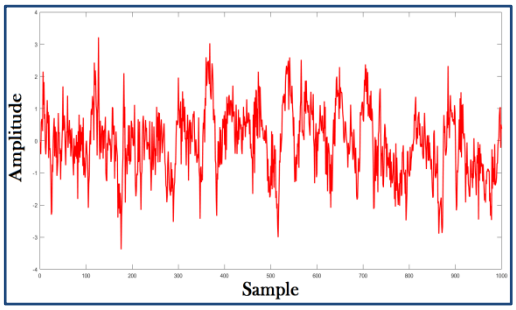

(E) Recovered signal Channel-5

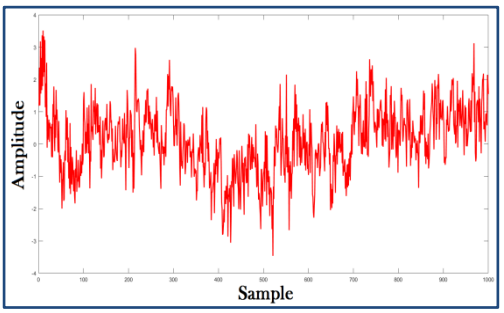

(F) Recovered signal Channel-6

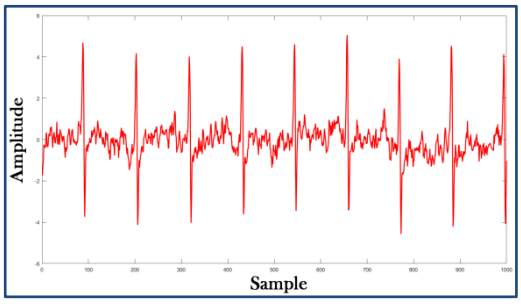

(G) Recovered Fetal signal Channel-7

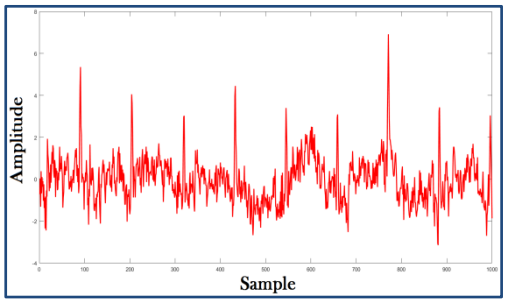

(H) Recovered signal Channel-8

Fig. 4.9 The extracted signals by JADE BBS algorithm

The previous figures show that every selected BSS algorithm has extracted fetal and mother ECG signals. However using the visual inspection, it very obvious that the noise has less effect on the extracted signals by STONE BSS algorithm. From the extracted signal for the mother and fetal it is so easy to calculate the fetal heart rate (FHR) which equal to (132 bpm) and mother heart rate (MHR) which is equal to (84 bpm).

By focusing on small part of each extracted signal of fetal ECG and mother ECG and specifically the QRS- Complex, the impact of noise appears more clearly as shown in the figs. 4.10, 4.11 and 4.12.

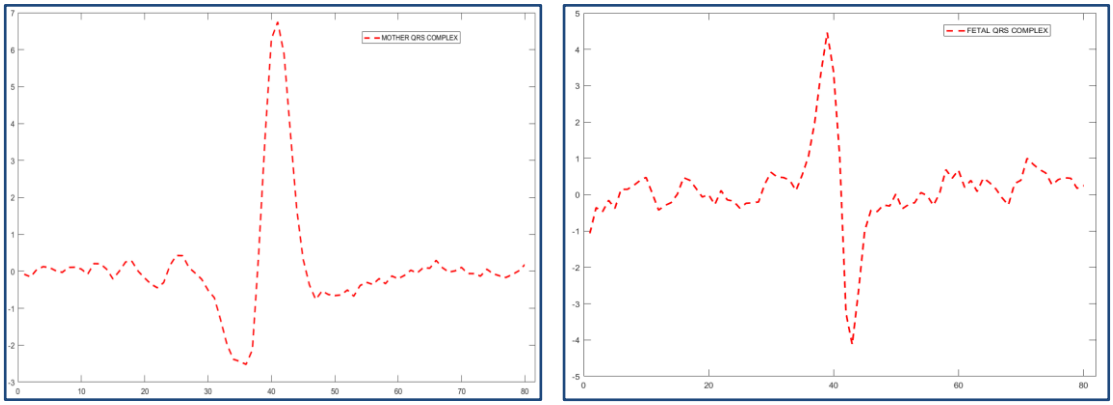

Fig. 4.10 The QRS complex for mother and fetal ECG after STONE

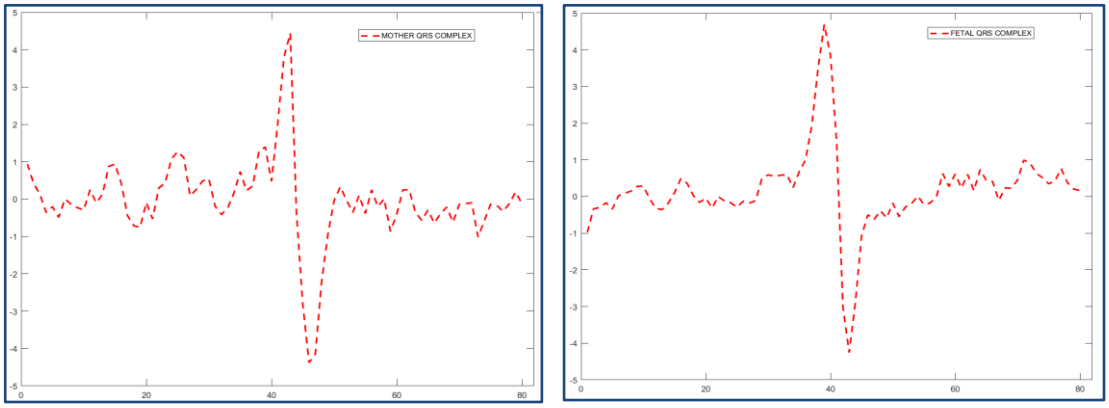

Fig. 4.11 The QRS complex for mother and fetal ECG after EFICA

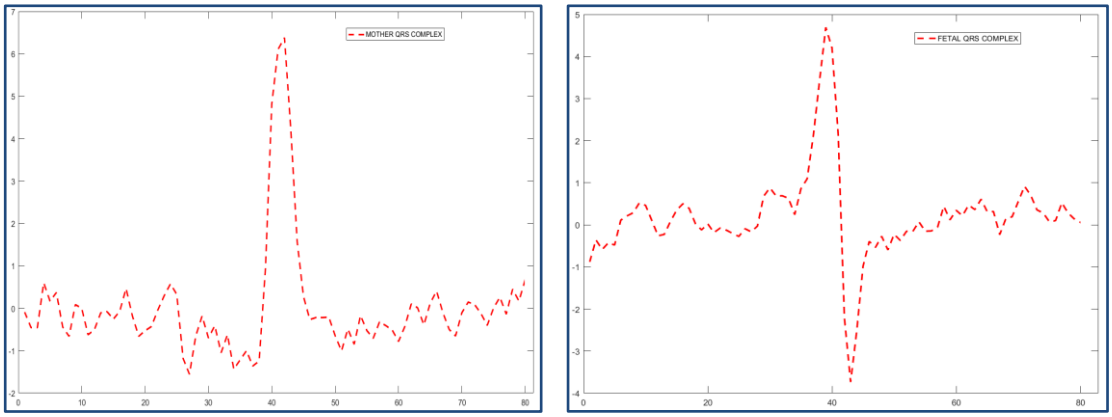

Fig. 4.12 The QRS complex for mother and fetal ECG after JADE BSS

For more clarification the down table 4.2 has been made to compare all restored signals (FECG & MECG) depending on the calculated power spectral density (PDS).

Power spectral density function (PSD) shows the strength of the variations(energy) as a function of frequency. In other words, it shows at which frequencies variations are strong and at which frequencies variations are weak. The unit of PSD is energy per frequency. We also can obtain energy within a specific frequency range by integrating PSD within that frequency range. Computation of PSD is done directly by the method called FFT or computing autocorrelation function and then transforming it.

Table 4.2 The recorded PSD for each signal

NO.	Signal	Real signal	Total power afte BPF	Total power after STONE	Total power after EFICA	Total power after JADE
1	FECG	101.3480	99.8504	0.8340	0.8727	0.8623
2	MECG	101.3480	99.8504	1.1098	1.0409	1.0289

Figures 4.13 and 4.14 demonstrate the obtained PSD for mother and fetal ECG signal.

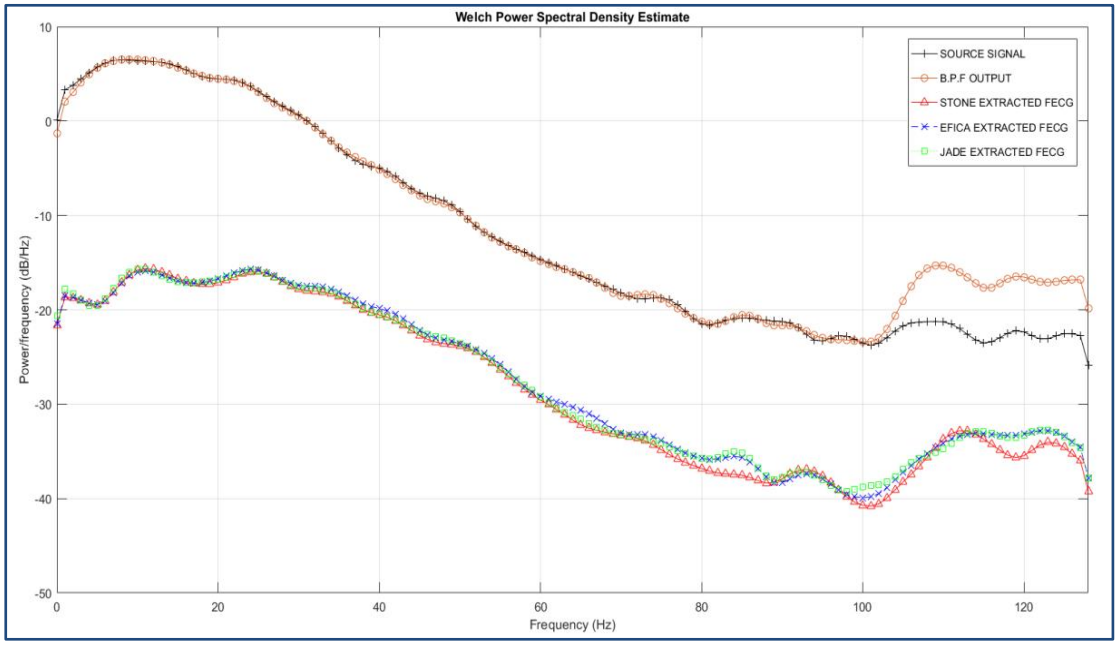

Fig. 4.13 The PSD for fetal ECG

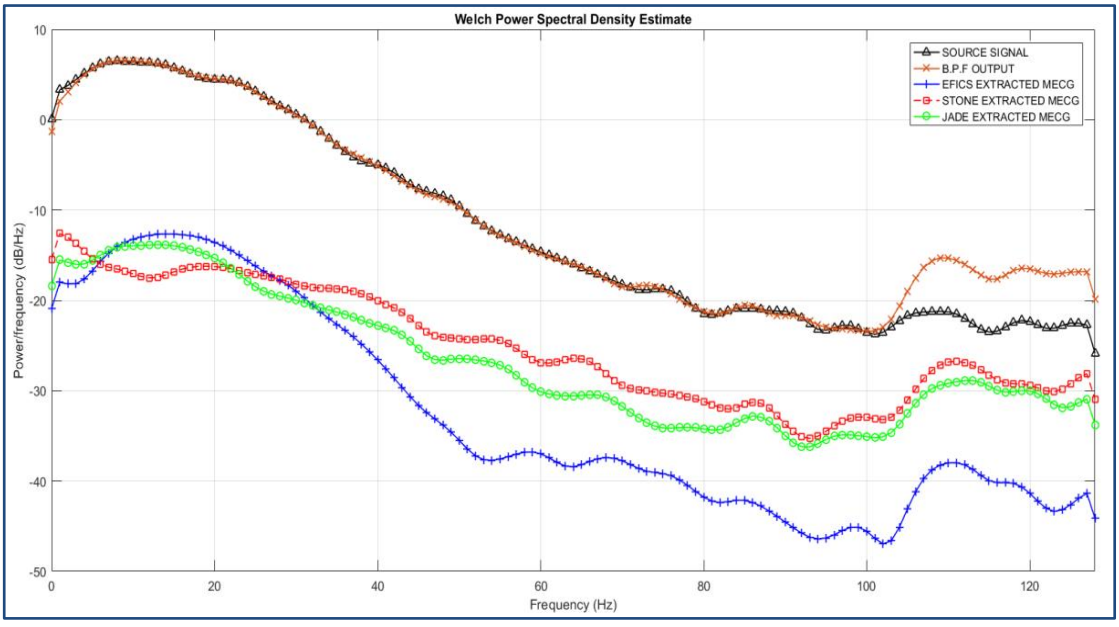

Fig. 4.14 The PSD for mother ECG

4.2.3 CASE 3: Twin Pregnancy Semi-Simulated data

As it has been mentioned previously in the simulated dataset part, one of the BSS algorithms out will be allowed to be the input to simulate the twin gestation case after doubling the signal of fetal. Three different noises, which have the biggest impact on the ECG signal extraction, are also added to be mixed with MECG, F1-ECG and F2-ECG. The extracted fetal and mother signal by Stone BSS in Case 2 will be depended to simulate twin gestation case. Figure 4.15 below represents the input signals to simulate the twin case gestation.

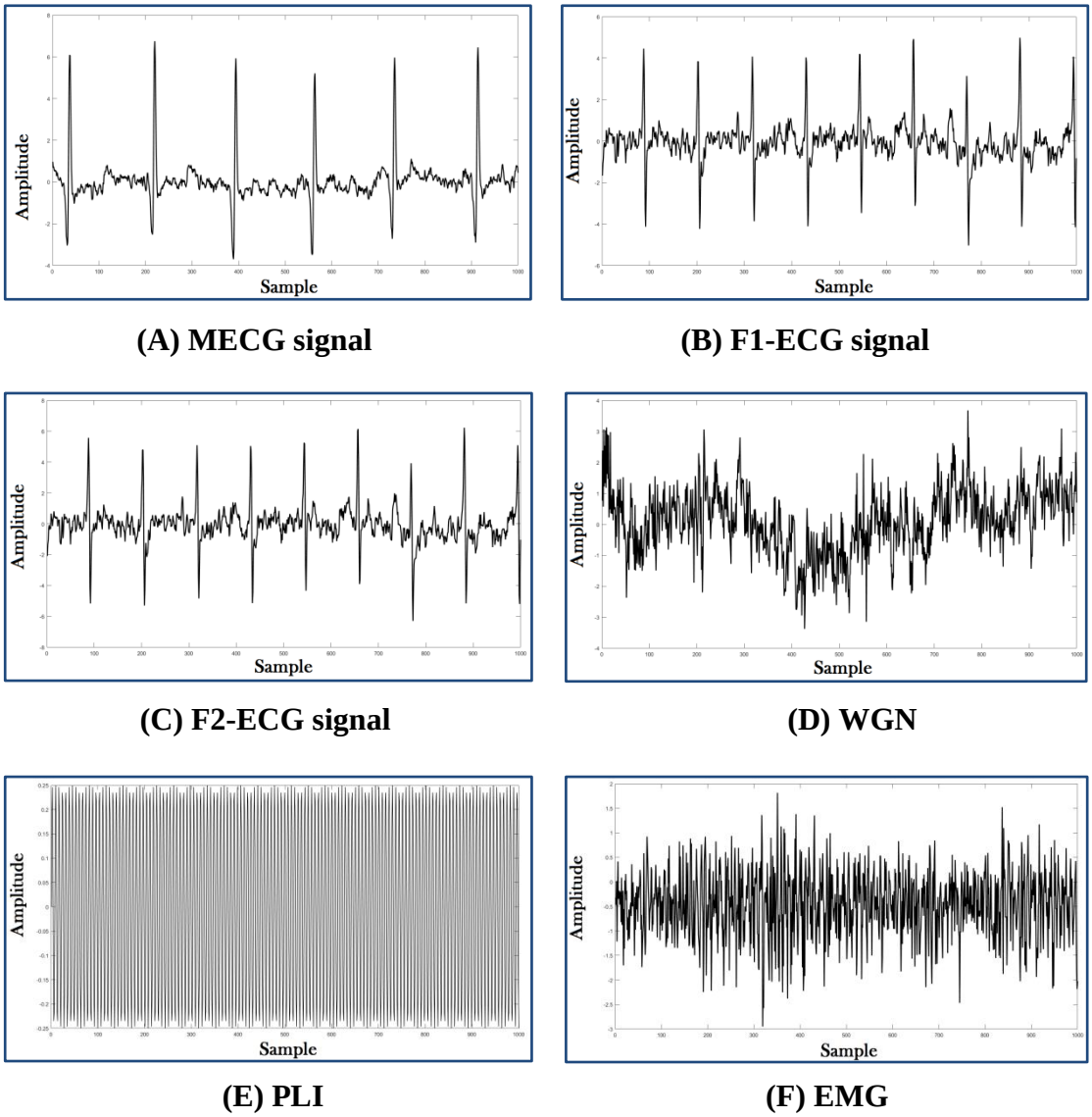

(A) MECG signal **(B) F1-ECG signal**

(C) F2-ECG signal **(D) WGN**

(E) PLI **(F) EMG**

Fig. 4.15 The input signals to simulate twin gestation

After all input signals have been determine, signals are randomly mixed together to get the mixture matrix. Figure 4.16 illustrates the shape of signals after being mixed randomly by the mixing matrix. It also shows how each channel affected by the other channel.

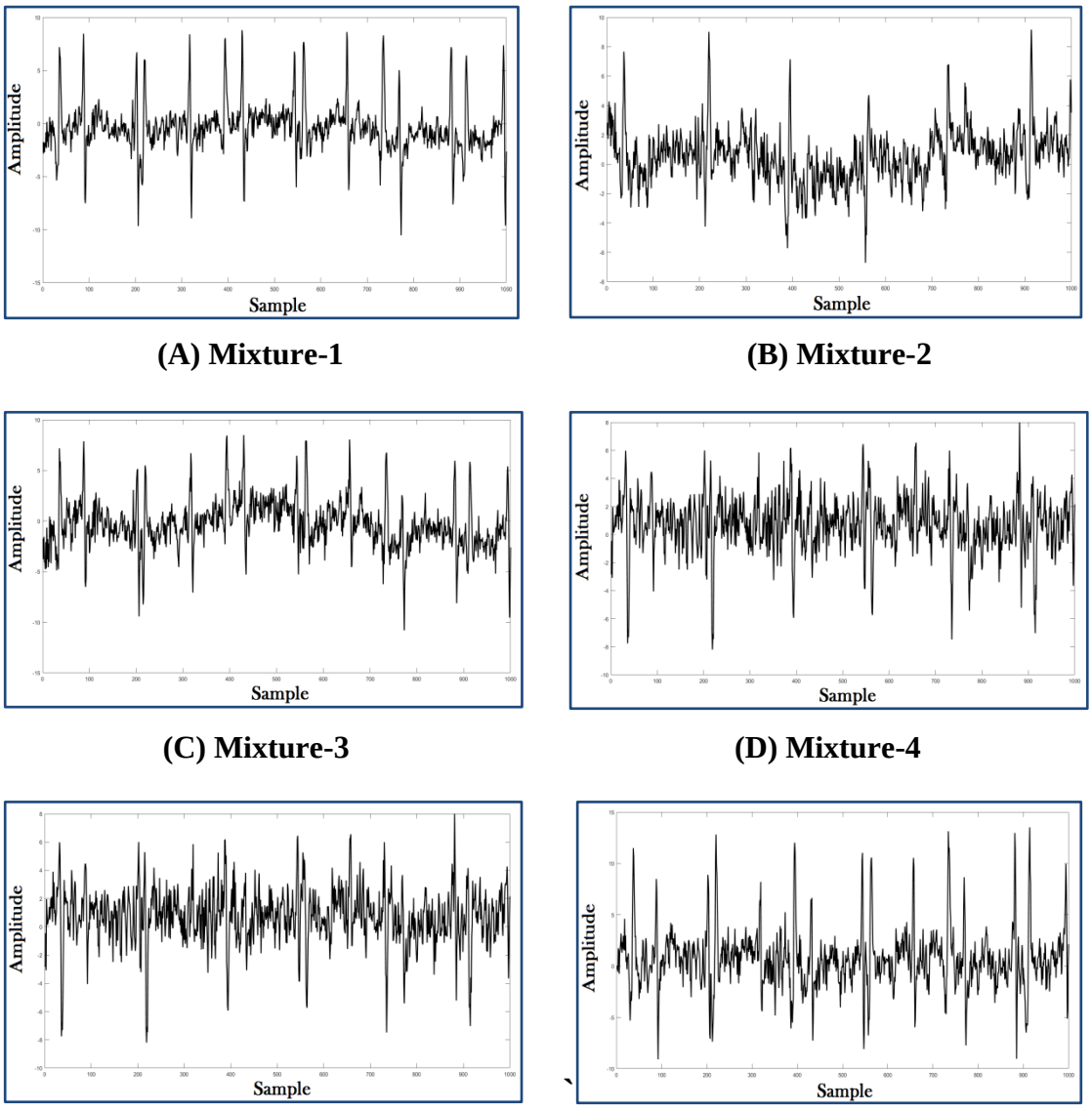

(A) Mixture-1 **(B) Mixture-2**

(C) Mixture-3 **(D) Mixture-4**

(E) Mixture-5 **(F) Mixture-6**

Fig. 4.16 The mixed signals to simulate twin gestation case

Figures 4.17, 4.18 and 4.19 show the recovered signals following the used BSS methods.

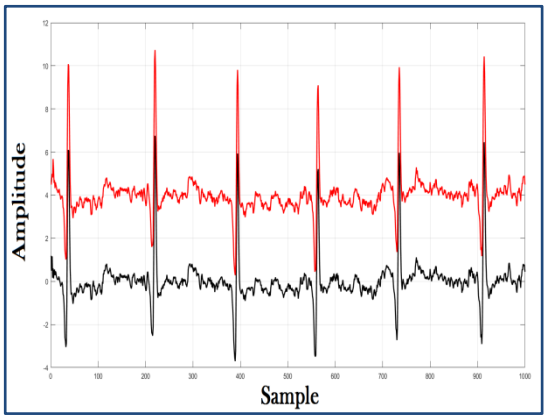

(A) Source and extracted signal

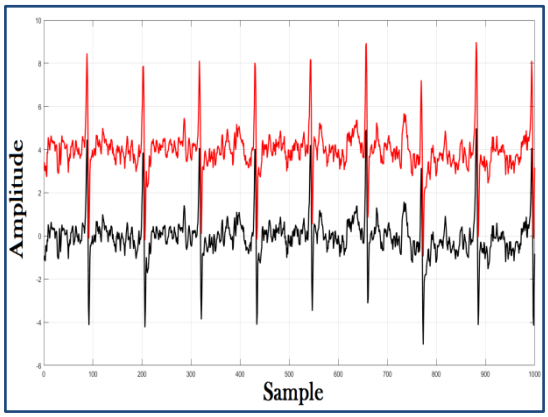

(B) Source and extracted signal

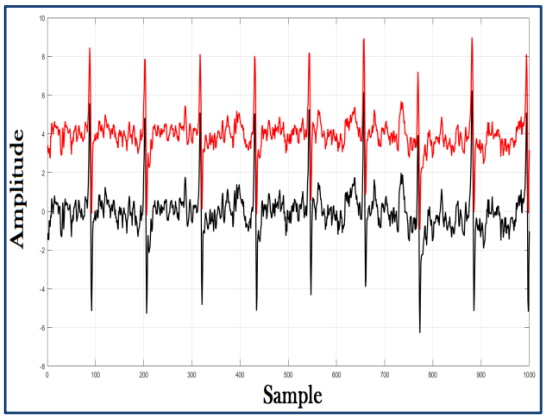

(C) Source and extracted signal

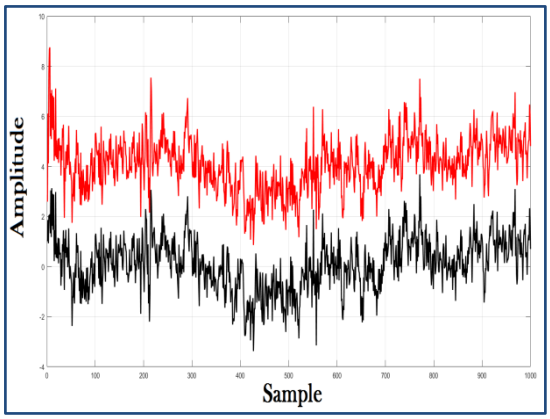

(D) Source and extracted signal

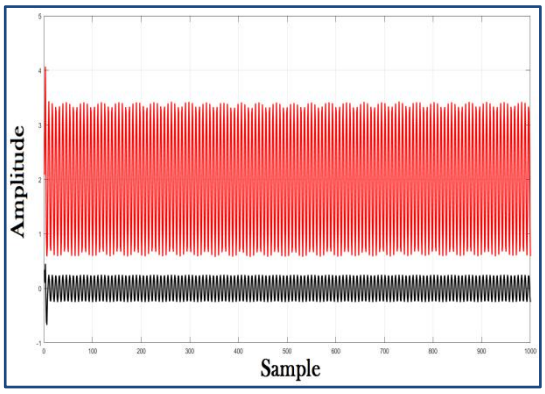

(E) Source and extracted signal

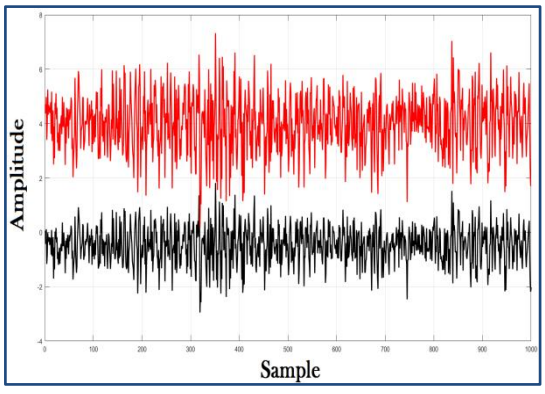

(F) Source and extracted signal

Fig. 4.17 The source and restored signals by Stone BBS algorithm

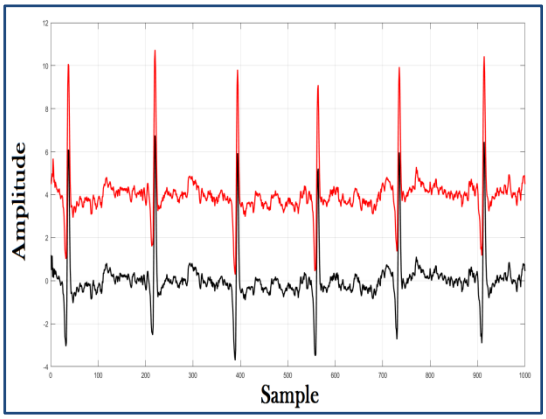

(A) Source and extracted signal

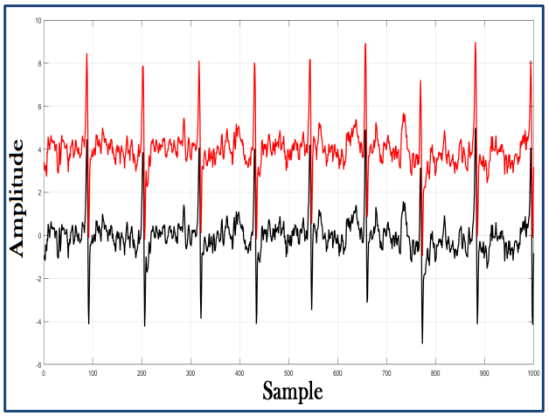

(B) Source and extracted signal

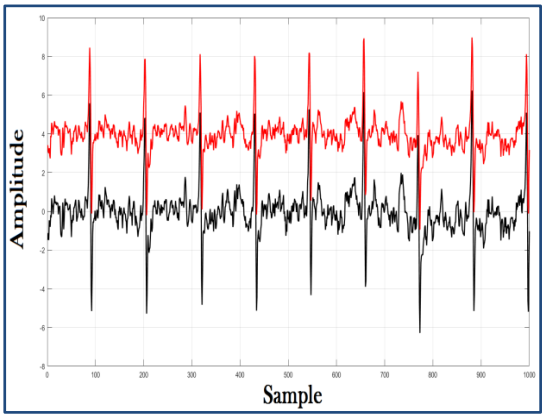

(C) Source and extracted signal

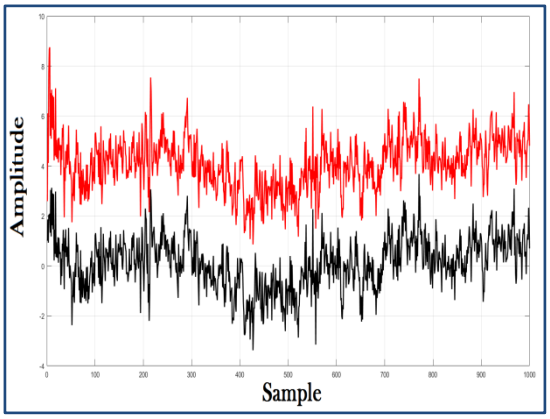

(D) Source and extracted signal

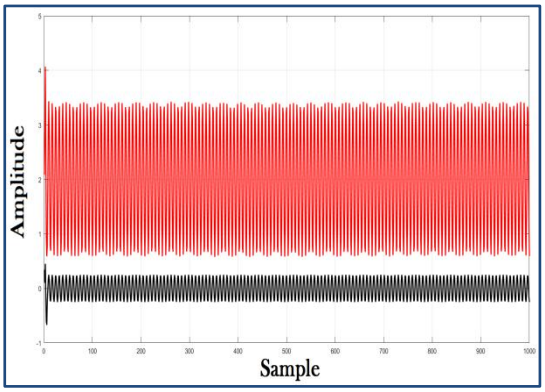

(E) Source and extracted signal

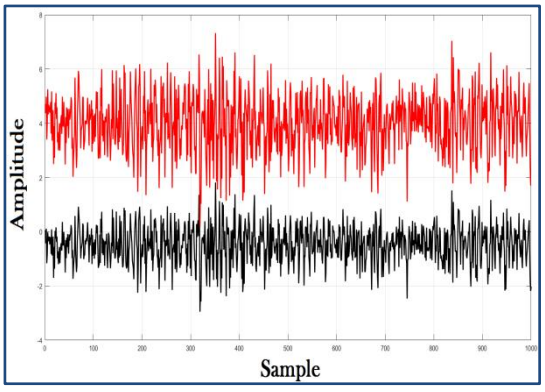

(F) Source and extracted signal

Fig. 4.18 The source and restored signals by EFICA BSS algorithm

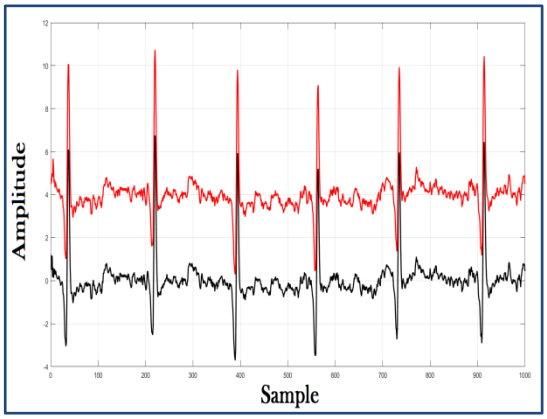

(A) Source and extracted signal

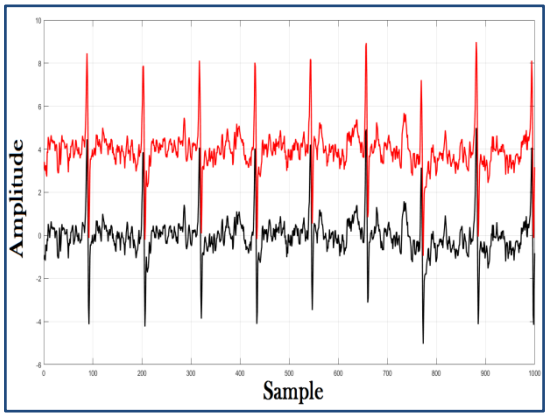

(B) Source and extracted signal

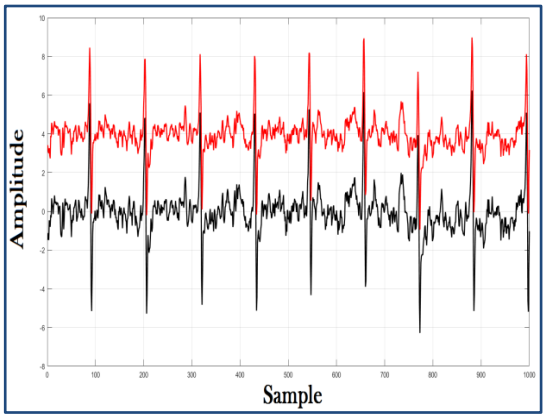

(C) Source and extracted signal

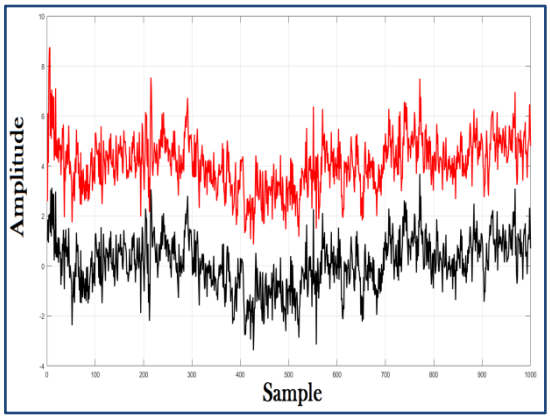

(D) Source and extracted signal

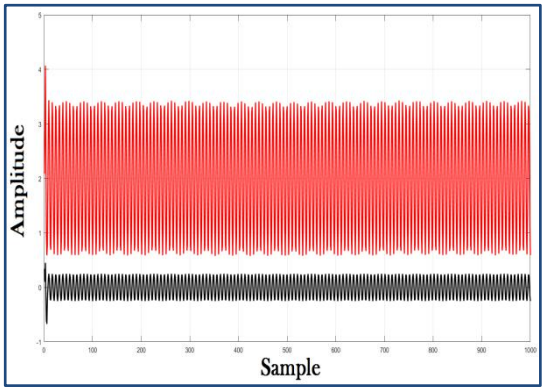

(E) Source and extracted signal

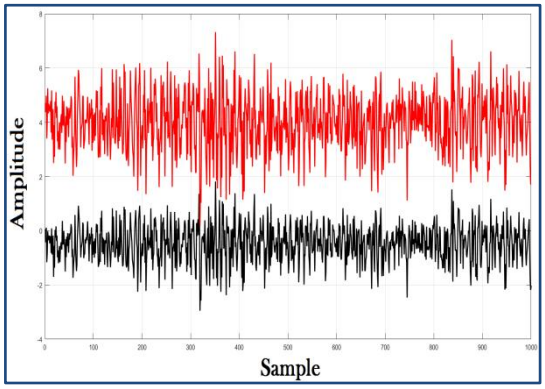

(F) Source and extracted signal

Fig. 4.19 The source and restored signals by JADE BBS algorithm

The red signal represents the recovered signal after using BSS technique while the black signal is the original signal. The above figures do not give an idea about the best BSS algorithm in the extraction of signals whereas all algorithms restore the signals perfectly. To verify the best algorithm, all registered SNR for (MECG, F1-ECG & F2-ECG) are compared in table 4.3.

Table 4.3 The recorded SNR in dB for each signal after each BSS algorithm

NO.	Signal	STONE	EFICA	JADE
1	MECG	16.0870	13.4229	14.0289
2	F1-ECG	26.1084	20.3604	21.6098
3	F2-ECG	13.7739	13.2550	13.3065

Table 4.3 proves that STONE BSS algorithm record the highest value of SNR comparing to the other BSS algorithms. STONE BSS has a better performance to restore and solve the problem of twin gestation than the EFICA and JADE BSS techniques.

Table 4.4 demonstrates the fitness between the restored signal and the original signal. STONE algorithm registers the highest value as well.

Table 4.4 The percentage of correlation between recovered and original signals

NO.	Signal	STONE	EFICA	JADE
1	MECG	98.77 %	89.55 %	90.4 %
2	F1-ECG	99.55 %	97.73 %	98.09 %
3	F2-ECG	95.92 %	88.59 %	89.62 %

4.3 PART- 2

The obtained results in this part are calculated depending on the modified Stone BSS. Modified Stone BSS has been demonstrated in Chapter Three.

4.3.1 CASE 1 The Abio-7 dataset

The same Abio-7 data, which has been used for testing the performance of the three used BSS algorithms (JADE, EFICA and Stone) are also used for testing the performance of MSBSS and comparing the achieved result with the results that have been obtained in Part-1.

Figure 4.20 illustrates the performance of the prepared fitness function. It shows how the fitness function descending from higher value toward zero during iterations changes in the same time the values of the long and short term.

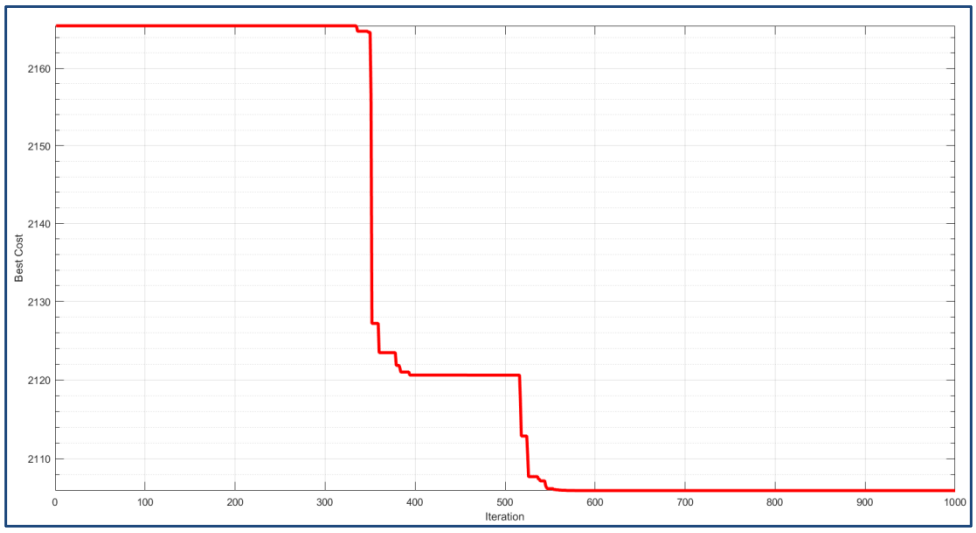

Fig. 4.20 The performance of the prepared fitness function of PSO for case-1

Figures 4.21 and 4.22 show how SNR and ISR values fluctuate during iterations depending on how the obtained values of long and short term change due to the performance of the fitness function.

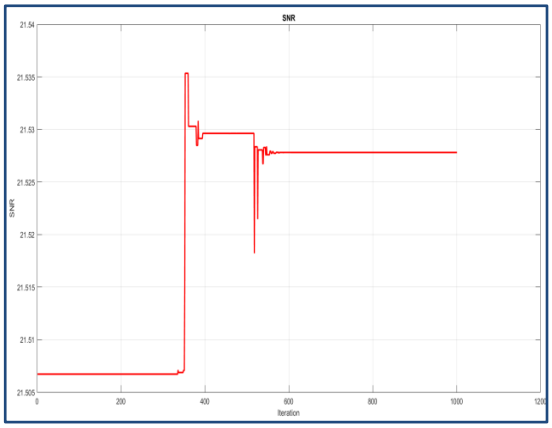

Fig. 4.21 The relation between SNR and iterations

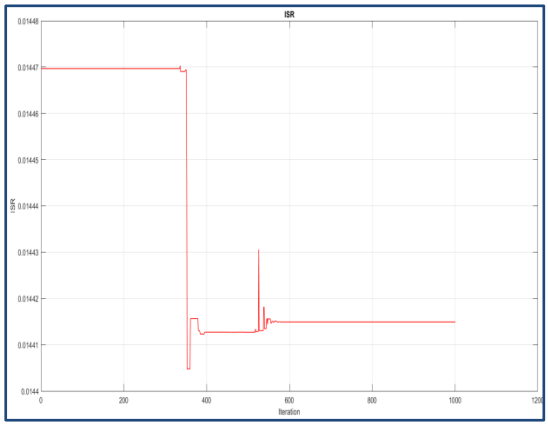

Fig. 4.22 The relation between ISR and iterations

After obtaining the best values for long and short term, the next step is setting the suitable value for max mask length. For original Stone BSS algorithm the max mask length is equal to 500. In this step the number is kept equal to 500, but the number of lives to make mask is changed to be (3) instead of (8) which is set by original Stone.

Figure 4.23 illustrates the recovered signal by MSBSS method. The signal with blue color denote to the extracted signal while the black one denotes the source signal.

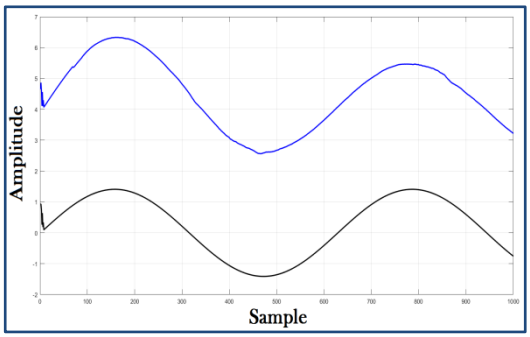

(A) Source and extracted signal

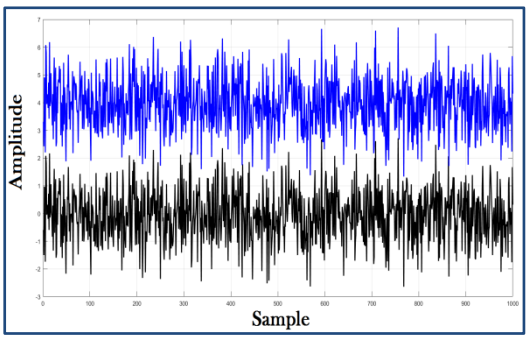

(B) Source and extracted signal

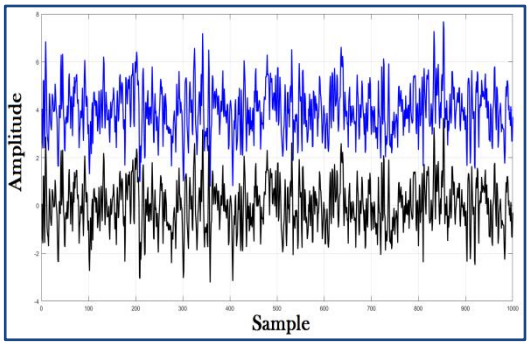

(C) Source and extracted signal

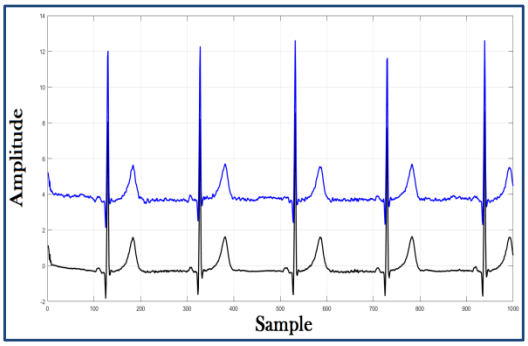

(D) Source and extracted signal

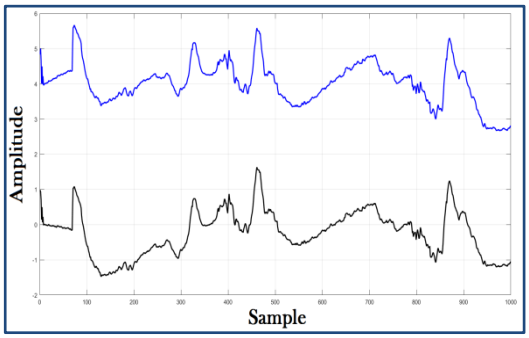

(E) Source and extracted signal

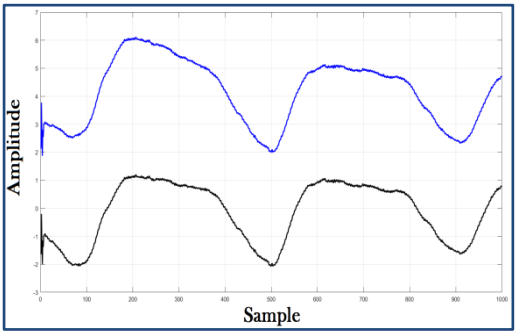

(F) Source and extracted signal

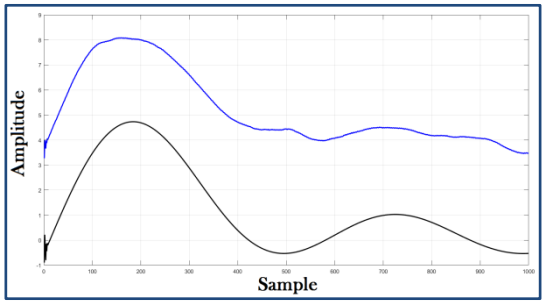

(G) Source and extracted signal

Fig. 4.23 The source and restored signals by MSBBS algorithm for Case-1

Tables 4.5 and 4.6 illustrate the recorded average of SNR and ISR as each one uses algorithm, including the MSBSS.

Table 4.5 The recorded average SNR in dB for each single algorithm

NO.	BSS Algorithm	Recorded Average SNR
1	STONE	16.88
2	EFICA	22.36
3	JADE	14.47
4	MSBSS	17.61

Table 4.6 The recorded average ISR in dB for each single algorithm

NO.	BSS Algorithm	Recorded Average ISR
1	STONE	-16.88
2	EFICA	-22.36
3	JADE	-14.47
4	MSBSS	-17.61

Tables 4.5 and 4.6 MSBSS records higher SNR and ISR values than original Stone and JADE. However it still records lower SNR and ISR than EFICA algorithm.

4.3.2 CASE 2: Single Pregnancy

MSBSS is also applied to process the same dataset which has been used in Part-1 (DaSIy dataset). Figure 4.24 shows the relation between fitness function and iterations.

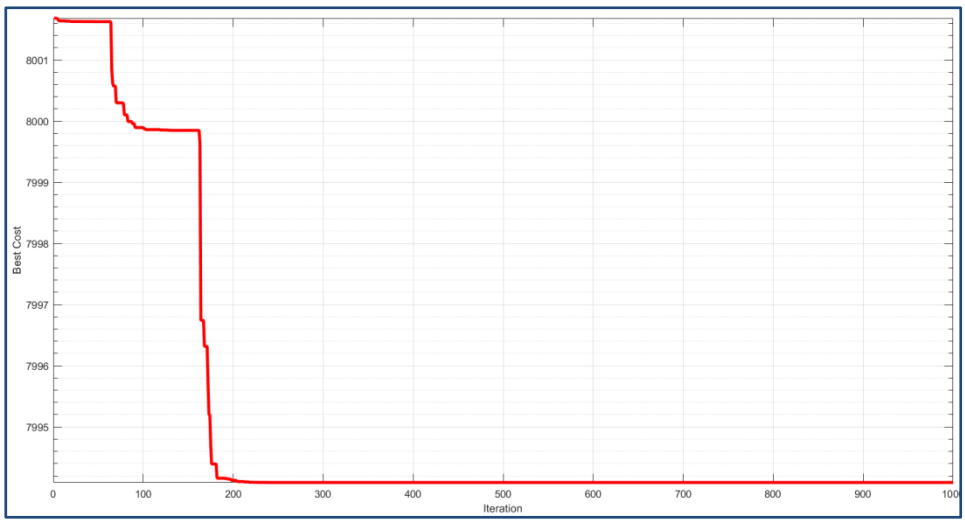

Fig. 4.24 The performance of the prepared fitness function of PSO for case-2

After obtaining the optimum values for long and short terms, the max mask length is set to equal 140. Selecting the value of the max mask length to be 140 is not arbitrary. FHR in normal case is between 140 to 160, so the selection of the max mask length depends on the value of the FHR. After setting the value of max mask length then the value of number of lives is needed to be set as well. Setting the number of lies to make mast is too important and affects directly on the recorded PSD for MECG and FECG. The value of the number of lives is set to get the best result PSD related to FECG signal since it represents the desired signal. Number of lives to make mask is set to 8.

Figure 4.25 illustrates the extracted MECG and FECG from the real 8 - channels signal.

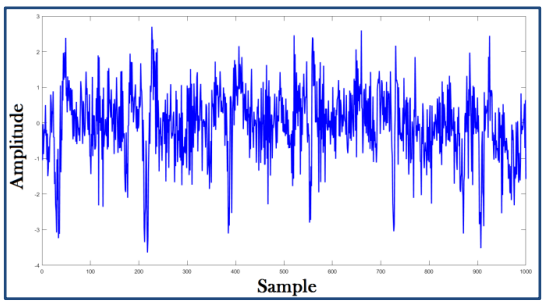

(A) Recovered signal Channel-1

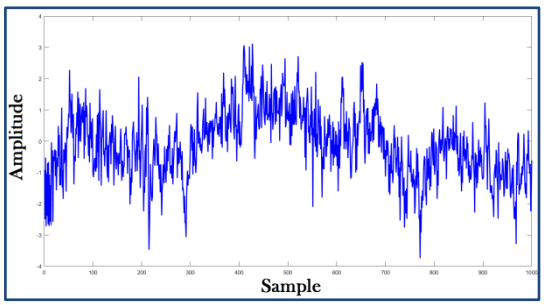

(B) Recovered signal Channel-2

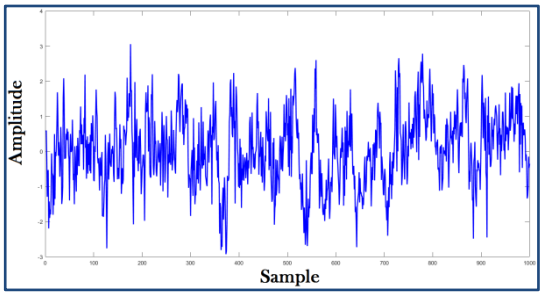

(C) Recovered signal Channel-3

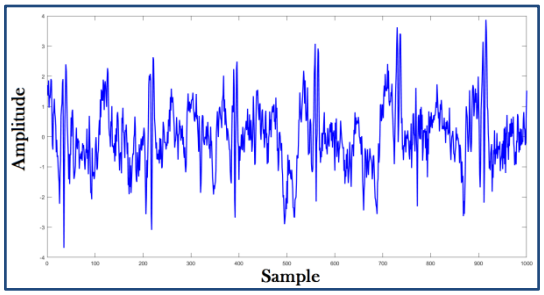

(D) Recovered signal Channel-4

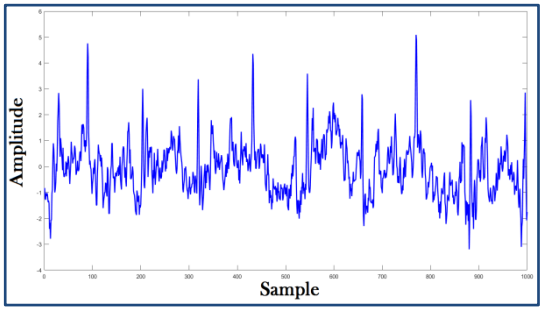

(E) Recovered signal Channel-5

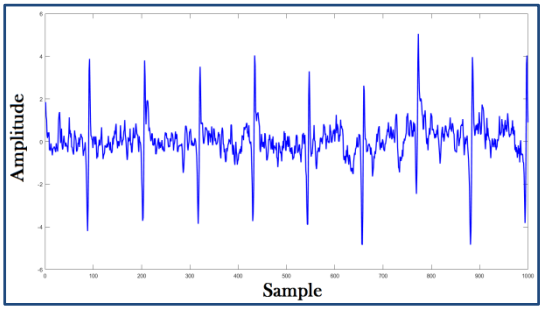

(F) Recovered Fetal signal Channel-6

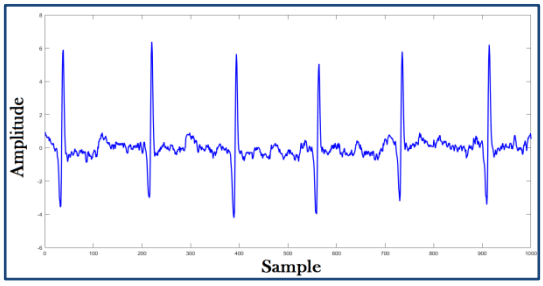

(G) Recovered Mother signal Channel-7

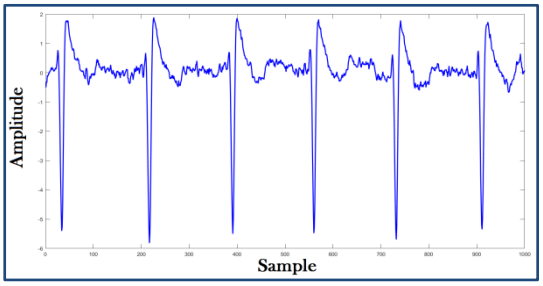

(H) Recovered signal Channel-8

Fig. 4.25 The extracted signals by MSBSS algorithm

Figures 4.26 and 4.27 represent the recorded PSD for the MECG signal and FECG signal respectively. Table 4.7 shows recorded PSD for MECG and FECG signal after every used BSS.

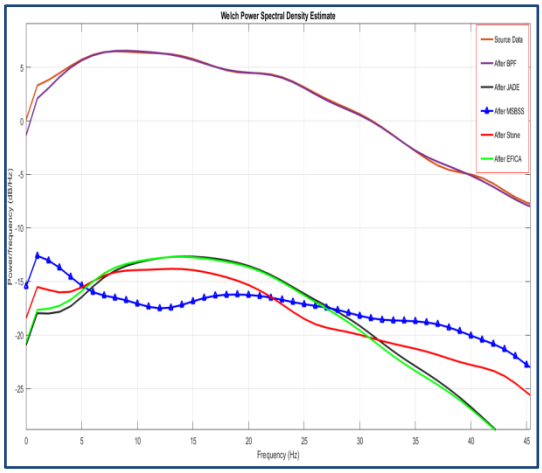

Fig. 4.26 The recorded PSD for MECG signal

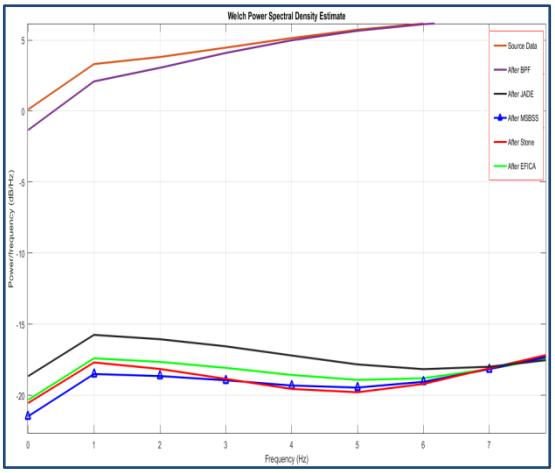

Fig. 4.27 The recorded PSD for FECG signal

Table 4.7 The recorded PSD for each signal

No.	Signal	Real signal	Total power after BPF	Total power after STONE	Total power after EFICA	Total power after JADE	Total power after MSBSS
1	FECG	101.3480	99.8504	0.8340	0.8727	0.8623	0.8078
2	MECG	101.3480	99.8504	1.1098	1.0409	1.0289	1.1143

4.3.3 CASE 3: Twin Pregnancy Semi-Simulated Data

The same inputs which have been used in Case-3 in Part-1 will be used for simulating twin case. All signals are randomly mixed together to create the mixture matrix. Then, the mixture matrix is a new input to MSBSS. Figure 4.28 shows the performance of the fitness function during iterations. It shows how the function starts descending from higher value toward zero.

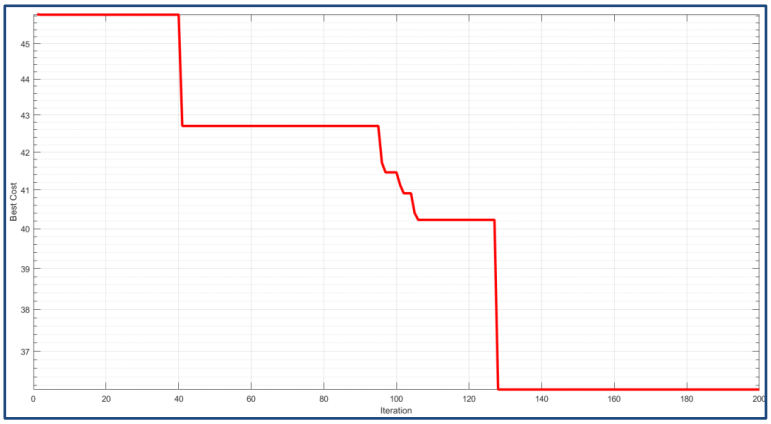

Fig. 4.28 The performance of the prepared fitness function of PSO for Case-3

SNR and ISR have been also calculated during iterations. Figures (4.29 and 4.30) show how the values of SNR and ISR change during iteration. The fluctuation in the values of SNR and ISR occurs due to the performance of the fitness function.

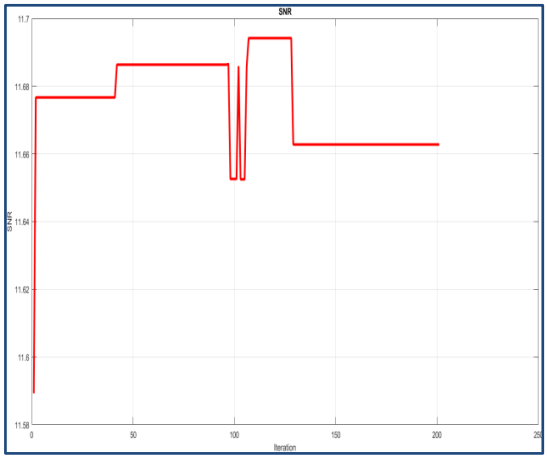

Fig. 4.29 The relation between SNR and iterations

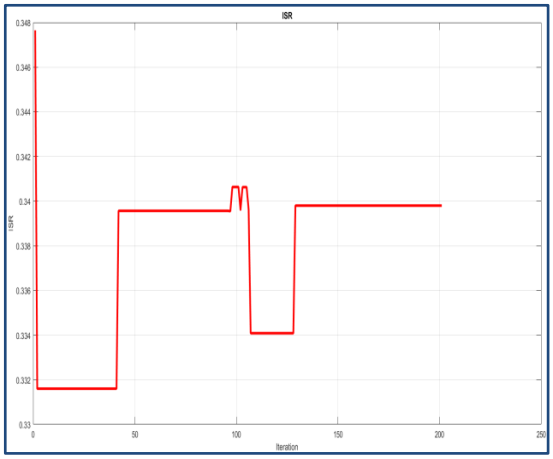

Fig. 4.30 The relation between ISR and iterations

After obtaining the optimum values for long and short term, the value of max mask length and number of lives to make mask are also needed to be set. As mentioned in Case-2 the value of max mask length would set to 140. The number of lives to make mask is equal to 2 instead

of 8 which has been set by original Stone. Figure 4.31 illustrates the extracted and source signals. The signals with blue color represent the extracted signals, while the signals with black color represent the source signals.

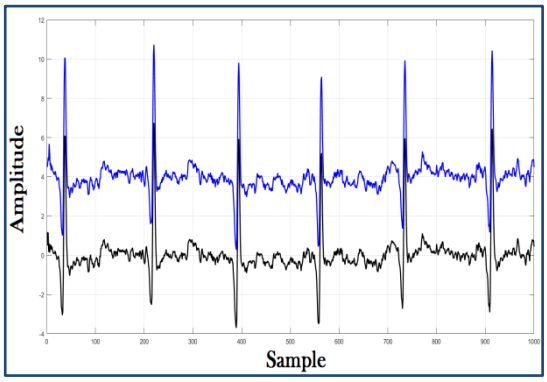

(A) Source and extracted signal

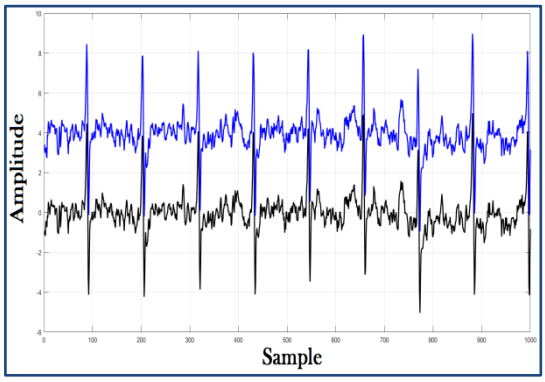

(B) Source and extracted signal

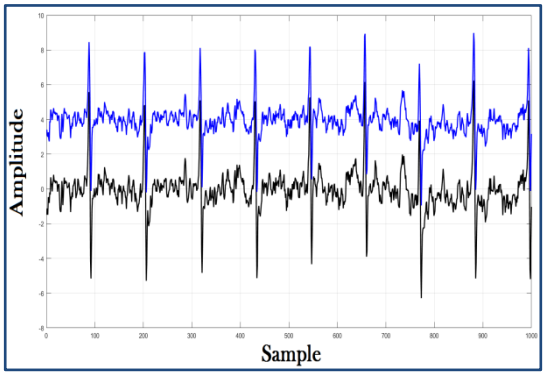

(C) Source and extracted signal

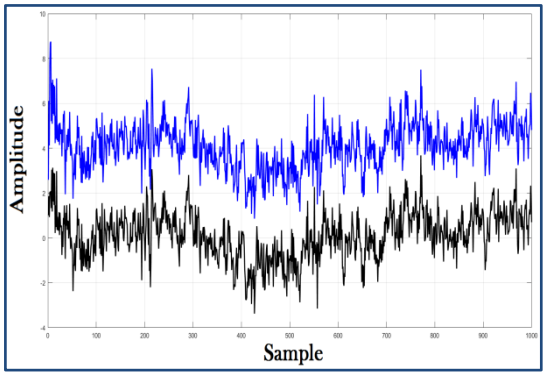

(D) Source and extracted signal

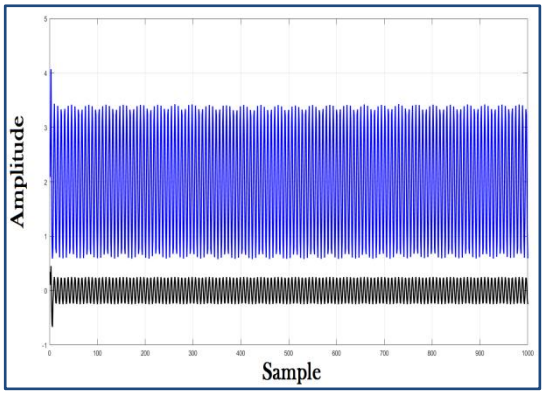

(E) Source and extracted signal

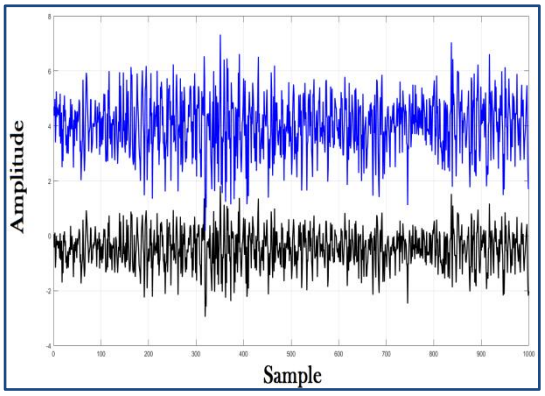

(F) Source and extracted signal

Fig. 4.31 The source and restored signals by MSBBS algorithm for Case-3

Tables 4.8 and 4.9 show the calculated SNR and ISR for each extracted signal.

Table 4.8 The recorded SNR in dB for each signal after each BSS algorithm

NO.	Signal	STONE	EFICA	JADE	MSBSS
1	**MECG**	**16.0870**	**13.4229**	**14.0289**	**23.9044**
2	**F1-ECG**	**26.1084**	**20.3604**	**21.6098**	**27.7191**
3	**F2-ECG**	**13.7739**	**13.2550**	**13.3065**	**13.8268**

Table 4.9 The recorded ISR in dB for each signal after each BSS algorithm

NO.	Signal	STONE	EFICA	JADE	MSBSS
1	**MECG**	**-16.0870**	**-13.4229**	**-14.0289**	**-23.9044**
2	**F1-ECG**	**-26.1084**	**-20.3604**	**-21.6098**	**-27.7191**
3	**F2-ECG**	**-13.7739**	**-13.2550**	**-13.3065**	**-13.8268**

Chapter Five

Conclusion and Suggestions for Future Work

CHAPTER FIVE
Conclusion and Suggestions for Future Work

5.1 Conclusion

The thesis demonstrates the need for reliable blind source separation technique to deal with the problem of fetal ECG extraction. It also shows that the abdominal ECG comes with different types of noises and interferences which need to be removed in order to obtain a clean ECG signal. The extraction of fetal ECG for twin case gestation has been also discussed.

In this research, Stone BSS algorithm has been utilized for the first time to deal with the problem of extracting fetal ECG. Furthermore, Stone algorithm is applied to separate between ECG signals of twin fetuses.

Different kinds of simulation have been used including different datasets. DaSIy dataset which has real in-vivo data for single fetal pregnancy; ABio-7 dataset which is obtained from ICALAB and simulated data for twin case gestation, represent the source data to this work.

In this research none of the traditional filters have been used. The reason of not using filters is to avoid losing some useful information since filters do not have perfect and ideal cutoff frequency. This may lead to waste part of the ECG signal.

The contribution of this thesis is a Modified Stone Blind Source Separation (MSBSS method). This method records higher results than the

other BSS techniques. The proposed algorithm is produced by combination of one of the soft computing algorithms (PSO) and Stone - BSS. The calculated Signal to Noise Ratio (SNR) and Power spectrum density (PSD) represent the performance index which have been used for comparing between the used algorithms (EFICA, JADE, Stone and MSBSS). The obtained results in this thesis are divided into three cases.

Case-1 depends on the ABio-7 data set as the source data to be mixed and then to be extracted. After that the SNR for each signal is calculated to every BSS technique. The aim of this case is to test the performance of each single BSS algorithm.

Case-2 uses the DaSIy real dataset to extract the mother ECG and fetal ECG. PSD is calculated for each technique to be compared. MSBSS records the best value of PSD in respect to fetal ECG as compared to the other BSS techniques.

Case-3 uses the simulated data to satisfy the case of twin gestation. The recorded SNR for mother and fetuses by MSBSS are high comparing with the other BSS techniques.

5.2 Suggestions for future work

With regard to the suggested future work, the obtained results by MSBSS are very encouraging to design and implement hardware equipment in future for recording and processing abdominal ECG having the MSBSS as an operating system.

In future, designing an algorithm that works with the fuzzy system concept to diagnose the health situation of fetal during gestation and works closely with MSBSS would be helpful. indeed the obtained results

by MSBSS is an accurate results and that provide an accurate diagnosis for defects which infect the heart of fetus for single and twin pregnancy.

Replacing the used optimization technique (PSO) to make modifications on Stone BSS with other developed optimization techniques like Shark Smell Optimization (SSO), Dolphin Swarm Optimization (DSO) and Gray Wolf Optimization (GWO) improve the performance of Stone BSS. This helps to get better results.

5.3 Limitations and Drawbacks

From the obtained results and specially CASE-1 in each part, Stone algorithm and MSBSS are not the most suitable algorithm to deal with the (Gaussian, Sub Gaussian and Supper Gaussian) signals. The algorithms is limited to deal with the problem of linear mixed signals only and not suitable for nonlinear mixed signal.

References

[1] A. V Rajesh and R. Ganesan, “Comprehensive study on fetal ECG extraction,” in 2014 International Conference on Control, Instrumentation, Communication and Computational Technologies, ICCICCT 2014, 2014.

[2] Reza Sameni, and Gari D. Clifford, “A Review of Fetal ECG Signal Processing Issues and Promising Directions,” The Open Pacing Electrophysiology & Therapy Journal, January 2010.

[3] A. Gupta, M. C. Srivastava, V. Khandelwal, and A. Gupta, “A novel approach to fetal ECG extraction and enhancement using Blind Source Separation (BSS-ICA) and adaptive fetal ECG enhancer (AFE),” in 2007 6th International Conference on Information, Communications and Signal Processing, ICICS, 2007, pp. 983–987.

[4] S. Comani, D. Mantini, G. Alleva, E. Gabriele, M. Liberati, and G. L. Romani, “Simultaneous monitoring of separate fetal magnetocardiographic signals in twin pregnancy,” Physiol. Meas., vol. 26, pp. 193–201, 2005.

[5] P. Comon and E. Jutten, “Handbook of Blind Source Separation: Independent Component Analysis and Applications,” in Handbook of Blind Source Separation Independent Component Analysis and Applications, 1st ed., Academic Press, 2009, p. 779_814.

[6] PubMed, “,” The U.S. National Library of Medicine and the National Institutes of Health, 2008. .

[7] L. S. Lilly, Pathophysiology of heart disease: a collaborative project of medical students and faculty, 6th ed. Lippincott Williams & Wilkins, 2012.

[8] E. A. Muirhead, “Muirhead 1848-1920,” Oxford Dictionary of National Biography. Oxford, Blackwell, 1926.

[9] J. V. Moises Rivera-Ruiz, Christian Cajavilca, “Einthoven’s String Galvanometer,” Tex. Heart Inst. J., vol. 35, no. 2, pp. 174–178, 2008.

[10] B. Guide, E. C. G. Interpretation, and M. Roman, Text Atlas of Practical Electrocardiography. .

[11] K.-C. Lai and J. J. Shynk, “A successive cancellation algorithm for fetal heart-rate estimation using an intrauterine ECG signal,” IEEE Trans. Biomed. Eng., vol. 49, no. 9, p. 943_954, 2002.

[12] B. De Moor, “Database for the Identification of Systems (DaISy).” 1997.

[13] A. L. Goldberger et al., “PhysioBank, PhysioToolkit, and PhysioNet,Components of a New Research Resource for Complex Physiologic Signals,” Circulation, vol. 110, no. 23, p. e215_e220, 2000.

[14] G. Walraven, ENCYCLOPEDIA OF MEDICAL DEVICES AND INSTRUMENTATION, 2nd ed., vol. 5. 2007.

[15] P. Várady, L. Wildt, Z. Benyó, and A. Hein, “An advanced method in fetal phonocardiography,” Comput. Methods Programs Biomed., vol. 71,

no. 3, p. 283_296, 2003.
[16] S. L. Bloom et al., “Fetal Pulse Oximetry and Cesarean Delivery,” Natl. Inst. Child Heal. Hum. Dev. Matern. Med. Units Netw., vol. 355, no. 21, p. 2195_2202, 2006.
[17] M. G. Signorini, G. Magenes, S. Cerutti, and D. Arduini, “Linear and nonlinear parameters for the analysis of fetal heart rate signal from cardiotocographic recordings,” IEEE Trans. Biomed. Eng., vol. 50, no. 3, p. 365_374, 2003.
[18] H. J. M. ter Brake et al., “Fetal magnetocardiography: clinical relevance and feasibility,” Phys. C Supercond., vol. 368, no. 1, pp. 10–17, 2002.
[19] P. Kligfield et al., “Recommendations for the standardization and interpretation of the electrocardiogram: part I: The electrocardiogram and its technology: a scientific statement from the American Heart Association Electrocardiography and Arrhythmias Committee, Council on Cli,” Circulation, vol. 115, no. 10. Journal of the American College of Cardiology, p. 1306_1324, 2007.
[20] A. Velayudhan and S. Peter, “Noise Analysis and Different Denoising Techniques of ECG Signal - A Survey,” in IOSR Journal of Electronics and Communication Engineering (IOSR-JECE), 2016, p. 40_44.
[21] J. G. Stinstra, “The reliability of the fetal magnetocardiogram,” Universiteit Twente, 2001.
[22] L. K. Hornberger and D. J. Sahn, “Rhythm abnormalities of the fetus,” Heart, vol. 93, no. 10, p. 1294_1300, 2007.
[23] E. Osei and K. Faulkner, “Fetal position and size data far dose estimation,” Br. J. Radiol., vol. 72, no. 856, p. 363_370, 1999.
[24] J. B. Roche and E. H. Hon, “The fetal electrocardiogram: V. Comparison of lead systems,” Am. J. Obstet. Gynecol., vol. 92, no. 8, p. 1149_1159, 1965.
[25] T. Rasheed, “Constrained blind source separation of human brain signals,” Department of Computer Engineering, Kyung Hee University, Seoul …, Seoul, 2010.
[26] A. K. Abdullah, Z. C. Zhu, L. Siyao, and S. M. Hussein, “Blind Source Separation Techniques Based Eye Blinks Rejection in EEG Signals,” Inf. Technol. J., vol. 13, no. 3, pp. 401–413, 2014.
[27] B. Ans, J. Herault, and C. Jutten, Adaptive neural architectures : Detection of primitives. Paris, 1985.
[28] B. Gao, “Single Channel Blind Source Separation,” Newcastle university, Newcastle, 2011.
[29] S. M. Hussein, “Design and Implementation of AI Controller Based on Brain Computer Interface,” Nahrain University, Baghdad, 2007.
[30] A. Hyvarinen, J. Karhunen, and E. Oja, Independent Component Analysis. New York: J. Wiley, 2001.
[31] M. Keralapura, M. Pourfathi, and B. Sirkeci-Mergen, “Impact of contrast functions in Fast-ICA on twin ECG separation,” IAENG Int. J. Comput. Sci., vol. 38, p. 1, 2011.
[32] Z. Chaozhu, A. K. Abdullah, and A. A. Abdullah,

"Electroencephalogram-Artifact Extraction Enhancement Based on Artificial Intelligence Technique," vol. 27, pp. 77–91, 2016.
[33] A. K. Abdullah and Z. C. Zhu, "Enhancement of Source Separation Based on Efficient Stone's BSS Algorithm," Int. J. Signal Process. Image Process. Pattern Recognit., vol. 7, no. 2, pp. 431–442, 2014.
[34] J. V Stone, "Blind deconvolution using temporal predictability," Neurocomputing, vol. 49, no. 1–4, pp. 79–86, 2002.
[35] J. V Stone, "Blind source separation using temporal predictability," Neural Comput., vol. 13, no. 7, pp. 1559–1574, 2001.
[36] J. V Stone, Independent component analysis: a tutorial introduction. MIT press, 2004.
[37] P. Tichavsk, "EXTENSION OF EFICA ALGORITHM FOR BLIND SEPARATION OF PIECEWISE STATIONARY NON GAUSSIAN SOURCES Zbyn˘ ek Koldovsk ´ Faculty of Mechatronic and Interdisciplinary Studies Technical University of Liberec , H ´ alkova 6 , 461 17 Liberec , Czech Republic Institute of Information Theory and Automation , P . O . Box 18 , 182 08 Prague 8 , Czech Republic Universit ´ e Paul Sabatier Toulouse 3 - Observatoire Midi-Pyr ´ en ´ ees - CNRS , Laboratoire d ' Astrophysique de Toulouse-Tarbes , 14 Av . Edouard Belin , 31400 Toulouse , France," pp. 2–5.
[38] R. Roy and M. S. Bepari, "Blind Source Separation : A Review and Analysis."
[39] R. Kalatehjari, A. S. A Rashid, N. Ali, and M. Hajihassani, "The contribution of particle swarm optimization to three-dimensional slope stability analysis," Sci. World J., vol. 2014, no. June, 2014.
[40] R. Poli, "Analysis of the Publications on the Applications of Particle Swarm Optimisation," J. Artif. Evol. Appl., vol. 2008, no. 2, pp. 1–10, 2008.
[41] S. D. Larks, "Present Status of Fetal Electrocardiography," Ire Trans. Biomed. Electron., vol. 9, no. 3, pp. 176–180, 1962.
[42] N. J. Outram, E. C. Ifeachor, P. W. J. V Eetvelt, and J. S. H. Curnow, "Techniques for optimal enhancement and feature extraction of fetal electrocardiogram," IEE Proc. - Sci. Meas. Technol., vol. 142, no. 6, p. 482_489, 1995.
[43] W. Xueyun and Z. Wei, "Application of kernel PCA for foetal ECG estimation," Electron. Lett., vol. 54, no. 6, pp. 340–342, 2018.
[44] E. Fotiadou, "Enhancement of low-quality fetal electrocardiogram based on time-sequenced adaptive filtering," 2018.
[45] M. Shao, K. E. Barner, and M. H. Goodman, "An interference cancellation algorithm for noninvasive extraction of transabdominal fetal electroencephalogram (TaFEEG)," IEEE Trans. Biomed. Eng., vol. 51, no. 3, pp. 471–483, 2004.
[46] P. D. Kushwaha, R. Narvey, and D. K. Verma, "Extraction Methods of Fetal ECG from Mother ECG Signal in Pregnancy," Int. J. Adv. Res. Comput. Commun. Eng., vol. 2, no. 6, pp. 2411-?, 2013.
[47] R. Sameni, "Extraction of Fetal Cardiac Signals from an Array of

Maternal Abdominal Recordings," Sharif University of Technology (SUT), 2008.
[48] R. Sameni, M. B. Shamsollahi, C. Jutten, and G. D. Clifford, "A Nonlinear Bayesian Filtering Framework for ECG Denoising," IEEE Trans. Biomed. Eng., vol. 54, no. 12, p. 2172_2185, 2007.
[49] A. M. Kaleem and R. D. Kokate, Performance Evaluation of Fetal ECG Extraction Algorithms. Springer Singapore.
[50] R. Kahankova, R. Martinek, and P. Bilik, "Non-invasive Fetal ECG Extraction from Maternal Abdominal ECG Using LMS and RLS Adaptive Algorithms," 2018.
[51] R. Sameni, M. B. Shamsollahi, and C. Jutten, "Model-based Bayesian filtering of cardiac contaminants from biomedical recordings," Physiol. Meas., vol. 29, no. 5, pp. 595–613, 2008.
[52] C. Li, C. Zheng, and C. Tai, "Detection of ECG characteristic points using wavelet transforms," IEEE Trans. Biomed. Eng., vol. 42, no. 1, pp. 21–28, 1995.
[53] A. H. Khamene and S. Negahdaripoure, "A new method for the extraction of fetal ECG from the composite abdominal signal," IEEE Trans. Biomed. Eng., vol. 47, no. 4, p. 507_516, 2000.
[54] S. Gaamouri, M. B. Salah, and R. Hamdi, "Denoising ECG Signals by Using Extended Kalman Filter to Train Multi-Layer Perceptron Neural Network 1," vol. 52, no. 6, pp. 528–538, 2018.
[55] M. Akay and E. Mulder, "Examining fetal heart-rate variability using matching pursuits," IEEE Eng. Med. Biol. Mag., vol. 15, no. 5, p. 64_67, 1996.
[56] H. He, Y. Tan, and Y. Wang, "Optimal base wavelet selection for ECG noise reduction using a comprehensive entropy criterion," Entropy, vol. 17, no. 9, pp. 6093–6109, 2015.
[57] M. S. S. Manjula, "Enhancement of SNR in fetal ECG signal extraction using combined SWT and WLSR in parallel EKF," Cluster Comput., vol. 4, 2018.
[58] P. P. Kanjilal, S. Palit, and G. Saha, "Fetal ECG extraction from single-channel maternal ECG using singular value decomposition," IEEE Trans. Biomed. Eng., vol. 44, p. 51_59, 1997.
[59] V. ZARZOSO, A. K. NANDI, and E. BACHARAKIS, "Maternal and foetal ECG separation using blind source separation methods," Math. Med. Biol. A J. IMA, vol. 14, no. 3, pp. 207–225, 1997.
[60] V. Zarzoso and A. K. Nandi, "Comparison between blind separation and adaptive noise cancellation tecmiuques for fetal electrocardiogram extraction," in IEE Colloquium on Medical Applications of Signal Processing, 1999, pp. 1/1--1/6.
[61] Z. L. Zhang and Z. Yi, "Extraction of temporally correlated sources with its application to non-invasive fetal electrocardiogram extraction," Neurocomputing, vol. 69, no. 7–9, p. 894_899, 2006.
[62] Y. Li and Z. Yi, "An algorithm for extracting fetal electrocardiogram," Neurocomput, vol. 71, no. 7–9, p. 1538_1542, 2008.

[63] M. B. Dembrani, K. B. Khanchandani, and A. Zurani, “Extraction of FECG Signal Based on Blind Source Separation Using Principal Component Analysis,” pp. 173–180, 2018.
[64] V. Ionescu and M. Hnatiuc, “Fetal heart rate detection and monitoring from noninvasive abdominal ECG recordings,” 2015 E-Health Bioeng. Conf. EHB 2015, vol. 2, pp. 5–8, 2016.
[65] R. Sameni, C. Jutten, and M. B. Shamsollahi, “Multichannel electrocardiogram decomposition using periodic component analysis,” IEEE Trans. Biomed. Eng., vol. 55, no. 8, p. 1935_1940, 2008.
[66] R. Sameni, C. Jutten, and M. B. Shamsollahi, “A deflation procedure for subspace decomposition,” IEEE Trans. Signal Process., vol. 58, no. 4, p. 2363_2374, 2010.
[67] T. Schreiber and D. T. Kaplan, “Nonlinear noise reduction for electrocardiograms,” Chaos, vol. 6, no. 1, p. 87_92, 1996.
[68] S. Nikam and S. Deosarkar, “Fast ICA based technique for non-invasive fetal ECG extraction,” Conf. Adv. Signal Process. CASP 2016, no. 1, pp. 60–65, 2016.
[69] L. Liao, W. Zhong, X. Guo, and G. Wang, A Mixed Approach for Fetal QRS Complex Detection. Springer Singapore.
[70] M. Richter, T. Schreiber, and D. T. Kaplan, “Fetal ECG extraction with nonlinear state-space projections,” IEEE Trans. Biomed. Eng., vol. 45, no. 1, p. 133_137, 1998.
[71] M. Akhavan-amjadi, “Fetal electrocardiogram modeling using hybrid evolutionary firefly algorithm and extreme learning machine,” Multidimens. Syst. Signal Process., 2019.
[72] H. Kantz and T. Schreiber, “Human ECG: nonlinear deterministic versus stochastic aspects,” vol. 145, no. 6, pp. 279–284, 1998.
[73] M. Kotas, “Projective filtering of time-aligned ECG beats,” IEEE Trans. Biomed. Eng., vol. 51, no. 7, p. 1129_1139, 2004.
[74] M. Kotas, “Projective filtering of time-aligned ECG beats for repolarization duration measurement,” vol. 5, pp. 115–123, 2006.
[75] M. J. O. Taylor et al., “Non-invasive fetal electrocardiography in singleton and multiple pregnancies,” BJOG Br. J. Obstet. Gynaecol., vol. 110, pp. 668–678, 2003.
[76] “SEPARATION OF TWINS FETAL ECG BY MEANS OF BLIND SOURCE SEPARATION (BSS) A. Kam and A. Cohen,” pp. 342–345.
[77] M. Burghoff and P. Van Leeuwen, “Separation of fetal and maternal magnetocardiographic signals in twin pregnancy using independent component analysis (ICA),” Neurol Clin Neurophysiol, vol. 39, pp. 1–4, 2004.
[78] M. Kotas, J. M. Leski, and J. Wrobel, “Sequential separation of twin pregnancy electrocardiograms,” Bull. Polish Acad. Sci. Tech. Sci., vol. 64, no. 1, 2016.
[79] M. Salmanvandi and Z. Einalou, “SEPARATION OF TWIN FETAL ECG FROM MATERNAL ECG USING EMPIRICAL MODE DECOMPOSITION TECHNIQUES,” Biomed. Eng. Appl. Basis

Commun., vol. 29, 2017.
[80] K. I. Ramachandran and U. K. Ceerthibala, “Approach To Extract Twin fECG For Different Cardiac Conditions During Prenatal,” in The 16th International Conference on Biomedical Engineering, 2017, pp. 106–110.
[81] W. J. Greville and M. J. Buehner, “Temporal predictability enhances judgements of causality in elemental causal induction from both observation and intervention,” Q. J. Exp. Psychol., 2016.
[82] and Y. K. K. Mahdi, R. A. Mohammad, “A theoretical discussion on the foundation of Stone’s blind source separation,” Springer:Signal, vol. 4, 2011.
[83] A. Cichocki, S. Amari, K. Siwek, T. Tanaka, and A. H. Phan, “ICALAB toolboxes, h http://www. bsp. brain. riken. jp,” ICALAB i, 2004.
[84] B. De Moor, P. De Gersem, B. De Schutter, and W. Favoreel, “DAISY: A database for identification of systems,” J. A, vol. 38, no. 3, pp. 4–5, 1997.
[85] S. Thalkar and D. Upasani, “Various techniques for removal of power line interference from ECG signal,” Int. J. Sci. Eng. Res., vol. 4, no. 12, 2013.

Appendices

Appendix A

Appendix A: Fetal Cardiovascular System

The Fig. A.1 below demonstrate general look to the Fetal Cardiovascular System.

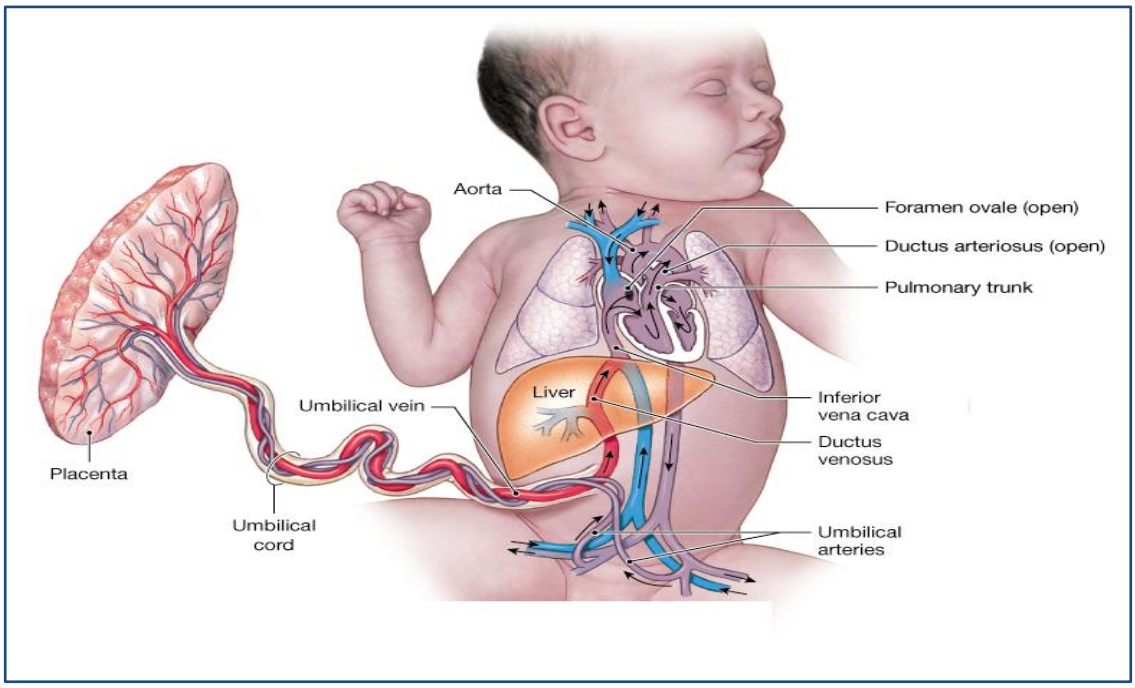

Figure A.1 The Fetal Cardiovascular System

Placenta

The circulatory system of the mother is not directly connected to that of the fetus, so the placenta functions as the respiratory center for the fetus as well as a site of filtration for plasma nutrients and wastes. Water, glucose, amino acids, vitamins, and inorganic salts freely diffuse across the placenta along with oxygen. The uterine arteries carry blood to the placenta, and the blood permeates the sponge-like material there. Oxygen then diffuses from the placenta to the chorionic villous, an alveolus-like structure, where it is then carried to the umbilical vein.

Heart

The fetal circulatory system includes three shunts to divert blood from undeveloped and partially functioning organs, as well as blood supply to and from the placenta. Below Fig A. 2 illustrate how the circulatory fetal system operates.

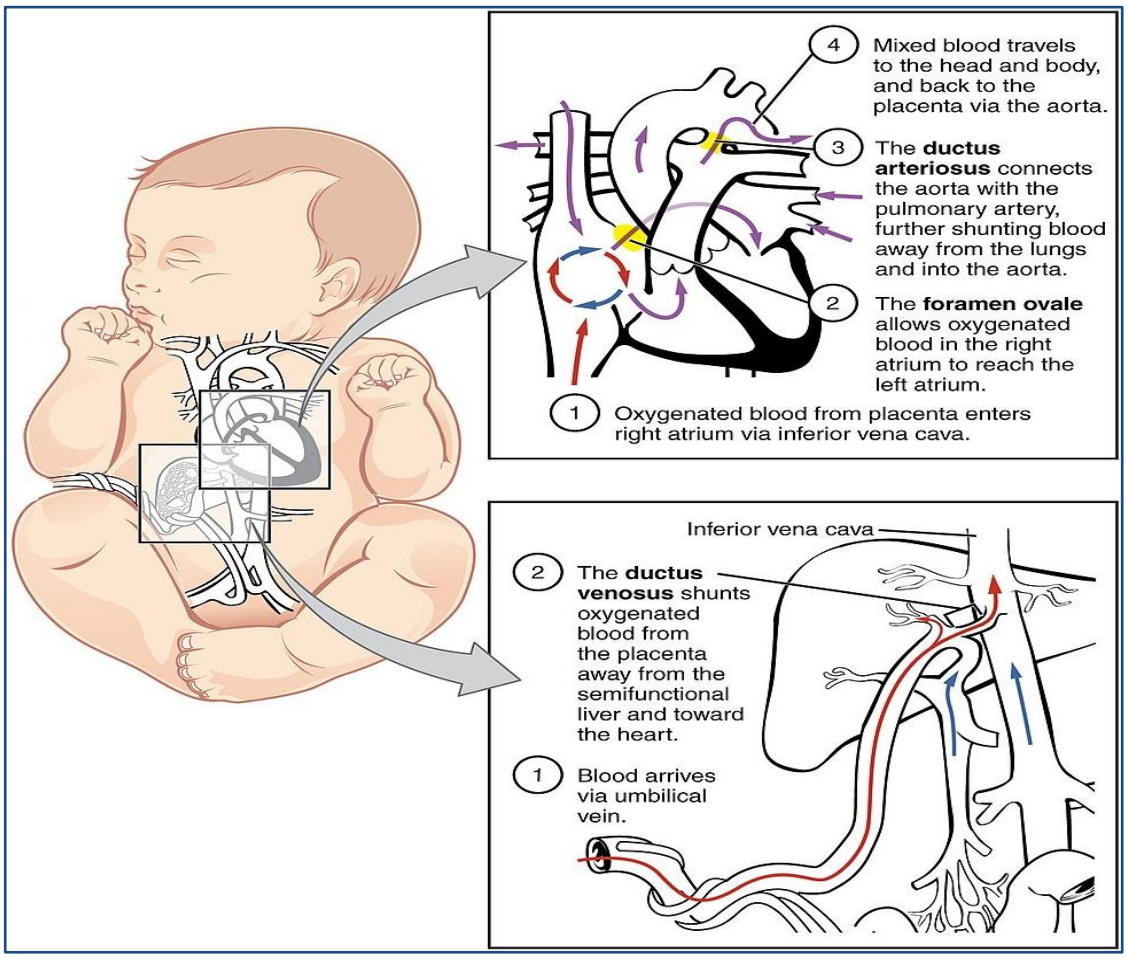

Figure A. 2 illustrate how the fetal heart and liver operate before fetal birth

Appendix B

Appendix B: Generation of simulated ECG data

The aim of the ECG simulator is to produce the typical ECG waveforms of different leads and as many arrhythmias as possible. My ECG simulator is a MATLAB based simulator and is able to produce normal lead II ECG waveform. The use of a simulator has many advantages in the simulation of ECG waveforms. First one is saving of time and another one is removing the difficulties of taking real ECG signals with invasive and noninvasive methods. The ECG simulator enables us to analyze and study normal and abnormal ECG waveforms without actually using the ECG machine. One can simulate any given ECG waveform using the ECG simulator.

Principle:

Fourier series

Any periodic functions which satisfy dirichlet's condition can be expressed as a series of scaled magnitudes of sin and cos terms of frequencies which occur as a multiple of fundamental frequency.

$$f(x) = (a_o/2) + \sum_{n=1} a_n cos(n\pi x/1) + \sum_{n=1} b_n sin\,(n\pi x/1)$$

$$a_o = (1/l) + \int_T f(x)dx \qquad ,T = 21 \qquad \text{.....(1)}$$

$$a_o = (1/l) + \int_T f(x)cos\,(n\pi x/1)dx \qquad ,n = 1,2,3\ldots \qquad \text{.....(2)}$$

$$a_o = (1/l) + \int_T f(x)\,sin\,(n\pi x/1)\,dx \qquad ,n = 1,2,3\ldots \qquad \text{.....(3)}$$

ECG signal is periodic with fundamental frequency determined by the heartbeat. It also satisfies the dirichlet's conditions:

- Single valued and finite in the given interval
- Absolutely integral
- Finite number of maxima and minima between finite intervals
- It has finite number of discontinuities

Hence Fourier series can be used for representing ECG signal.

Calculations:

If we observe figure1, we may notice that a single period of a ECG signal is a mixture of triangular and sinusoidal wave forms. Each significant feature of ECG signal can be represented by shifted and scaled versions one of these waveforms as shown below.

- QRS, Q and S portions of ECG signal can be represented by triangular waveforms
- P, T and U portions can be represented by triangular waveforms

Once we generate each of these portions, they can be added finally to get the ECG signal.

Let's take QRS waveform as the centre one and all shifting takes place with respect to this part of the signal.

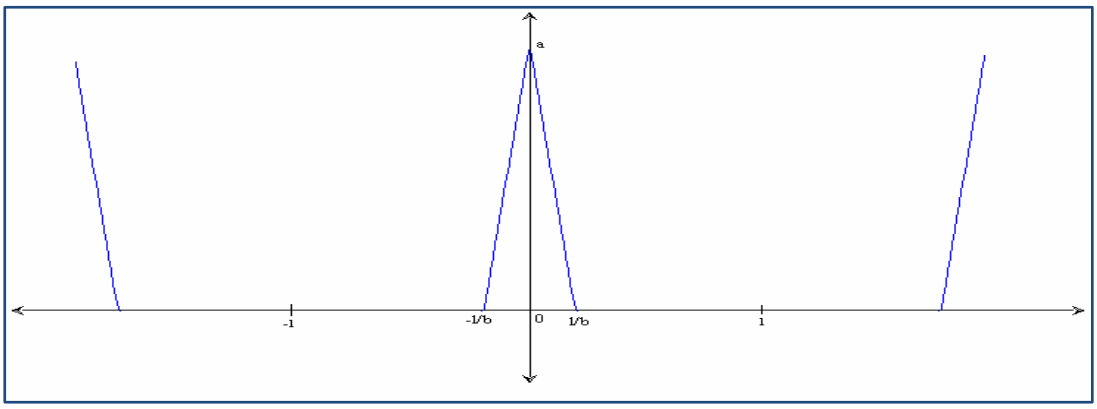

Figure B. 1 generating QRS waveform

From equation (1), we have

$f(x) = (-\text{bax/l}) + a \qquad 0 < x < (l/b)$

$$= (-\text{bax/l}) + a \qquad (-l/b) < x < 0$$

$$a_o = (1/l) f(x) dx$$

$$= (a/b) * (2 - b)$$

$$a_o = (1/l) + \int_T f(x)\, cos(n\pi x/l)\, dx$$

$$= (1ba/(n^2\pi^2)) * (1 - cos\ (n\pi/b))$$

$$b_n = (1/l) + \int_T f(x)\, sin(n\pi x/l)\, dx$$

$$= 0\ (becuase\ the\ waveform\ is\ a\ even\ function)$$

$$f(x) = (a_o/2) + \sum_{n=1}^{\infty} a_o cos\ (n\pi x/l)$$

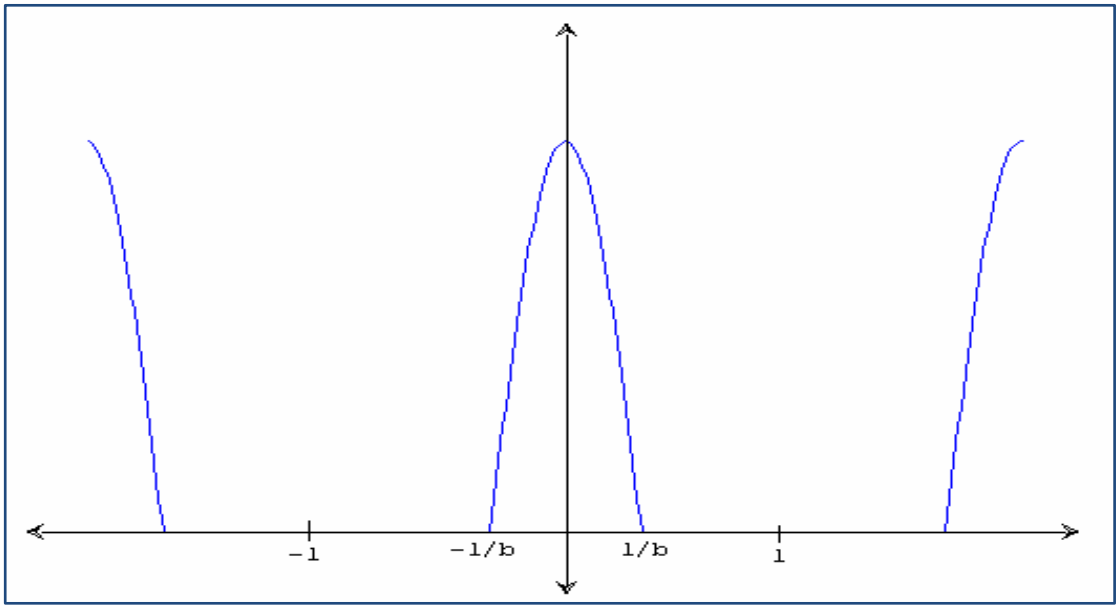

Fig B. 2 generation of p-wave

$$f(x) = cos((\pi bx)/(2l)) \qquad (-l/b) < x < (l/b)$$

$$a_o = (1/l) \int_T cos\ ((\pi bx)/(2l)) dx$$

$$= (a/(2b))(2 - b)$$

$$a_o = (1/l) \int_T cos(\pi bx/2l)\, cos\ (n\pi x/l)dx$$
$$= ((2ba)/(i^2\pi^2))(1 - cos(n\pi/b))\, cos\ ((n\pi x)/l)$$

$$b_o = (1/l) \int_T cos(\pi bx/2l)\, sin\ (\text{n}\pi\text{x/l})\text{dx}$$
$$= 0 \text{ (becuase the waveform is a even function)}$$

$$\text{f(x)} = (\text{a}_\text{o}/2) + \sum_{\text{n=1}}^{\infty} \text{a}_\text{n}\text{cos}\ (\text{n}\pi\text{x/l})$$

Implementation in MATLAB:

Code:

Save the below file as complete.m

```
x=0.01:0.01:2;
default=input('Press 1 if u want default ecg signal else press 2:\n');
if(default==1)
    li=30/72;

    a_pwav=0.25;
    d_pwav=0.09;
    t_pwav=0.16;

    a_qwav=0.025;
    d_qwav=0.066;
    t_qwav=0.166;

    a_qrswav=1.6;
    d_qrswav=0.11;
```

```
    a_swav=0.25;
    d_swav=0.066;
    t_swav=0.09;

    a_twav=0.35;
    d_twav=0.142;
    t_twav=0.2;

    a_uwav=0.035;
    d_uwav=0.0476;
    t_uwav=0.433;
else
   rate=input('\n\nenter the heart beat rate :');
   li=30/rate;
   %p wave specifications
   fprintf('\n\np wave specifications\n');
   d=input('Enter 1 for default specification else press 2: \n');
   if(d==1)
      a_pwav=0.25;
      d_pwav=0.09;
      t_pwav=0.16;
   else
     a_pwav=input('amplitude = ');
     d_pwav=input('duration = ');
     t_pwav=input('p-r interval = ');
     d=0;
   end
   %q wave specifications
```

```
fprintf('\n\nq wave specifications\n');
d=input('Enter 1 for default specification else press 2: \n');
if(d==1)
   a_qwav=0.025;
   d_qwav=0.066;
   t_qwav=0.166;
else
  a_qwav=input('amplitude = ');
  d_qwav=input('duration = ');
  t_qwav=0.1;
  d=0;
end
%qrs wave specifications
fprintf('\n\nqrs wave specifications\n');
d=input('Enter 1 for default specification else press 2: \n');
if(d==1)
   a_qrswav=1.6;
   d_qrswav=0.11;
else
  a_qrswav=input('amplitude = ');
  d_qrswav=input('duration = ');
  d=0;
end
%s wave specifications
fprintf('\n\ns wave specifications\n');
d=input('Enter 1 for default specification else press 2: \n');
if(d==1)
   a_swav=0.25;
   d_swav=0.066;
```

```
    t_swav=0.125;
else
   a_swav=input('amplitude = ');
   d_swav=input('duration = ');
   t_swav=0.125;
   d=0;
end
%t wave specifications
fprintf('\n\nt wave specifications\n');
d=input('Enter 1 for default specification else press 2: \n');
if(d==1)
    a_twav=0.35;
    d_twav=0.142;
    t_twav=0.18;
else
   a_twav=input('amplitude = ');
   d_twav=input('duration = ');
   t_twav=input('s-t interval = ');
   d=0;
end
%u wave specifications
fprintf('\n\nu wave specifications\n');
d=input('Enter 1 for default specification else press 2: \n');
if(d==1)
    a_uwav=0.035;
    d_uwav=0.0476;
    t_uwav=0.433;
else
   a_uwav=input('amplitude = ');
```

```
      d_uwav=input('duration = ');
      t_uwav=0.433;
      d=0;
   end
end
 pwav=p_wav(x,a_pwav,d_pwav,t_pwav,li);
 %qwav output
 qwav=q_wav(x,a_qwav,d_qwav,t_qwav,li);
 %qrswav output
 qrswav=qrs_wav(x,a_qrswav,d_qrswav,li);
 %swav output
 swav=s_wav(x,a_swav,d_swav,t_swav,li);
%twav output
 twav=t_wav(x,a_twav,d_twav,t_twav,li);
%uwav output
 uwav=u_wav(x,a_uwav,d_uwav,t_uwav,li);
 %ecg output
 ecg=pwav+qrswav+twav+swav+qwav+uwav;
 figure(1)
 plot(x,ecg);
```

Save the below file as p_wav.m

```
function [pwav]=p_wav(x)
l=1;
a=0.25
x=x+(1/1.8);
b=3;
n=100;
p1=1/l
p2=0
```

```
for i = 1:n
   harm1=(((sin((pi/(2*b))*(b-(2*i))))/(b-
(2*i))+(sin((pi/(2*b))*(b+(2*i))))/(b+(2*i)))*(2/pi))*cos((i*pi*x)/l);
   p2=p2+harm1
end
pwav1=p1+p2;
pwav=a*pwav1;
```

Save the below file as q_wav.m

```
function [qwav]=q_wav(x)
l=1;
x=x+l/6
a=0.025;
b=15;
n=100;
q1=(a/(2*b))*(2-b);
q2=0
for i = 1:n
   harm5=(((2*b*a)/(i*i*pi*pi))*(1-cos((i*pi)/b)))*cos((i*pi*x)/l);
   q2=q2+harm5;
end
qwav=-1*(q1+q2);
```

Save the below file as qrs_wav.m

```
function [qrswav]=qrs_wav(x)
l=1;
a=1;
b=5;
n=100;
qrs1=(a/(2*b))*(2-b);
qrs2=0
```

```
for i = 1:n
   harm=(((2*b*a)/(i*i*pi*pi))*(1-cos((i*pi)/b)))*cos((i*pi*x)/l);
   qrs2=qrs2+harm;
end
qrswav=qrs1+qrs2;
```

Save the below file as s_wav.m

```
function [swav]=s_wav(x)
l=1;
x=x-l/6
a=0.25;
b=15;
n=100;
s1=(a/(2*b))*(2-b);
s2=0
for i = 1:n
   harm3=(((2*b*a)/(i*i*pi*pi))*(1-cos((i*pi)/b)))*cos((i*pi*x)/l);
   s2=s2+harm3;
end
swav=-1*(s1+s2);
```

Save the below file as t_wav.m

```
function [twav]=t_wav(x)
l=1;
a=0.35
x=x-(1/1.8);
b=7;
n=20;
t1=1/l
t2=0
for i = 1:n
```

```
    harm2=(((sin((pi/(2*b))*(b-(2*i))))/(b-
(2*i))+(sin((pi/(2*b))*(b+(2*i))))/(b+(2*i)))*(2/pi))*cos((i*pi*x)/l);
    t2=t2+harm2
end
twav1=t1+t2;
twav=a*twav1;
```

Save the below file as u_wav.m

```
function [uwav]=u_wav(x)
l=1;
a=0.03;
x=x-(1/1.1);
b=21;
n=100;
u1=1/l;
u2=0;
for i = 1:n
    harm4=(((sin((pi/(2*b))*(b-(2*i))))/(b-
(2*i))+(sin((pi/(2*b))*(b+(2*i))))/(b+(2*i)))*(2/pi))*cos((i*pi*x)/l);
    u2=u2+harm4;
end
uwav1=u1+u2;
uwav=a*uwav1;
```

precautions:

- All the files have to be saved in the same folder
- Save the files in the names mentioned above the code
- While entering the specification, give the amplitude in mV and duration in seconds

Default Specification

Heart beat :72

Amplitude:

P wave 25mV

R wave 1.60mV

Q wave 0.025mV

T wave 0.35mV

Duration:

P-R interval 0.16s

S-T interval 0.18s

P interval 0.09s

QRS interval 0.11s

Not all the default values are specified here. They can be obtained from the code of the simulator from the file complete.m. The user can enter their desired values of specifications too. Other concepts of the code are simple and are self explanatory.

A typical output for the above specification will be like this:

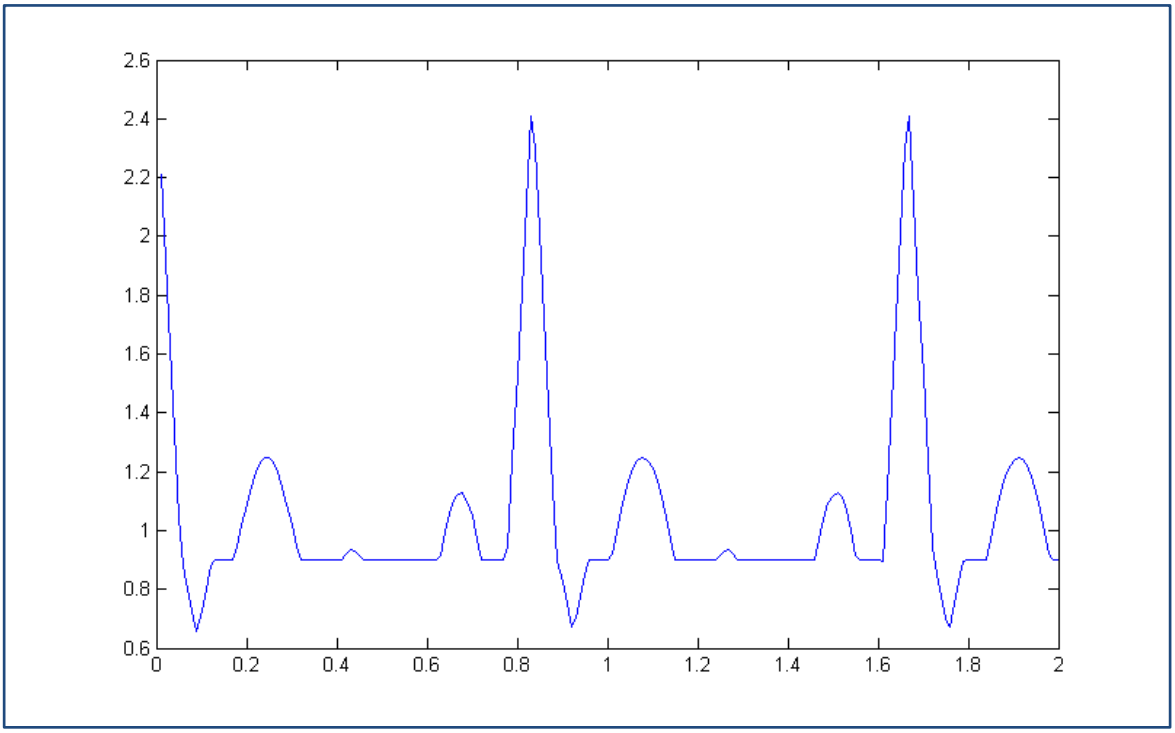

Figure B. 3 Complete ECG signal